NWT Open Report 2011-010
Paleoclimatological Assessment of the Northwest Territories and Implications for the Long-Term Viability of the Tibbitt to Contwoyto Winter Road, Part II: March 2010 Field Season Results

Macumber, A.L., Neville, L.A., Galloway, J.M., Patterson, R.T., Falck, H., Swindles, G., Crann, C., Clark, I., Gammon,P., and Madsen, E.

Recommended Citation: ***Macumber, A.L., et al., 2012.*** Paleoclimatological Assessment of the Northwest Territories and Implications for the Long-Term Viability of the Tibbitt to Contwoyto Winter Road, Part II: March 2010 Field Season Results*; Northwest Territories Geoscience Office, NWT Open Report 2011-010, 83 p.*

>>> NORTHWEST TERRITORIES GEOSCIENCE OFFICE

PO Box 1500, 4601-B 52 Avenue, Yellowknife, NT X1A 2R3

NWT Open Report 2011-010

Paleoclimatological Assessment of the Northwest Territories and Implications for the Long-Term Viability of the Tibbitt to Contwoyto Winter Road, Part II: March 2010 Field Season Results

Andrew L. Macumber, Lisa A. Neville, Jennifer M. Galloway, R. Timothy Patterson, Hendrik Falck, Graeme Swindles, Carley Crann, Ian Clark, Paul Gammon and Erik Madsen (see next page for authors' affiliations and addresses)

This publication may be obtained from the Northwest Territories Geoscience Office

4601-B 52 Avenue
P.O. Box 1500
Yellowknife, NT, X1A 2R3 Canada
867-669-2636
www.nwtgeoscience.ca

Author's addresses:

Andrew L. Macumber[1], Lisa A. Neville[1], Jennifer M. Galloway[2], R. Timothy Patterson[1], Hendrik Falck[3], Graeme Swindles[4], Carley Crann[1], Ian Clark[6], Paul Gammon[7] and Erik Madsen[5]

[1]Departmentof Earth Sciences and Ottawa-Carleton Geoscience Centre
Carleton University
1125 Colonel By Drive, Ottawa, Ontario, K1S 5B6

[2]Geological Survey of Canada, Calgary
3303-33rd Street NW, Calgary, AB, T2L 2A7

[3]Northwest Territories Geoscience Office
P.O. Box 1500, Yellowknife, NT, X1A 2R3

[4]School of Geography, University of Leeds,
Leeds, LS2 9JT, UK

[5]Tibbitt to Contwoyto Winter Road Joint Venture,
Diavik Diamond Mines Inc.,
P.O. Box 2498 5007 – 50th Ave, Yellowknife, NT X1A 2P8

[6]Department of Earth Sciences and Ottawa-Carleton Geoscience Centre
University of Ottawa
75 Laurier Avenue East, Ottawa, ON, K1N 6N5

[7]Geological Survey of Canada, Ottawa
601 Booth Street, Ottawa, ON, K1A 0E8

Table of Contents

Introduction

SUMMARY
We characterize water quality and present biological and chemical data from lake sediments in support of an NSERC Strategic Project mandated to investigate background climate variability over the past ca. 3500 years in the southern Northwest Territories (NT). Goals of the project "Paleoclimatological assessment of the central Northwest Territories: Implications for the long-term viability of the Tibbitt to Contwoyto Winter Ice Road" include providing data to increase the understanding of natural climate variability in the southern NT in general, and the Tibbitt to Contwoyto Winter Road (TCWR) in particular. A complete understanding of past climate systems is critical to predicting future climate variability and impacts on northern ecosystems.

Eighteen lakes were sampled during March 2010 (Appendix C – Table C01): a total of thirteen freeze cores, sixty Glew cores, twenty sediment-water interface samples, twenty bottom and top water samples and twenty vertical lake profiles were collected. The eighteen lakes sampled are spread along a latitudinal transect that spans the length of the TCWR from Tibbitt Lake to Lac de Gras. Lake sediment cores are composed mainly of mud, although a few contain intervals of sand and gravel. Freeze coring was performed with a custom designed device that captured sediments on two faces and was successful in capturing the unconsolidated sediment-water interface. Sediment cores were digitally imaged and sedimentologically described and a subset was X-Ray imaged. Limnological properties and chemical characterization of lake water will be used in concert with analyses of sediment-water interface samples to develop thecamoebian (arcellacean) and diatom-based transfer functions. These transfer functions will be used to quantify the paleoclimate record of the central NT over the past 3000 years. This research represents the first analysis of fossil and modern assemblages of arcellaceans in the southern NT and is only the second investigation involving arcellaceans, after Dallimore et al. (2000), to occur in the territory. Other microfossil techniques, such as palynology and microscopic charcoal analysis, will permit reconstruction of treeline movement and the response of fire regime to past climate change.

ACKNOWLEDGEMENTS

This research is funded by a Natural Sciences and Engineering Research Council of Canada Strategic Project Grant to Dr. R. Timothy Patterson and co-investigators. Direct and in-kind funding is also provided by the Northwest Territories Geoscience Office, The Department of Aboriginal Affairs and Northern Development Canada, the Geological Survey of Canada, the Tibbitt to Contwoyto Winter Road Joint Venture, and the North Slave Métis Alliance. Staff of the three maintenance camps, Dome, Lockhart and Lac de Gras, provided essential information and made our stay enjoyable. Special thanks must be given to Brett Wildman, Shaun Tone and Dallas Bridges of the Lockhart Camp and Kirk Kellar, Allan Mischuk, Terry Sharun, Keith White, Don Cockburn and Ryan Lepine of the Lac de Gras Camp; their knowledge of the study sites was invaluable. Discussions with the North Slave Métis Alliance (Sheryl Grieve) assisted our study design. Robert Mercredi was integral to the success of this project, and we thank him for providing his services. This research was carried out under Aurora Research Institute License No. 14965.

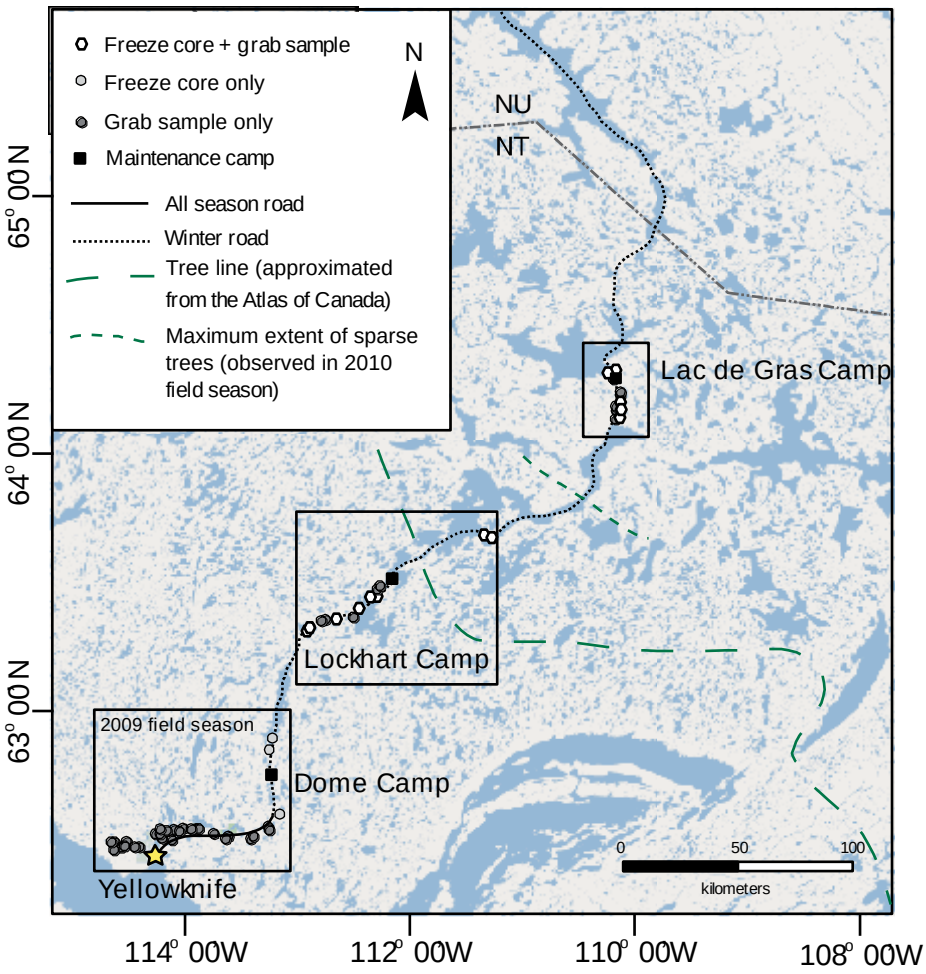

Figure A01. Map of TCWR with sampling locations from 2009 (within box) & 2010 field seasons. Hashed circles delineate geographical zones (Boreal Forest (A), Sparse Trees (B), and Tundra (C)). Map from Google Earth.

Table 01. Geographical co-ordinates and vegetational zonations of the 20 study sites. ♦ = Boreal Forest, Δ = Sparse Trees, • = Arctic Tundra

	SITE	LAT(N)	LONG(W)		SITE	LAT(N)	LONG(W)
♦	P26-1	63°23.297	112°51.768	•	P48-1	64°14.592	110°06.995
♦	P27-1	63°28.616	112°50.972	•	P49-1	64°15.571	110°05.878
♦	P28-1	63°23.974	112°50.514	•	P51-1	64°16.605	110°05.015
♦	P30-1	63°25.195	112°41.314	•	P52-1A	64°17.394	110°03.694
♦	P33-1	63°27.551	112°32.785	•	P52-1B	64°17.381	110°03.701
♦	P34-2	63°28.547	112°32.250	•	P53-1A	64°19.921	109°59.921
♦	P39-1	63°35.141	112°18.393	•	P53-1B	64°22.554	110°00.944
♦	P40-1	63°35.615	112°17.649	•	P54-1	64°24.717	110°06.199
Δ	P46-1	63°44.963	111°18.560	•	P54-2	64°25.114	110°06.449
Δ	P47-1	63°44.538	111°12.957	•	P55-1	64°25.794	110°08.168

BACKGROUND

The diamond industry is an essential component of the economy of the NT and the TCWR is the sole infrastructure for the ground transportation of goods and services to and from mines and projects north of Yellowknife. Cold winter temperatures are critical to the viability of the road, as 87% of the TCWR's 600 km length is composed of frozen lakes. Changing ice stability, thickness, and duration of ice cover associated with recent climate variability has dramatically impacted the use of the road. For example, an unusually mild and stormy winter in 2006 associated with the El Niño/Southern Oscillation (ENSO) resulted in a substantially shortened road operation (26 days below average) and significant financial losses for industry. High costs for alternative transportation, such as air, negatively influences the feasibility of new mining operations, so it is critical for policy makers, planners, land users, and mine developers to understand the potential impact of future climate variability on the TCWR.

The detrimental fiscal impact of the 2006 winter underscored the need for a more complete understanding of which climate phenomena impact the region and how the region responds to natural climate variability. Instrumental records are few in number and only began in the 1940s. Even so they show a strong correlation to the positive and negative phases of the Pacific Decadal Oscillation (PDO) (Pisaric et al 2008), a phenomenon driven by sea surface temperatures of the Pacific Basin. Previous climate reconstructions in the NT have shown that the climate of the NT has changed substantially and rapidly in the past (Pienitz et al., 1997a; Rühland et al., 2003; Huang et al., 2004; Rühland and Smol, 2005). Employing only vegetational histories, sediment-water interface samples or single indicators of past climate or environmental change, these studies provide only a low spatial and temporal resolution (i.e. centennial-scale) that is insufficient to analyze climate variability on decadal and multi-decadal time scales (i.e. PDO and ENSO). Exceptions include the recent work of MacDonald et al. (2009) at Lake S41 where a temporal resolution of 90 years (including dating error) was achieved and the comprehensive studies conducted at Queen's Lake (MacDonald et al., 1993; Wolfe and Härtling, 1996; Pienitz et al., 1999) and Toronto Lake (Moser and MacDonald, 1990; MacDonald et al., 1993; Pienitz et al., 1999). A more complete understanding of which climate phenomenon impact this region and their presence through time can only be achieved utilizing a high temporal resolution climate reconstruction, which is completely lacking in this region of the world.

Lakes are abundant in the central NT and their sediments contain continuous archives of biological, chemical, and physical proxies of recent and past environmental conditions that can be linked to climate (Chen et al., 2004; Conroy et al., 2008; MacDonald et al., 2009). For example, arcellaceans (thecamoebians) are abundant in benthic lacustrine habitats and research on this group has shown that arcellaceans are excellent proxies for paleolimnological and paleoclimatic study because their populations respond rapidly to changes in trophic status, pH, temperature, contamination, nutrients, and oxygen levels that can in turn, be linked to climate (Patterson et al., 1985; McCarthy et al., 1995; Booth 2001; Neville et al., 2010; Roe et al., 2010) including at high latitudes in Canada (e.g. Kliza and Schröeder-Adams, 1999; Dallimore et al., 2000). Extant arcellacean community

composition in sediment-water interface samples will be statistically correlated to measured environmental variables. A transfer function will apply the modern biological community-environment relationship to sub-fossil arcellacean community compositions preserved in the freeze cores. This approach will permit the quantitative reconstruction of environmental variables associated with climate for at least the past 3000 years. Another proxy of interest, particle size, is thought to reflect the energy of the surrounding catchment (Sun et al., 2002; Chen et al., 2004; Conroy et al., 2008; Kirby et al., 2010). When precipitation is greater, resulting in larger freshets, there is an increase in larger grains washing into the lake. The alternation between coarser and finer average particle sizes in the core samples records the oscillations of climate phenomena in the area. Using time series analysis the signals of various climate phenomena can be reconstructed. These signals can they be compared to known global climate phenomenon.

By combining a multiproxy approach and a high resolution analysis, decadal to multi-decadal climate phenomenon will be resolved in the sediment cores. Qualitative and quantitative environmental reconstructions of the past 3500 years will aid in our understanding of how this region has responded to natural climate variability. This is the type of knowledge that is required to assess the impact of future climate variability whether natural, anthropogenic, or a combination of the two.

OBJECTIVES

Physical and chemical properties of lake sediments and surface and lake bottom waters will be used to characterize the biological, physical, and chemical properties of lacustrine systems along the TCWR. These types of data characterize the limnology of the basin and can be used to develop quantitative transfer functions to link the distribution of biological organisms during winter months to seasonal changes in water chemistry, for example. The results of this analysis will be applied to sediment core archives to reconstruct paleoenvironments during the last 3500 yrs. By investigating these paleoenvironments a qualitative climate history of the NT can be elucidated, and utilizing time series analysis cyclicity of various climate phenomena can be recognized. Understanding which climate phenomenon impact this region and their effects on the regional watershed, will provide a robust and comprehensive scientific basis to evaluate the viability of present and future projects. The objectives of the March 2010 field season were to collect freeze cores, Glew cores (Glew, 1991), water samples, and water quality measurements from lakes north of the 2009 field season sites (Galloway et al. 2010) to complete the latitudinal transect along the TCWR.

STUDY SITE

The 2010 sampling program continued the north-south transect started during the 2009 field season to include sites from below, at, and above treeline (Figure A01; Table 01). The study region is located within the Taiga Shield Ecozone (Lands Directorate, 1986). West of Hudson Bay, this ecozone spans northern Manitoba and Saskatchewan, southern portions of Nunavut, and the south central area of the NT. The climate of the Taiga Shield Ecozone is subarctic and continental, and is

characterized by short summers and long, cold winters. Annual precipitation is low (175-200 mm) and mean daily January temperatures range from -17.5°C to -27.5°C while the mean daily July temperatures range from 7.5°C to 17.5°C. Boreal forests make up most of the groundcover of this ecozone and are dominated by stands of black spruce (*Picea mariana* (Mill.) BSP.) and white spruce (*Picea glauca* (Moench) Voss), with tamarack (*Larix laricina* (Du Roi) K. Kock) and pine (*Pinus* L.). Deciduous trees, including birch (*Betula* L.), trembling aspen (*Populus tremuloides* Michx.), alder (*Alnus* Mill.), and willow (*Salix* L.), grow in moist habitats. Along the northern limits of the ecozone, the boreal tree line is reached and forest stands are open and lichen woodlands merge into areas of shrub tundra. The tundra vegetation cover can be discontinuous on rocky substrates and is dominated by lichen-heath, mosses, sedges, grasses, and diverse herbs (MacDonald et al. 2009). Small shrubs, most typically *Betula glandulosa* (dwarf birch), *Salix* (willow), alder (*Alnus crispa*), and various ericoids are common (Pienitz et al., 1997a; Huang et al., 2004; MacDonald et al., 2009). Peat bogs in low-lying areas are dominated by *Cyperaceae* and *Sphagnum* (Pienitz et al., 1997a; Huang et al., 2004).

Methodology

Site Characterization

Lake selection

The overall size and inflow outflow parameters were used to select target sites. In the absence of detailed bathymetry, the anecdotes of the Tibbitt Contwoyto Winter Road Joint Venture (TCWRJV) maintenance camp staff were used to improve the selection set. In addition several lakes identified as "problem lakes" by the maintenance camp staff were examined. The features that define problem lakes include lakes that freeze late and thaw early, that develop large areas of weak ice, and those associated with the escape of large amounts of methane from the substrate. Lake 26-1, Lake 27-1 and Lake 33-1 were identified as 'problem lakes' by the TCWRJV and were incorporated into the study. Small lakes, ponds, and bogs located adjacent to the TCWR were not targeted for coring for two reasons: 1) the truck equipped with a rear-mounted auger of adequate width for freeze coring was unable to leave the TCWR; and 2) there is specific interest in how climate change may impact lakes along the TCWR. Future field work will target those sites that lie adjacent to the TCWR in 2011.

Coring location

Ideal coring sites were more than 3 meters from shore, less than 8 m deep and contained a muddy substrate of suitable thickness (Galloway et al., 2010). It was also important that coring locations where the water column was greater than 2 meters as to avoid the disruption to lake sediment caused by ice freezing to the lake bottom. During the annual lake thaw, as the surface melts, the ice frozen to the bottom of the lake floats up, pulling up lake sediment with it, thus removing part of the lake history. A fish finder and sounding line were used to measure water depth and a 'pilot' Glew core was used to investigate substrate type and thickness. If all criteria were met, the lake was cored with the freeze corer. GPS coordinates in NAD 83 were recorded at all sampling locations.

Water quality characterization

Winter water quality characteristics (dissolved oxygen, temperature, and conductivity) were recorded at each core location using an YSI multi-meter probe (Appendix B). Measurements were taken per meter depth at deeper sites and half-meter depth at shallower sites. Surface water pH was measured with a hand held pH meter. All equipment was calibrated according to manufacturer's instructions. Ambient weather conditions (cloudiness, air temperature) were recorded for each day. Lake bottom water was sampled using a Kemmerer sampler and surface water was sampled directly. See Table 02 for sample treatment in field prior to analysis. Cations and dissolved metals were analyzed using both ICP-MS and ICP-ES, alkalinity was measured using an automatic titration method (PC-Titrate), and trace anions were measured using a DIONEX EG40 coupled with ion chromatography. Samples measured for dissolved organic carbon (DOC) and dissolved inorganic carbon (DIC) were run on an OI Analytical "TIC-TOC" Analyser Model 1030 (St-Jean,

2003). Samples for inorganic nutrient molecule analysis (P, NH_3, N) were submitted to Caduceon Environmental Laboratories, Ottawa, Canada.

Table 02. Sample treatment in field.

Analysis	Bottle	Filter	Preserve
Cations & Dissolved Metals	60 mL HDPE	Y	Nitric Acid
Anions	60 mL HDPE	Y	No
Stable Isotopes	60 mL HDPE	Y	No
Total Nutrients	2x125 mL HDPE	N	Sulphuric
DIC	40 mL amber w/ septum	Y	No
DOC	40 mL amber w/ septum	Y	No

Surface Sediment Sampling

Lake sediment-water interface samples were collected using a Glew corer (Glew, 2001). In most cases, a top, middle, and bottom sample were sub-sampled from the Glew corer using the extruding device (Glew, 2001). Selection criteria for suitable Glew coring sites followed the selection process for freeze coring. Due to speed of collection with the Glew coring method, more lakes were sampled (Appendix C - Table C01). Triplicate cores were collected from each lake to provide enough material for multiple analyses. Each site was approximately 0.3 m apart. Lake sediment-water interface samples were analyzed for a suite of analysis (see *Core Analysis* for methodology): microfossils (arcellaceans, chironomids, diatoms, and pollen), microscopic charcoals, loss on ignition (%moisture, % organics, % carbonate), particle size analysis, biogenic silica, oxygen and carbon isotopes and magnetic susceptibility. Phosphorus was also examined using the Olsen's phosphorus (Olsen P) extraction method, which provides a measure of bio-available phosphorus (Zhou et al. 2001) and is a suitable extraction method for samples of neutral to alkaline pH. Phosphorus concentrations were determined using phosphomolybdate colorimetric technique (Watanabe and Olsen 1965). Results will be used in conjunction with samples collected during summer 2009, summer 2011, and to develop both arcellacean and diatom-based transfer functions (Galloway et al., 2010; ter Braak & Prentice, 1988).

Freeze Coring

Coring

Two freeze corers, a single-faced and a double-faced freeze corer, were employed to collect continuous successions of lake sediment. Freeze corers are ideally suited for the recovery of high quality sedimentary successions, especially the unconsolidated and water saturated sediment near the sediment-water interface that is difficult to recover undisturbed using the open-tube corers (Lotter, 1997; Glew, 2001; Kulbe and

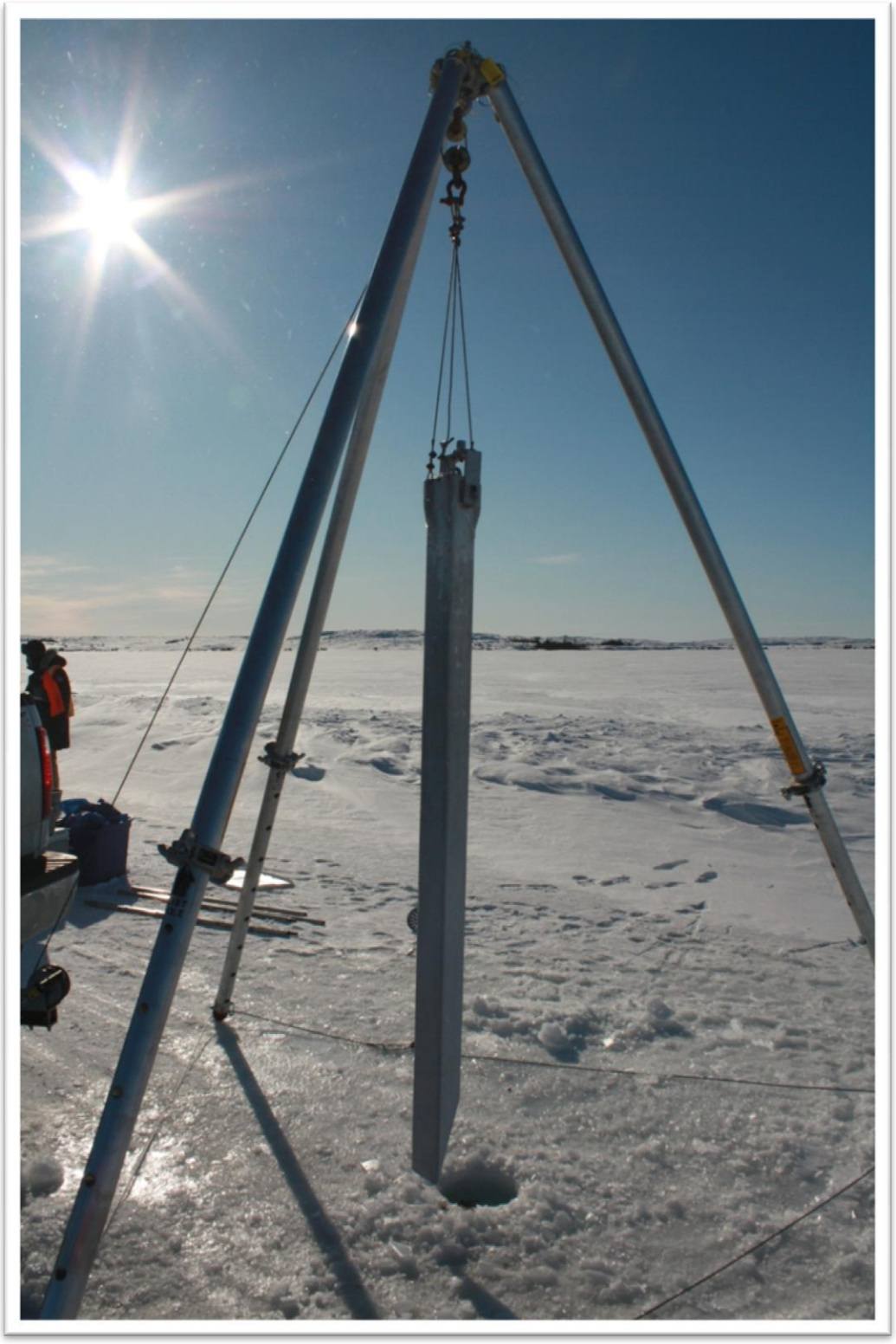

Figure 01. Deployment of tri-pod suspending double faced freeze corer during freeze coring on lake P47-1 (March 10th, 2010; TCWR, NT).

Niederreiter Jr., 2003; Blass et al., 2007). A single faced freeze corer was used during the March 2009 field season as described by Galloway et al., 2010. A custom-designed double-faced freeze corer, consisting of a rectangular pyramid chamber with one face covered by a wood board and the other two faces bare metal was also employed in March 2010 (Figure 01).

The exposed metal faces are used to collect the sediment. Each face is fifteen centimeters in width and over 2 m in length. The freeze core methodology employed was identical to that described by Galloway et al. (2010). An aluminum tri-pod with telescopic legs in conjunction with a boat winch (fastened to a modified trailer hitch) was used to raise and lower the freeze corers (Figure 01). The use of the telescopic legs allowed us to completely raise the freeze corer above the surface of the ice, facilitating successful recovery of undisturbed sediment.

Removal of sediment & sediment core preparation

Sediment was mostly completely frozen upon removal from the lake. Nonetheless, we allowed an extra ~10 minutes of freezing prior to transport. Freeze cores with frozen sediment were wrapped in a tarp and brought back to the maintenance camp where sediment was removed in frozen slabs. Slabs were laid on plastic wrapped wooden planks, information was recorded on the planks, and the slabs were encased in plastic wrap and secured with duct tape. Cores were then placed in coolers with dry ice and shipped frozen to Carleton University, Ottawa, Ontario, for detailed analyses.

Freeze cores are named as follows: (Project & Year)-(Lake Number or Name). Lakes along the TCWR are numbered according to what land portage they follow. P (portage)-39-1; is the first lake after the 39th land portage. P34-2 is the second lake after the 34th land portage. Some lakes, such as Lac de Gras, are referred to by a proper name when it exists, but also have a lake number assigned to them. Glew cores and water samples were named as follows: (Lake Number or Name)-(Replicate Hole Number) (Top, Middle or Bottom). 39-1-2T represents a Glew core collected from Lake 39-1, from the second replicate hole, and collected from the top of the Glew core.

Sedimentological description

Sediment cores were unwrapped in the laboratory for sedimentological description following procedures and nomenclature outlined in Schnurrenberger et al., 2003. The upper surface (1 mm or less) of the cores was allowed to come to a temperature of ~4^{o}C; the remainder of the sediment core was kept frozen. Sediment colour and grain size were determined using Munsell colour charts. Digital photos were taken of the cores (Francus et al., 2004) using a Canon EOS Rebel T1i EOS 500D camera with a Canon EFS 18-55mm lens (Appendix C – Figures C01-C27). The camera was set to automatic under indoor lighting. An 18% gray card, printed gray scale and a 2.5y Munsell Colour Card were used as standards. Cores were X-Rayed at the Merivale Medical Imaging Centre using a Philips 527593, Bucky Diagnost TH and Fuji FCR (Appendix C – Figures C01-C27).

Core Analysis

Bulk sediment samples and plant remains (e.g., twigs) were submitted to the 14CHRONO Lab, Queen's University, Belfast, and Beta Analytic Inc., Florida, U.S.A. for AMS radiocarbon dating (Appendix D – Table D01). Age-depth relationships shown in Figure D01 include more dates then are displayed in Table D01, since the age-depth relationships were updated after submission of this report. Those cores with a suitable age model were then selected to be sub-sampled at a mm-scale resolution using a freeze core microtome (Macumber et al., 2011).

Material was collected at various resolutions for a suite of analysis including: particle size analysis with a Beckman Coulter LS13 320 Laser Diffraction Analyser. Particle size variations reflect the variability in catchment energy as a result of changes in levels of precipitation and inflow to the lake. Low frequency magnetic susceptibility has been shown to reflect erosional rates and switches in source provenance. Loss on ignition using a (muffle oven), gives results about the shifts in moisture content, total organic carbon, carbonate and sediment content in the soil. Shifts in these percentages reflect variability in lake productivity and increases in erosional rates. Oxygen and carbon isotope analysis can track variations in lake levels and overall productivity. Microfossil assemblages (thecamoebians, diatoms, chironomids) are being analyzed to quantitatively reconstruct the paleoclimate of the region. Pollen and microscopic charcoal are being used to reconstruct vegetation and fire regimes of the region. Tree-ring analysis (dendrochronology) will be used at low latitude sites along the TCWR to provide an annually resolved terrestrial climate record to which other proxies can be compared.

Results & Discussions

Site Characterization

Lake selection & Coring Location

Sites sampled span from latitude N62°27.600 to latitude N64°25.794 and from longitude W109°59.921 to longitude W114°43.603. A recent forest fire (~1997) occurred in close proximity to Lake 34-2 (Danny's Lake). Charcoal that has been deposited within the lake can be used as a chrono-stratigraphic marker. A burn is evident on air photos north of this site and Lake 46-1. Lake 46-1 and Lake 47-1 (Portage Lake) are located at the treeline (near the Snap Lake Mine turnoff). Lake 47-1 is a multi-basin lake, but is isolated from Mackay and P46-1. Lake McKay is almost 100 km in length. A sediment core from this lake was collected at the northern end within a sub-basin. Lake 53-1 (Gravel Pit Lake) is located next to an esker with large lenses of frozen ice near the Lac de Gras maintenance camp. Lake 54-2 (Echo Lake) contained clear water and is located next to the Lac de Gras maintenance camp.

Water quality characterization

Site Characterization - Twenty one water samples (surface water and bottom water) were retrieved from eighteen lakes (Figure A01; Table C01). Water quality data was collected from all eighteen lakes (Appendix B: Table B01). Water from Lake 40-1 and Lac de Gras had a sulfur smell. Water was tea-coloured, possibly due to a high concentration of dissolved organic carbon or humic substances. Peaty fragments were also observed in the Glew cores collected from these sites. Lake 49-1 also contained tea-coloured water.

Physical Parameters – The 18 study lakes were generally between 10 to 1000 hectares in size but some very large lakes (P48-1 & P55-1) were included (surface area ranged from 2.3 to 97600 ha; median = 49.9 ha) (Table C01). The lakes were also generally shallow (maximum depth ranged from 1 to 6.5 m; median = 3.5 m) (Table C01). There were no significant differences ($p<0.05$; Table 3) and no pattern was seen lake surface area or water depth across the three ecozones (Figure 2a & c). Surface area was negatively correlated at the $p<0.01$ level with silica (Table 4). Depth was negatively correlated at the $p<0.01$ level with conductivity, and various dissolved elements (Ba, Ca, K, Mg) and at the $p<0.05$ level with dissolved organic/inorganic carbon (DOC, DIC) and various dissolved elements (As, B, Cl, Li) (Table 4). Temperature profiles revealed all lakes to be isothermal to inversely stratified (Figure B01). Inverse stratification occurs in winter and is related to the maximum density of water being 4°C Celsius, resulting in this water mass coming to underlay the colder less dense surface waters. There were no significant differences ($p<0.05$; Table 3), but a slight trend of decreasing bottom water temperatures as one moves north (Figure 2b). Dissolved oxygen profiles revealed most lakes to have homogenous oxygen levels, with a few exceptions (P30-1 and P34-2) (Figure B01). Dissolved oxygen levels were significantly different ($p<0.05$; Table 3) between the lakes within the Boreal Forest and the Arctic Tundra and there is a general trend of

Table 3. Comparison of significant differences (two-tailed t-test results) of measured variables across the three vegetational zones [Boreal Forest (BF), Sparse-Trees (ST), Arctic Tundra (AT). Highlighted numbers indicates significantly different ($p < 0.05$). DO = Dissolved Oxygen. TKN = Total Kjeldalh Nitrogen. P-acid = Acid Extracted Phosphorous. TP = Total phosphorous. DOC = Dissolved Organic Carbon. DIC = Dissolved Inorganic Carbon.

Variable		BF vs ST	ST vs AT	BF vs AT
Depth	(m)	0.4641	0.3045	0.8010
DO	(%)	0.2479	0.6721	0.0115
DO	(mg/L)	0.2640	0.6367	0.0111
NH_3	(µg/g)	0.5921	0.3148	0.0133
TKN	(µg/g)	0.4607	0.3822	0.0001
P-acid	(µg/g)	0.0671	0.1620	0.5483
TP	(µg/g)	0.6535	0.4957	0.0171
Temp	(˚C)	0.7340	0.6468	0.1955
Alkalinity	(ppm)	0.0549	0.8099	0.0544
Conductivity	(µS/cm)	0.0567	0.4942	0.1416
DOC	(ppm)	0.1100	0.0907	0.1715
DIC	(ppm)	0.0922	0.4349	0.1775
δ^{13}C DOC	(vpdb)	0.0332	0.0755	0.4066
δ^{13}C DIC	(vpdb)	0.2303	0.3493	0.0851
Br	(ppm)	0.1086	0.0002	0.9652
Cl	(ppm)	0.0805	0.4398	0.3941
F	(ppm)	0.0472	0.0136	0.0000
NO_3	(ppm)	0.2367	0.9035	0.2394
SO_4	(ppm)	0.8029	0.3368	0.3233
pH	(units)	0.0157	0.0331	0.4196
Al	(ppb)	0.1565	0.0691	0.2078
As	(ppb)	0.1671	0.1118	0.7588
B	(ppb)	0.0012	0.1439	0.0235
Ba	(ppb)	0.0977	0.3553	0.2262
Ca	(ppm)	0.0917	0.9264	0.0966
Ce	(ppb)	0.1520	0.3453	0.1678
Cl	(ppm)	0.0472	0.4661	0.2600
Co	(ppb)	0.2618	0.2414	0.2532
Cr	(ppb)	0.0852	0.1966	0.1690
Cs	(ppb)	0.0871	0.0317	0.6645
Cu	(ppb)	0.0810	0.0068	0.2268
Fe	(ppm)	0.2117	0.2551	0.3867
Gd	(ppb)	0.0974	0.0738	0.1264
K	(ppm)	0.0506	0.4969	0.1159
La	(ppb)	0.1380	0.6492	0.1449
Li	(ppb)	0.1915	0.2369	0.6300
Mg	(ppm)	0.0760	0.4438	0.2286
Mn	(ppb)	0.1826	0.4198	0.4277
Na	(ppm)	0.0205	0.7401	0.0263
Nd	(ppb)	0.1372	0.4888	0.1504
Ni	(ppb)	0.1717	0.0444	0.2758
Pb	(ppb)	0.0470	0.0983	0.0955
Pr	(ppb)	0.1364	0.4693	0.1497
Rb	(ppb)	0.1020	0.4135	0.2738
S	(ppm)	0.4470	0.2383	0.5207
Si	(ppm)	0.0381	0.4077	0.0583
Sm	(ppb)	0.1174	0.2042	0.1422
Sr	(ppb)	0.1655	0.7254	0.1482
U	(ppb)	0.0001	0.3151	0.0001
V	(ppb)	0.1291	0.1172	0.1977
Y	(ppb)	0.0813	0.1231	0.1105
Yb	(ppb)	0.0901	0.1518	0.1219
Zn	(ppb)	0.0210	0.0388	0.0823

increasing dissolved oxygen levels as one moves north (Figure 2i), with a few exceptions (P26-1, P27-1, P28-1, P51-1). Dissolved oxygen is negatively correlated at the $p<0.01$ level with alkalinity, conductivity, DOC, DIC, and various dissolved elements (Al, B, Ba, Ca, Ce, Fe, K, Mg, Mn, Na, Pr, Si, Zn) (Table 4).

pH (Appendix B: Table B01) – Lake pH values were significantly different ($p<0.05$; Table 3) in the Sparse Trees ecozone from those found in the Boreal Forest and Arctic Tundra ecozones. pH was not significantly correlated with any other environmental parameters (Table 4). There is a trend of increasing pH values from South to North (Figure 2d) with some exceptions (P27-1, P39-1, P46-1, P47-1). The pH range (6.3 to 7.4 with a median of 7.0) (Table B03) is smaller than that recorded by in previous studies (Rühland et al. 2003). Interestingly, a circum-neutral pH (range = 6.75 – 7.68) was recorded in all 'problem lakes' (P26-1, P27-1, & P33-1).

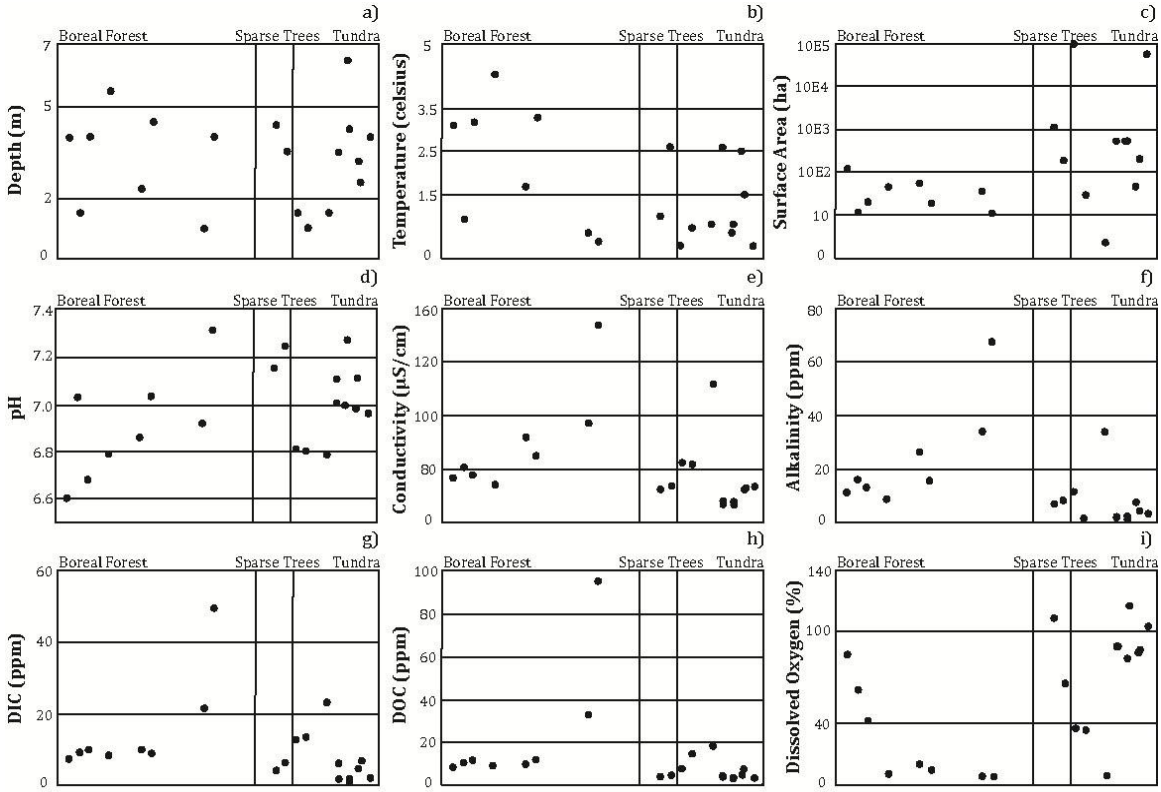

Figure 2. Trends in selected variables across ecozones. Sites are placed in latitudinal order along the x-axis, with the leftmost site being the sourthern most. Sites are classified into ecozones along the x-axis, the value of the measured environmental variable for each lake is given along the y-axis.

Trends in conductivity, alkalinity, and DIC (Appendix B: Table B01) - Lake water conductivity measurements show dilute waters that vary from 8 µS cm^{-1} to 93 µS cm^{-1}. Tundra lakes have a median conductivity of 12.75 µS cm^{-1} (range = 8 to 64.2), lakes in the Sparse Trees zone have a median conductivity of 16.5 µS cm^{-1} (range = 13.5 to 17.1), and lakes in the Boreal Forest zone have a median conductivity of 26.8 µS cm^{-1} (range = 12.8 to 93). The highest conductivity measured was in lake P40-1 (median = 93 µS cm^{-1}). There were no significant differences ($p<0.05$; Table 3) in conductivity levels between ecozones, although differences between the Boreal Forest and Sparse Trees ecozone did approach it ($p=0.0567$). Conductivity shows positive correlations at the $p<0.01$ level with alkalinity, DIC, DOC, and various dissolved elements (Al, As, B, Ba, Ca, Ce, Cl, Fe, K, Li, Mg, Mn, Na, Pr, Si, Zn). Rühland et al. (2003) found that conductivity was positively correlated with Ca, Mg, Na, K, Cl, DIC. We found a similar trend to that reported by Rühland et al. (2003), of increasing ionic concentrations from Arctic Tundra to Boreal forest lakes. Rühland et al. (2003) interpreted this as the result of more restricted groundwater flow in tundra lakes that restrict net yield of base cations. Soils are also poorly developed relative to sites in the Boreal forest. Decreasing ionic concentration with latitude is also reported in other limnological studies near the Canadian treeline (Pienitz et al., 1997a, b; Rühland and Smol, 1998; Duff et al., 1998; Fallu and Pienitz, 1999;

Table 4. Pearson Correlation matrix for measured environmental variables (following transformation) of the 18 lakeset. Light grey and dark grey indicate significant correlations at P <0.05 and P<0.01, respectively, based on Bonferroni-adjusted probabilities.

	DEPTH	*AREA*	*TEMP*	*pH*	*ALK*	*COND*	*DO*	*DIC*	*DOC*	*TP*	*TKN*	*NH3*	*Al*	*As*	*B*	*Ba*	*Ca*	*Ce*	*Cl*	*Cs*	*Cu*	*Fe*	*K*	*Li*	*Mg*	*Mn*	*Na*	*Pb*	*Pr*	*S*	*Si*	*U*	*Zn*
DEPTH	1.00																															
AREA	0.18	1.00																														
TEMP	0.52	-0.39	1.00																													
pH	0.07	0.07	-0.19	1.00																												
ALK	-0.64	-0.44	-0.01	-0.10	1.00																											
COND	-0.76	-0.48	-0.28	-0.18	0.84	1.00																										
DO	0.54	0.54	0.03	0.19	-0.73	-0.81	1.00																									
DIC	-0.72	-0.55	-0.06	-0.20	0.76	0.89	-0.77	1.00																								
DOC	-0.68	-0.60	-0.19	-0.11	0.73	0.90	-0.82	0.90	1.00																							
TP	0.13	-0.18	0.14	-0.26	0.34	0.29	-0.18	0.29	0.20	1.00																						
TKN	-0.10	-0.55	0.27	-0.16	0.58	0.48	-0.38	0.55	0.48	0.81	1.00																					
NH3	0.01	-0.45	0.33	0.09	0.55	0.32	-0.21	0.30	0.25	0.49	0.73	1.00																				
Al	-0.52	-0.61	-0.19	0.00	0.61	0.76	-0.86	0.72	0.88	0.11	0.36	0.10	1.00																			
As	-0.66	-0.44	-0.49	-0.03	0.48	0.81	-0.63	0.73	0.82	-0.01	0.14	0.00	0.76	1.00																		
B	-0.68	-0.54	-0.09	-0.34	0.73	0.90	-0.80	0.82	0.79	0.32	0.51	0.21	0.69	0.62	1.00																	
Ba	-0.80	-0.48	-0.34	-0.16	0.82	0.95	-0.80	0.89	0.91	0.20	0.45	0.26	0.80	0.85	0.80	1.00																
Ca	-0.74	-0.50	-0.23	-0.17	0.88	0.98	-0.81	0.90	0.90	0.33	0.57	0.41	0.76	0.75	0.87	0.95	1.00															
Ce	-0.60	-0.52	-0.21	-0.01	0.78	0.85	-0.90	0.78	0.88	0.22	0.47	0.27	0.94	0.71	0.77	0.87	0.88	1.00														
Cl	-0.69	-0.21	-0.28	-0.29	0.74	0.77	-0.39	0.62	0.58	0.24	0.32	0.42	0.29	0.56	0.61	0.70	0.74	0.44	1.00													
Cs	-0.56	-0.53	-0.23	0.02	0.29	0.48	-0.51	0.57	0.61	-0.18	0.09	-0.16	0.66	0.70	0.41	0.63	0.44	0.51	0.15	1.00												
Cu	-0.37	-0.33	-0.21	-0.20	0.34	0.54	-0.55	0.56	0.66	0.13	0.18	0.04	0.61	0.65	0.47	0.59	0.50	0.59	0.32	0.47	1.00											
Fe	-0.61	-0.61	-0.29	-0.05	0.67	0.85	-0.79	0.76	0.85	0.17	0.39	0.16	0.93	0.85	0.76	0.87	0.84	0.92	0.49	0.62	0.56	1.00										
K	-0.74	-0.47	-0.32	-0.17	0.79	0.98	-0.76	0.86	0.89	0.31	0.47	0.30	0.73	0.82	0.88	0.91	0.96	0.82	0.77	0.45	0.63	0.83	1.00									
Li	-0.70	-0.57	-0.33	-0.02	0.57	0.87	-0.64	0.82	0.86	0.09	0.29	0.12	0.72	0.93	0.75	0.86	0.82	0.70	0.60	0.71	0.59	0.82	0.89	1.00								
Mg	-0.75	-0.51	-0.28	-0.15	0.80	0.99	-0.84	0.89	0.90	0.25	0.44	0.28	0.78	0.84	0.90	0.94	0.97	0.85	0.72	0.53	0.55	0.86	0.97	0.90	1.00							
Mn	-0.50	-0.62	-0.05	-0.17	0.68	0.82	-0.78	0.83	0.82	0.25	0.49	0.31	0.79	0.78	0.70	0.87	0.82	0.81	0.50	0.54	0.55	0.86	0.76	0.76	0.82	1.00						
Na	-0.64	-0.52	-0.15	-0.21	0.86	0.94	-0.79	0.83	0.89	0.40	0.61	0.46	0.75	0.65	0.87	0.87	0.96	0.86	0.74	0.30	0.52	0.78	0.94	0.73	0.91	0.74	1.00					
Pb	-0.50	-0.49	-0.12	-0.20	0.60	0.65	-0.69	0.63	0.73	0.11	0.30	0.13	0.81	0.63	0.58	0.71	0.66	0.81	0.41	0.53	0.76	0.80	0.67	0.59	0.64	0.65	0.67	1.00				
Pr	-0.54	-0.48	-0.21	0.01	0.76	0.82	-0.87	0.73	0.82	0.25	0.47	0.28	0.92	0.67	0.72	0.82	0.86	0.99	0.42	0.43	0.53	0.91	0.79	0.64	0.82	0.78	0.84	0.79	1.00			
S	-0.59	-0.08	-0.41	0.00	0.40	0.63	-0.56	0.44	0.39	-0.02	-0.10	-0.16	0.38	0.57	0.63	0.54	0.52	0.45	0.42	0.38	0.32	0.50	0.62	0.62	0.68	0.40	0.42	0.30	0.42	1.00		
Si	-0.56	-0.76	0.07	-0.15	0.83	0.83	-0.87	0.83	0.89	0.29	0.63	0.42	0.88	0.62	0.80	0.84	0.87	0.91	0.50	0.56	0.49	0.85	0.79	0.69	0.82	0.81	0.87	0.77	0.88	0.30	1.00	
U	-0.14	-0.52	0.24	-0.20	0.65	0.51	-0.55	0.46	0.57	0.49	0.72	0.69	0.53	0.15	0.51	0.44	0.59	0.63	0.40	-0.04	0.27	0.47	0.49	0.20	0.46	0.43	0.75	0.51	0.65	-0.14	0.73	1.00
Zn	-0.58	-0.38	-0.17	-0.33	0.62	0.69	-0.77	0.70	0.72	0.30	0.44	0.05	0.76	0.55	0.77	0.73	0.71	0.80	0.36	0.46	0.67	0.74	0.70	0.54	0.70	0.64	0.71	0.78	0.77	0.38	0.74	0.48

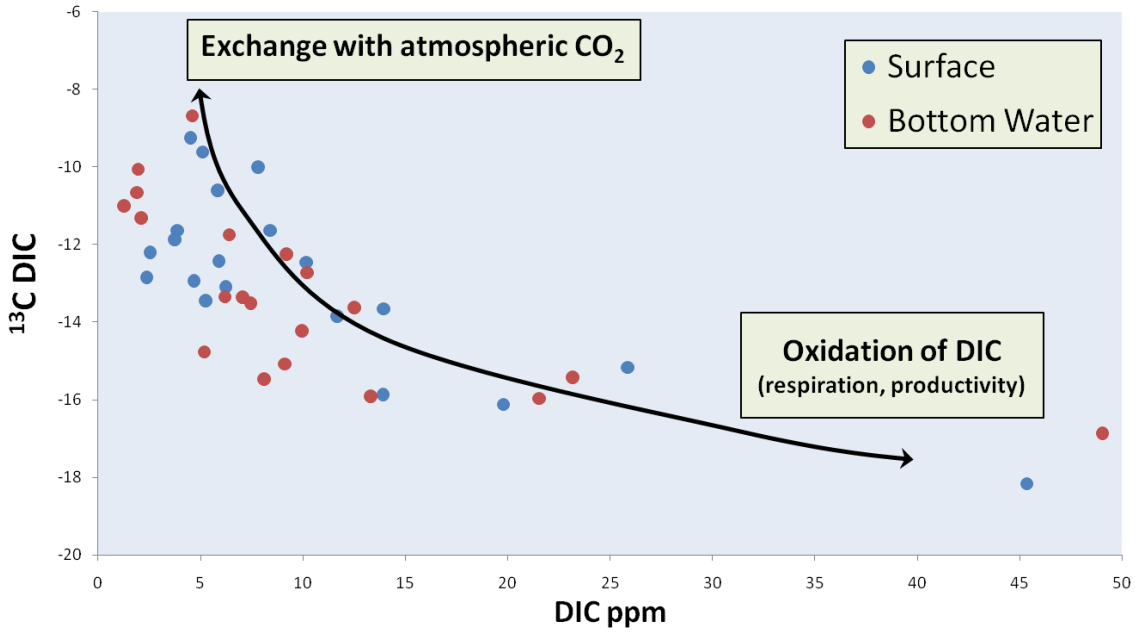

Figure 03. Scatterplot of ^{13}C DIC vs. DIC ppm with oxidation of DIC trendline. This figure illustrates that there is very little respiration or primary productivity during the winter. Lake P40-1 plots far to the right.

Gregory-Eaves et al., 2000; Fallu et al., 2002). Alkalinity values range from 2 to 72 ppm with a median of 9 ppm (Table B03). The difference in alkalinity values approach significance between the Boreal forest and Sparse Trees ecozones ($p=0.0549$) and the Arctic Tundra ecozones ($p=0.0544$) (Table 3). There is a slight trend for decreasing alkalinity values moving from south to north (Figure 2f), with some exceptions (P49-1, P51-1). Alkalinity is positively correlated at the $p<0.01$ level with conductivity, DIC, and various dissolved elements (B, Ba, Ca, Ce, Cl, K, Mg, Na, Pr, Si), at the $p<0.05$ level with Fe and Mn (Table 4). Alkalinity is negatively correlated with dissolved oxygen ($p<0.01$; Table 4). The strong correlation of conductivity and alkalinity can be interpreted as these lakes representing closed systems. DIC ranges from 2.4 to 49 ppm with a median of 7.8 ppm, with similar values seen in surface and bottom water samples (Table B03). DIC did not show significant difference in values across the three ecozones ($p<0.05$; Table 3). There appears to be homogeneity in values for DIC with a few exceptions (P34-2, P49, P51) (Figure 2g). DIC displays a negative correlation to depth and dissolved oxygen ($p<0.05$ & 0.01, respectively), a positive correlation at the $p<0.01$ level with alkalinity, conductivity, DOC, and various dissolved elements (As, B, Ba, Ca, Ce, Fe, K, Li, Mg, Mn, Na, Pr, Si) and at the $p<0.05$ level with Al and Zn. Dissolved inorganic carbon (DIC) and dissolved organic carbon (DOC) can be used to interpret the state of organics, respiration of organisms and the overall mixing within a lake. This sub-set of lakes is generally well-mixed, with little to no respiration by organisms (Figure 03).

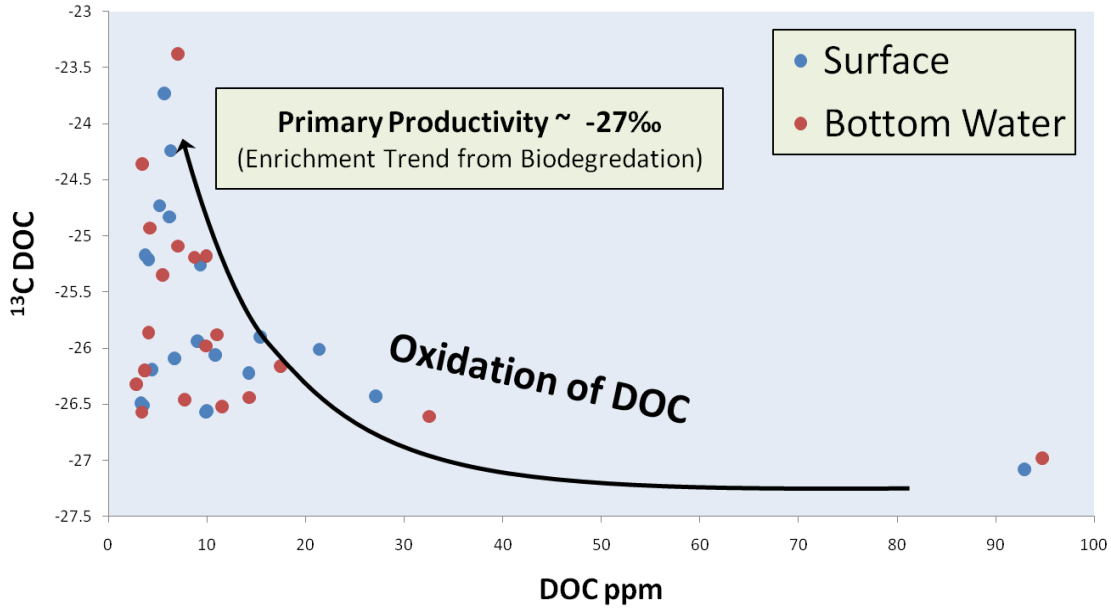

Figure 04. Scatterplot of ^{13}C DOC vs. DOC ppm with oxidation of DOC trendline. This figure illustrates that there is enrichment due to the biodegradation of organics within the lakes. Lake P40-1 plots away from the main cluster of samples.

Trends in DOC – DOC values range from 2.8 to 94.7 ppm and have a median of 7.4 ppm (Table BO3), with surface and bottom water samples showing similar values. DOC did not show significant difference in values across the three ecozones ($p<0.05$; Table 3), although Boreal Forest δ ^{13}C DOC values are significantly different from Sparse Trees sites ($p<0.05$; Table 3) and approach significance in their differences from Arctic Tundra sites ($p=0.0755$). DOC displays a negative correlation to depth and dissolved oxygen ($p<0.05$ & 0.01, respectively), a positive correlation at the $p<0.01$ level with conductivity, DIC, and various dissolved elements (Al, As, B, Ba, Ca, Ce, Fe, K, Li, Mg, Mn, Na, Pb, Pr, Si) and at the $p<0.05$ level with Cu and Zn. Dissolved inorganic carbon (DIC) and dissolved organic carbon (DOC) can be used to interpret the state of organics, respiration of organisms and the overall mixing within a lake. There is an enrichment trend due to the biodegradation of organics (Figure 03).

There appears to be a slight trend for lower values in the Arctic Tundra sites (4.8 ppm; Table B03) versus the Boreal Forest sites (10.5 ppm; Table B03), with a few exceptions (P34-2, P49, P51) (Figure 2h). Rühland et al. (2003) found similar results and attributed this to drainage of catchments with coniferous leaf litter, and wetlands bringing in high amounts of allochthonous DOC. They also found a relationship between water colour and DOC values. In our study, Lake P40-1, P49-1, and P55-1 all contained dark tea-coloured water. P40-1 does show extremely elevated DOC values compared to other study sites, while P49-1 shows only a slightly elevated value compared to other Arctic Tundra sites and P55-1 displays one of the lowest DOC values (Figure 2h). Two lakes with elevated DOC values P39-1 and P51-1 did not have tea-coloured water.

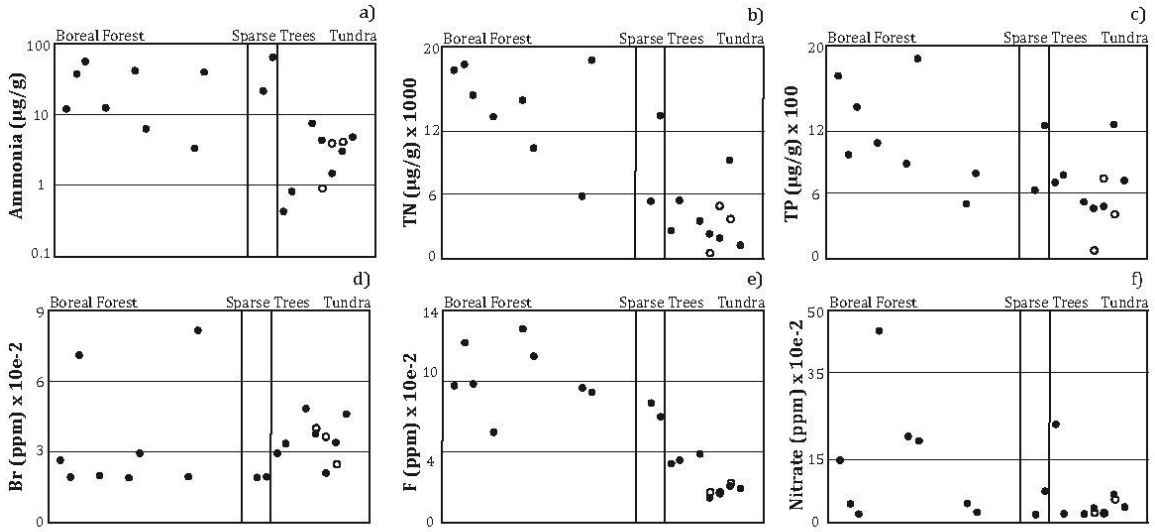

Figure 5. Trends in nutrients and selected anions across ecozones. Sites are placed in latitudinal order along the x-axis, with the leftmost site being the sourthern most. Sites are classified into ecozones along the x-axis, the value of the measured environmental variable for each lake is given along the y-axis. Open circles represent the second lake/site where two lakes/sites share the same portage (e.g. P54-1 closed, P54-2 open).

Trends in nutrients – Ammonia values ranged from 0.440 to 7.820 µg/g with a median of 3.595 µg/g (Table B03). There was a significant difference ($p<0.05$; Table 3) between Boreal Forest sites and Arctic Tundra sites. Ammonia is positively correlated with total kjeldahl nitrogen (TKN) ($p<0.01$; Table 4). There is a clear trend (Figure 5a) for higher ammonia values in Boreal Forest sites (median 26.050 µg/g) and lower values in the Arctic Tundra sites (median 3.595 µg/g). TKN values ranged from 438 to 18800 µg/g with a median of 5595 µg/g. There was a significant difference ($p<0.05$; Table 3) between Boreal Forest sites and Arctic Tundra sites. TKN is positively correlated with ammonia and total phosphorus (TP) ($p<0.01$; Table 4). There is a clear trend (Figure 5b) for higher TKN values in Boreal Forest sites (median 15200 µg/g), lower values in the Sparse Trees sites (median 9475 µg/g), and lowest values in the Arctic Tundra sites (median 3025 µg/g). TP values ranged from 85.9 to 1890 µg/g with a median of 777.5 µg/g. There was a significant difference ($p<0.05$; Table 3) between Boreal Forest sites and Arctic Tundra sites. TP is positively correlated with TKN ($p<0.01$; Table 4). There is a clear trend (Figure 5c) for higher TP values in Boreal Forest sites (median 1031.5 µg/g), lower values in the Sparse Trees sites (median 955 µg/g), and lowest values in the Arctic Tundra sites (median 633.5 µg/g).

All three nutrient parameters show clear trends (Figure 5a to c) of decreasing values from as one moves from south to north. Rühland et al. 2003 found similar results and thought that the higher nutrient values in the Boreal Forest sites was related to higher runoff, higher precipitation, dense vegetation, increased breakdown of terrestrial litter and a longer growing season in combination with warmer temperatures elevating primary productivity and intensifying nutrient circulation. While in the Arctic Tundra sites, shorter growing seasons, cooler conditions, restricted hydrological processes, continuous permafrost and

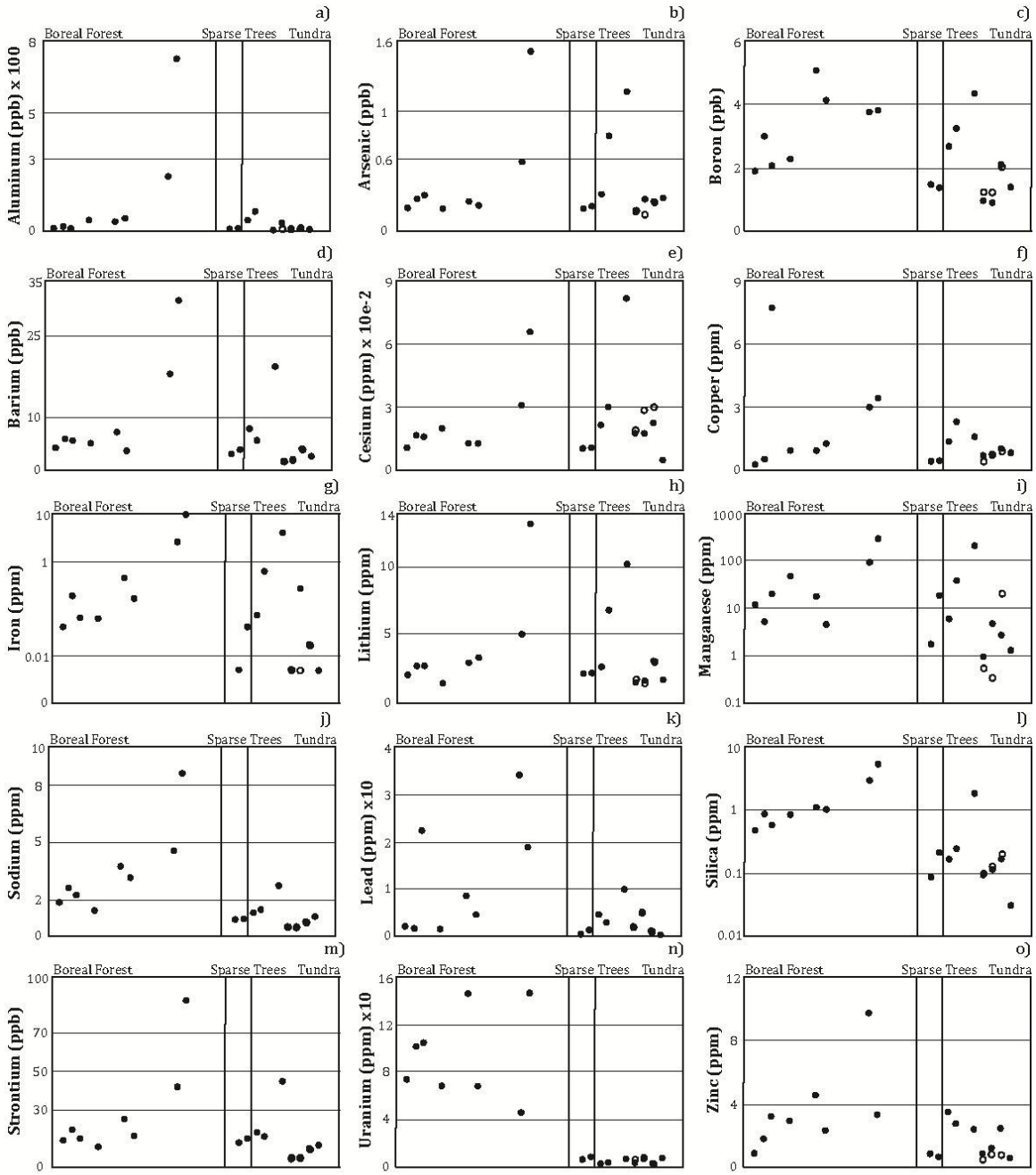

Figure 6. Trends in elements across ecozones. Sites are placed in latitudinal order along the x-axis, with the leftmost site being the sourthern most. Sites are classified into ecozones along the x-axis, the value of the measured environmental variable for each lake is given along the y-axis. Open circles represent the second lake/site where two lakes/sites share the same portage (e.g. P54-1 closed, P54-2 open).

diminished catchment-derived nutrients resulted in overall lower primary productivity (Rühland et al. 2003).

Trends in dissolved elements – Concentrations for most of the dissolved elements were within the ranges provided by the Canadian Council of Ministers of

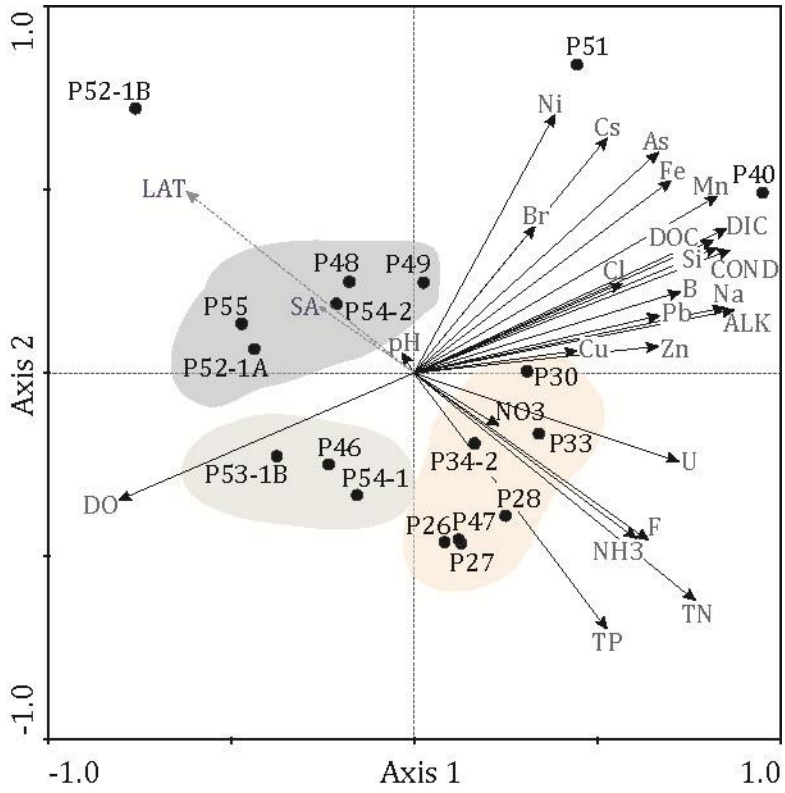

Figure 07. Principal components analysis (PCA) of March 2010 sediment-water interface samples and environmental parameters. Sample sites listed as portage numbers (i.e. P (ortage) 26). Environmental variables: ALK-alkalinity, DIC-dissolved inorganic carbon, DOC-dissolved organic carbon, DO-dissolved oxygen, Lat-latitude,, NH3-Ammonia, NO3-nitrite, TP-total phosphorus, TN-total nitrogen.

Environment (CCME, 2008), except for Fe concentrations (CCME guideline is 0.3 ppm) in P39, P40 and P51 which showed elevated concentrations (range = 2.5 to 9.5 ppm) (Table B02). These elevated Fe concentrations could be reflective of reducing conditions within these lakes (Davison, 1993). Reducing conditions are common in lakes which have low oxygen levels, are shallow, and have a substantial amount of organic matter that can be subjected to decomposition (Davison, 1993). P39, P40 and P51 show reduced oxygen levels (Table B01), and are shallow (Table C01). Further analysis will need to be done to see if the sediments are high in organic matter, and if these conditions are permanent or rather a function of the winter ice cover. F, B, Cl, Na, Pb, Si, U, Zn all showed significant differences in values between Boreal Forest sites and Sparse Trees sites (Table 3). Br, F, Cs, Cu, Ni, Zn all showed significant differences in values between Sparse Trees sites and Arctic Tundra sites (Table 3). F, B, Na, U all showed significant differences in values between Boreal Forest sites and Arctic Tundra sites (Table 3). Several dissolved elements displayed positive correlations amongst each other (Table 4). B, Fe, Mn, Na, Si, and U show trends from south to north of decreasing values (Figure 5). Several lakes always display higher values in comparison to lakes found close by (P39-1, P40-1, P51-1) (Figure 5).

Ordination (PCA) – Principal components analysis (PCA), a multivariate ordination technique, was used to interpret the major patterns of variation in the environmental data by examining the strengths of each variable in explaining the principal directions of variation for 18 of the 20 sites (duplicate sites from P49 and P53 were excluded since they showed similar values). Data was normalized using the natural log so that all environmental variables were comparable. PCA was carried out using the computer program CANOCO version 4.0 (ter Braak & Šmilauer1998). Since we were primarily interested in determining the interrelationships among the chemical and physical variables across the vegetational gradient, we treated latitude as a passive variable. The large differences in surface area between lakes also required that it too be run passively.

The study lakes in figure 07 cluster into three separate groups. Boreal Forest sites cluster together in lower right quadrant. These lakes are generally high in organics, and have moderate dissolved element concentrations. Of note is the relatively high concentration of uranium within these sites. A second grouping of sites in the lower left quadrant includes mostly Arctic Tundra sites. These lakes have low to moderate levels of nutrients but very dilute waters (low dissolved elements). The final grouping in the top left quadrant are Arctic Tundra sites that have very low nutrient values and low to moderate levels of dissolved elements. Overall all sites can be said to be relatively dilute, except for a few exceptions. Lakes P40 and P51 show relatively elevated dissolved element concentrations.

Surface Sediment Sampling

Twenty sediment-water interface samples were retrieved from eighteen lakes using the top sample from a Glew core (Glew, 2001) (Figure A01; Appendix C - Table C01). All sediment-water interface samples were surveyed for thecamoebians, diatoms, pollen and ostracods. All microfossils were present in abundance. Although present in the sediment-water interface samples, sediment cores were barren of ostracods. It is likely that acidification of sediments during decomposition of organic material dissolved the calcitic shells of ostracods. In northern lakes with high organic content and high concentrations of humic acids, it is unlikely that ostracods will be preserved in sedimentary successions.

These sediment-water interface samples will form part of a larger sampling training set (Summer 2009, Summer 2011, Winter 2012) that will form the basis both thecamoebian and diatom-based transfer functions.

Freeze Coring

Coring

Thirteen sediment cores from eighteen lakes were retrieved using the freeze corer, and the latitudinal transect along the TCWR was completed (Figure A01; Appendix C - Table C01). The latitudinal transect along the TCWR crosses three biogeographical zones and study sites are grouped accordingly: Boreal Forest (A: Figure A01 & Table C01), Sparse Trees (B: Figure A01 & Table C01), and Arctic Tundra (C: Figure A01 & Table C01). Sedimentary successions varying in length from 27.3 cm (P39-1) to 152.3 cm (P30-1) (median = 87.1 cm) were retrieved.

Sedimentological description & Core analysis

All core descriptions make reference to photos and X-Rays displayed in Appendix C (Table C01 & Figures C01–C27). Lake sediment-water interface was successfully captured in all freeze cores. Where the lake sediment-water interface is not a flat line, the middle point between its highest and lowest occurrence is used as the zero mark when measuring total core depth for descriptive purposes only.

ROAD10-BRIDGE1 (Appendix C: Table C01, Figure C01-02) – A freeze core was collected from P26-1 using the two-face freeze corer. The sediment-water interface was successfully captured on both faces. Face 1 was 60.9 cm in length and face 2 was 64.8 cm in length. The top 1 cm contained oxidized organic debris in a light grey/brown matrix (10yr 2/2). A gradual colour change to brown (10yr 2/1) takes place around 30 cm. There is a sharp colour change at 35.7 cm to light grey fine gray clay at (5y 3/2). X-Ray analysis reveals banding at the base of face 2 within the clay fraction. Face 2 captured a longer sequence of the clay interval than face 1. No sub-samples were sent radiocarbon dating.

ROAD10-BRIDGE2 (Appendix C: Table C01, Figure C03-04) - A freeze core was collected from P26-1 using the one-face freeze corer. The sediment-water interface was successfully captured. The core is 98.6 cm in length. The core is massive, with a gradual change from darker brown mud (10yr 2/1) to light brown mud (10yr 3/3) over the top 45.1 cm. There is colour change to lighter brown mud (2.5y 4/3) at 64.6 cm. There is a sharp transition to light grey (5y 3/2), fine grain mud at 79.1 cm. X-Ray analysis reveals little internal structure but does show that there is a density change that corresponds with the visual colour change. No sub-samples were sent radiocarbon dating.

Attempts by Dr. Graeme Swindles, Leeds University, UK, to isolate crypto-tephra in Road10-Bridge1 were unsuccessful. One cm sub-samples were analysed for the presence of cryptotephra following Turney (1998) and Swindles et al. (2010). It appears that the Bridge River and White River ash plumes were not deposited in Bridge Lake, despite reports of the latter visible in peatlands west of Yellowknife (Robinson, 2001).

ROAD10-PAT'S LAKE (Appendix C: Table C01, Figure C05-07) - A freeze core was collected from P30-1 using the one-face freeze corer. The sediment-water interface was successfully captured, although it must be noted that the interface for this lake is extremely soupy. The extremely high water content of the surface sediments of this lake makes it difficult to discern a true sediment-water interface. The core is 152.3 cm in length. The core is massive and made up of dark brown organic mud (10yr 2/1). X-Ray analysis reveals no internal structure that cannot be explained by artifacts of the analysis or coring procedure. No sub-samples were sent radiocarbon dating.

ROAD10-DANNY'S LAKE (Appendix C: Table C01, Figure C08-12) – A freeze core was collected from P34-2 using the two-face freeze corer. The sediment-water

interface was successfully captured on both faces. Face 1 is 118 cm in length and face 2 is 116.2 cm in length. Both faces show similar colour changes and are made up of similar sediment. The faces are massive and made up of fine organic mud. The upper 70cm are homogenous dark brown organic mud (10yr 2/2). The next 24.1 cm see several gradual colour changes from dark brown to a lighter brown/yellow (to 7.5yr 2.5/2 to 2.5y 3/2). A distinct colour change from (2.5y 3/2 to 2.5y 4/3) takes place at 93.9 cm in face one and at 90.6 in face two. An indistinct colour change takes place at the base from (2.5y 4/3 to 2.5y 2/1). X-Ray analysis reveals little internal structure but does show that there is a density change that corresponds with the distinct visual colour change.

Thirteen bulk material sub-samples have been submitted for radiocarbon dating (Table DO1). The age-model (Figure D01c) shows a roughly consistent sedimentation pattern over the last 8112 ^{14}C yr with one age reversal at the base of the core. The average sedimentation rate for this core is 0.01 cm/yr.

NOTE ON RADIOCARBON DATING FREEZE CORES IN NT - Chronological control is critical to establish sedimentation rates and estimating the temporal resolution of each sub-sample. Age-depth relationships of sediment cores were modeled using the Clam computer program (version 1.0.2; Blaauw, 2010; Appendix D – Figure D01). All radiocarbon ages were calibrated using the IntCal09 dataset (Reimer et al., 2009). An old carbon reservoir effect may occur in some of the lakes. We know the sediment-water interface to have been captured (visual determination), yet the radiocarbon-based age-depth models suggest that surface samples may be as much as 400 years old. Old-carbon may be derived from carbonates contained in glacially derived surficial geology in the central NT (Sutherland, 1980). An alternative hypothesis is that if ice froze to lake bottom, then recently accumulated sediments may be frequently disturbed. To address the discrepancy between our visual observations of sediment-water interface core capture and age-depth relationships based on radiocarbon, we are using 210-Pb dating, unaffected by reservoir effects, of upper sediments of cores.

ROAD10-39-1A (Appendix C: Table C01, Figure C13-14) – A freeze core was collected from P39-1 using the two-face freeze corer. The sediment-water interface was successfully captured on both faces. Face 1 is 27.3 cm in length and face 2 is 27.9 cm in length. Both faces are massive and made up of dark brown (2.5y 2.5/1) fine organic mud. X-Ray analysis reveals no internal structure that cannot be explained by artifacts of the analysis or coring procedure.

Three bulk material sub-samples have been submitted for radiocarbon dating (Table D01). The age-model (Figure D01d) shows that the top of this core is abnormally old (3597 ^{14}C yr at 10 cm). P39-1 is a very shallow lake 1 to 1.25 m in depth. Thus if this lake freezes to bottom during the winter surface sediments could be rafted to the surface, explaining the age of the top of the core.

ROAD10-39-1B (Appendix C: Table C01, Figure C15) – A freeze core was collected from P39-1 using the one-face freeze corer. The sediment-water interface was successfully captured. The core is 29.3 cm in length. The core is massive and made

up of dark brown (2.5y 2.5/1) fine organic mud. This core was not submitted for X-Ray analysis and no sub-samples were sent for radiocarbon analysis.

ROAD10-46-1 (Appendix C: Table C01, Figure C16-17) – A freeze core was collected from P46-1 using the two-face freeze corer. The sediment-water interface was successfully captured on both faces. Face 1 is 33.3 cm in length and face 2 is 36.9 cm in length. Both faces are massive, made up of fine organic mud, and show similar colour changes. The top 5 cm of the cores is made up of a dark grey/green algal mix (2.5y 5/2) followed by an indistinct colour change to (5y 4/1). The rest of the cores show a gradual change to a lighter grey. At 12 cm there is an indistinct colour change to (5y 3/2), at 17 cm an indistinct change to (5y 4/1), and finally at 23 cm an indistinct change to (2.5y 4/1). The X-Ray reveals a slumping texture in the middle of face 2. From the left side to right side, there is a gradual incline with a sharp drop to the right visible in several layers. This may be due to topographic differences or as an artifact due to the coring method. No sub-samples were sent for radiocarbon analysis.

ROAD10-47-1 (Appendix C: Table C01, Figure C18) – A freeze core was collected from P47-1 using the one-face freeze corer. The sediment-water interface was successfully captured. The core is 85.7 cm in length. The entire core is massive and made up of light brown (2.5y 3/2) fine organic mud. X-Ray analysis reveals no internal structure that cannot be explained by artifacts of the analysis or coring procedure.

Four bulk material sub-samples have been submitted for radiocarbon dating (Table D01). The age-model (Figure D01e) shows that the top of this core is abnormally old (4218 ^{14}C yr at 13.5 cm). Unlike P39-1, P47-1 is not a very shallow lake at 4.85 m in depth (Table C01). It is a relative large lake (194.9 ha) compared to a lake like P34-2 (19.2 ha), and is also connected to an even larger lake P46-1 (1108.3). Thus the bottom sediments might be subjected to bottom currents that can develop through wind fetch in such large systems.

ROAD10-49-1A (Appendix C: Table C01, Figure C19) – A freeze core was collected from P49-1 using the two-face freeze corer. The sediment-water interface was successfully captured on both faces, but the interface on Face 1 shows a strong inclination. Face 1 is 70.8 cm in length and face 2 is 88.3 cm in length. Both faces are massive, made up of fine organic mud, and show similar colour changes. The majority of the faces is made up of brown mud (2.5y 3/2 and at the base of Face 2 there is a gradual colour change to a darker brown mud (2.5y 4/3). This core was not submitted for X-Ray analysis and no sub-samples were sent for radiocarbon analysis.

ROAD10-49-1B (Appendix C: Table C01, Figure C20-21) – A freeze core was collected from P49-1 using the one-face freeze corer. The sediment-water interface was successfully captured. The core is 111.2 cm in length. The entire core is massive and made up of light brown (2.5y 3/2) fine organic mud. There is a gradual transition from light to darker brown (2.5y 4/3) mud towards the base of the core.

X-Ray analysis reveals no internal structure that cannot be explained by artifacts of the analysis or coring procedure.

Three bulk material sub-samples have been submitted for radiocarbon dating (Table DO1). The age-model (Figure D01f) shows a roughly consistent sedimentation pattern over the last 5663 ^{14}C yr. The average sedimentation rate for this core is 0.02 cm/yr.

ROAD10-52-1 (Appendix C: Table C01, Figure C22-24) – A freeze core was collected from P52-1 using the two-face freeze corer. The sediment-water interface was successfully captured on both faces. Face 1 is 101.6 cm in length and face 2 is 104.7 cm in length. Both faces are massive and made up of fine organic mud. The upper 53 cm are homogenous dark brown organic (10yr 3/3) mud. The next 23 cm see a gradual colour change from dark brown to a lighter brown (2.5y 4/3). An indistinct colour change from (2.5y 4/3 to 2.5y 5/2) takes place at 76 cm. X-Ray analysis of face two reveals no internal structure that cannot be explained by artifacts of the analysis or coring procedure.

Seven bulk material sub-samples have been submitted for radiocarbon dating (Table DO1). The age-model (Figure D01g) shows a roughly consistent sedimentation pattern over the last 8011 ^{14}C yr. The average sedimentation rate for this core is 0.01 cm/yr.

ROAD10-ECHO (Appendix C: Table C01, Figure C25) – A freeze core was collected from P54-2 using the two-face freeze corer. The sediment-water interface was successfully captured on both faces. Face 1 is 87.7 cm in length and face 2 is 86.5 cm in length. Both faces are massive, poorly sorted (mud-pebble), dark brown (2.5y 3/2) sediment. There is an indistinct transition from dark brown to light brown (10yr 3/3) towards the base of the core. This lake is located near an esker, a source of gravel for land portages, and is the likely source of gravel that may have been transported to the basin during periods of high runoff. This core was not submitted for X-Ray analysis and no sub-samples were sent for radiocarbon analysis.

ROAD10-LACDEGRAS (Appendix C: Table C01, Figure C26-27) – A freeze core was collected from P55-1 using the two-face freeze corer. The sediment-water interface was successfully captured on both faces, except face 1 shows a depression in the interface. Face 1 is 44.7 cm in length and face 2 is 49.2 cm in length. Face 1 appears to be distorted and could be due to the coring process. Face 2 shows several colour and stratigraphic changes. The upper 0.5 cm is composed of what appears to be oxidized orange/red (2.5yr 4/8) sediment. Several colour changes take place below this oxidized layer from a dark grey (2.5y 3/1) to: (2.5y 4/1) at 5 cm, (5y 5/1) at 8 cm, (2.5y 4/1) at 15.8 cm, (5y 4/1) at 17.4 cm, and (10yr 4/1) at 23 cm. Dark inclusions were noted at 17 and 21 cm. Small black specks are noted throughout the core. X-Ray analysis of face 1 confirms that the sedimentary layers have been distorted, while X-Ray analysis of face 2 shows that the sedimentary layers have been preserved. Of note is distinct laminations at the base of the core.

Three bulk material sub-samples have been submitted for radiocarbon dating (Table DO1). The age-model (Figure D01h) is rather troublesome for this core, with an age reversal and a abnormally old age at the top of the core.

Conclusions

Eighteen lakes were investigated during the 2010 field season. Thirteen freeze cores, twenty sediment-water interface samples, and twenty-one surface and bottom water samples were collected. Water quality data and vertical temperature-dissolved depth profiles were generated for each study site. Water quality data shows similar trends to a previous study by Rühland et al. (2003).The latitudinal transect along the Tibbitt to Contwoyto Winter Road was successfully completed. We now have data collected from lakes that span from latitude N62°27.600 to latitude N64°25.794 and from longitude W109°59.921 to longitude W114°43.603 in the central NT.

Sedimentological description and X-Ray imaging demonstrate that the majority of sediment cores exhibit a massive sedimentological structure, consist of fine organic mud with both abrupt and gradual colour changes, and show little density variation. No varves or annual layering was observed. Age modelling of a subset of the freeze cores confirms that there are lakes that will be suitable for high resolution paleoclimatic reconstruction. Material collected during the 2010 field program is being used to meet the mandates of on-going research programs. Sediment-water interface samples will be combined with samples collected during August 2011 and during future field expeditions and from the basis of both thecamoebian and diatom based transfer functions.

References

Blass A., Bigler C., Grosjean, M., and Sturm, M., 2007. Decadal-scale autumn temperature reconstruction back to AD 1580 inferred from the varved sediments of Lake Silvaplana (southeastern Swiss Alps); Quaternary Research, v. 68, p. 184-195.

Blaauw, M., 2010. Methods and code for 'classical' age-modelling of radiocarbon sequences; Quaternary Geochronology, v. 5(5), p. 512-518.

Booth, R., 2001. Ecology of testate amoebae (Protozoa) in two Lake Superior coastal wetlands: Implications for paleoecology and environmental monitoring; Wetlands, v. 21, p. 564-576.

Canadian Council of Ministers of Environment, 2008. Canadian water quality guidelines. Retrieved January 16, 2012, from Canadian Council of Ministers of Environment Web site: www.ccme.ca/publicationsarchives.html

Chen, J., Wan, G., Zhang, D.D., Zhang, F., Huang R., and 2004. Environmental records of lacustrine sediments in different time scales: Sediment grain size as an example. Science in China Series D: Earth Sciences 47 (10):954-60.

Conroy, J.S., Overpeck, J.T., Cole, J.E., Shanahan, T.M., and Steinitz-Kannan, M., 2008. Holocene changes in eastern tropical pacific climate inferred from a Galapagos lake sediment record. Quaternary Science Reviews, v. 27 (11-12), p. 1166-80.

Dallimore, A., Schröder-Adams, C.J., Dallimore, S.R., 2000. Holocene environmental history of thermokarst lakes on Richards Island, Northwest Territories, Canada: Thecamoebians as paleolimnological indicators; Journal of Paleolimnology, v. 23(3), p. 261-283.

Davison, W., 1993. Iron and manganese in lakes; Earth-Science Reviews, v. 34 (2), p. 199 – 163.

Duff, K.E., Laing, T.E., Smol, J.P., and Lean, D.R.S., 1998. Limnological characteristics of lakes located across arctic treeline in Northern Russia; Hydrobiologia, v. 391, p. 205-222.

Fallu, M.A. and Pienitz, R., 1999. Diatomeés lacustres de Jamésie-Hudsonie (Québec) et modèle de reconstitution des concentrations de carbone organique dissous; Ecoscience, v. 6, p. 603-620.

Fallu, M.A., Allaire, N., Pienitz, R., 2002. Distribution of freshwater diatoms in 64 Labrador (Canada) lakes: species-environment relationships along latitudinal gradients and reconstruction models for water colour and alkalinity; Canadian Journal of Fisheries and Aquatic Science, v. 59, p. 329-349.

Francus, P., Bradley, R.S., and Thurow, J., 2004. An introduction to image analysis, sediments and paleoenvironments; In: Francus, P. (eds). Image analysis, sediments, and paleoenvironments, v. 7, p. 1-7.

Galloway, J.M., Macumber, A., Patterson, R.T., Falck, H., Hadlari, T., and Madsen, E., 2010. Paleoclimatalogical assessment of the southern Northwest Territories and implications for the long-term viability of the Tibbitt to Contwoyto winter road, part I: Core collection; Northwest Territories Geoscience Office, Report # 2010-002.

Glew, J.R., 1991. Miniature gravity corer for recovering short sediment cores; Journal of Paleolimnology, v. 5, p. 285-287.

Glew, J.R., Smol, J.P., Last, W.M., 2001. Sediment core collection and extrusion; In: Last W.M., Smol J.P. (eds). Tracking environmental changes using lake sediments: Volume 1: Basin analysis, coring and chronological techniques; Kluwer Academic Publishers, Dordrecht, p. 73-106.

Gregory-Eaves, I., Smol, J.P., Finney, B.P., Lean, D.R.S., and Edwards, M.E., 2000. Characteristics and variation in lakes along a north-south transect in Alaska; Archives of Hydrobiology, v. 147, p. 193-223.

Huang, C.C., MacDonald, G., and Cwynar, L., 2004. Holocene landscape development and climatic change in the low arctic, northwest territories, Canada; Palaeogeography, Palaeoclimatology, Palaeoecology, v. 205(3-4), p. 221-234.

Kirby, M.E., Lund, S.P., Patterson, W.P., Anderson, M.A., Bird, B.W., Ivanovici, L., Monarrez, P., and Nielsen, S., 2010. A Holocene record of Pacific Decadal Oscillation (PDO)-related hydrologic variability in southern California (Lake Elsinore, CA); J Paleolimnol., v. 44, p. 819-839.

Kliza, D.A. and Schröeder-Adams, C.J., 1999. Holocene thecamoebians in freshwater lakes on Bylot Island, Northwest Territories, Canada; Journal of Foraminifera Research, v. 29, p. 26-36.

Kulbe, T., Niederreiter Jr, R., 2003. Freeze coring of soft surface sediments at a water depth of several hundred meters. Journal of Paleolimnology, v. 29, p. 257-263.

Lotter, A.F., Renberg, I., Hansson, H., Stöckli, R., and Sturm, M., 1997. A remote controlled freeze corer for sampling unconsolidated surface sediments. Aquatic Sciences, v. 59, p. 295-303.

MacDonald, G.M., Edwards, T.W.D., Moser, K.A., Pienitz, R., and Smol, J.P., 1993. Rapid response of treeline vegetation and lakes to past climate warming; Nature, v. 361(6409), p. 243.

MacDonald, G., Porinchu, D., Rolland, N., Kremenetsky, K., and Kaufman, D., 2009. Paleolimnological evidence of the response of the central Canadian treeline zone to radiative forcing and hemispheric patterns of temperature change over the past 2000 years; Journal of Paleolimnology, v. 41(1), p. 129-141.

Macumber, A.L., Patterson, R.T., Neville, L.A., and Falck, H., 2011. A sledge microtome for high resolution subsampling of freeze cores; Journal of Paleolimnology, v. 45, p. 307-310.

McCarthy, F.M.G., Collins, E.S., McAndrews, J.H., Kerr, H.A., Scott, D.B., and Medioli, F.S., 1995. A comparison of postglacial arcellacean ("thecamoebian") and pollen succession in Atlantic Canada, illustrating the potential of arcellaceans for paleoclimatic reconstruction; Journal of Paleontology, v. 69(5), p. 980-993.

McNeely, R.N., Neimanis ,V.P., and Dwyer, L., 1979. *Water quality sourcebook: A guide to water quality parameters*. -Water Quality Branch, Inland Waters Directorate, Environment Canada, Ministry of Supply and Services, Ottawa, Canada: 88 pp.

Moser, K.A. and MacDonald, G.M., 1990. Holocene vegetation change at treeline north of Yellowknife, Northwest Territories, Canada; Quaternary Research, v. 34(2), p. 227-239.

Neville, L.A., McCarthy, F.M.G., and MacKinnon, M.D., 2010. Seasonal environmental and chemical impact on thecamoebian community composition in an Oil Sands reclamation wetland in Northern Alberta; Palaeontologia Electronica, v. 13(13A), 14p.

Patterson, R.T., MacKinnon, K.D., Scott, D.B., Medioli, F.S., 1985. Arcellaceans (thecamoebians) in small lakes of New Brunswick and Nova Scotia: Modern distribution and Holocene stratigraphic change; Journal of Foraminiferal Research, v. 15, p. 114-137.

Pienitz, R., Smol, J.P., and Lean, D.R., 1997a. Physical and chemical limnology of 24 lakes located between Yellowknife and Contwoyto Lake, Northwest Territories (Canada); Canadian Journal of Fisheries and Aquatic Sciences, v. 54(2), p. 347-358.

Pienitz, R., Smol, J.P., and Lean, D.R.S., 1997b. Physical and chemical limnology of 59 lakes located between the southern Yukon and the Tuktoyaktuk Peninsula, Northwest Territories (Canada); Canadian Journal of Fisheries and Aquatic Sciences, v. 54, p. 330-346.

Pienitz, R., Smol, J.P., and MacDonald, G.M., 1999. Paleolimnological reconstruction of Holocene climatic trends from two boreal treeline lakes, Northwest Territories, Canada; Arctic, Antarctic, and Alpine Research, v. 31(1), p. 82-93.

Reimer, P.J., Baillie, M.G.L., Bard, E., Bayliss, A., Beck, J.W., Blackwell, P.G., Bronk Ramsey, C., Buck, C.E., Burr, G.S., Edwards, R.L., Friedrich, M., Grootes, P.M., Guilderson, T.P., Hajdas, I., Heaton, T.J., Hogg, A.G., Hughen, K.A., Kaiser, K.F., Kromer, B., McCormac, F.G., Manning, S.W., Reimer, R.W., Richards, D.A., Southon, J.R., Talamo, S., Turney, C.S.M., van der Plicht, J., and Weyhenmeyer, C.E., 2009. IntCal09 and Marine09 radiocarbon age calibration curves, 0-50,000 years cal BP; Radiocarbon, v. 51, p. 1111-1150.

Robinson, S.D., 2001. Extending the Late Holocene White River Ash distribution, Northwestern Canada; Arctic, v. 54, p. 157-161.

Roe, H.M., Patterson, R.T., and Swindles, G.T., 2010. Controls on the contemporary distribution of lake thecamoebians (testate amoebae) within the Greater Toronto Area and their potential as water quality indicators; Journal of Paleolimnology, v. 43, p. 955-975.

Rühland, K. and Smol, J.P., 1998. Limnological characteristics of 70 lakes spanning Arctic treeline from Coronation Gulf to Great Slave Lake in the central Northwest Territories, Canada; International Review of Hydrobiology, v. 83, p. 183-203.

Rühland, K.M., Smol, J.P., Wang, X., and Muir, D.C.G., 2003. Limnological characteristics of 56 lakes in the central Canadian arctic treeline region; Journal of Limnology, v. 62(1), p. 9-27.

Rühland, K. and Smol, J.P., 2005. Diatom shifts as evidence for recent subarctic warming in a remote tundra lake, NWT, Canada; Palaeogeography, Palaeoclimatology, Palaeoecology, v. 226(1-2), p. 1-16.

Schnurrenberger, D., Russell, J., and Kelts, K., 2003. Classification of lacustrine sediments based on sedimentary components; Journal of Paleolimnology, v. 29, p. 141-154.

St-Jean, G., 2003. Automated quantitative and isotopic (13C) analysis of dissolved inorganic carbon and dissolved organic carbon in continuous-flow using a total organic carbon analyser. Rapid Communication in Mass Spectrometry, v.17, p. 418-428.

Sun D., Bloemendal, J., Rea, D.K., Vandenberghe, J., Jiang, F., An, Z., and Su, R., 2002. Grain-size distribution function of polymodal sediments in hydraulic and Aeolian environments, and numerical partitioning of the sedimentary components; Sediment Geol, v. 152(3-4), p. 263-77.

Sunderland, D.G., 1980. Problems of radiocarbon dating deposits from newly deglaciated terrain: some examples from the Scottish Lateglacial; In: Lowe J.J., Gray J.M., and Robinson, J.E. (eds); Studies in the Lateglacial of North-West Europe, Oxford. Pergamon Press, p. 123 – 138.

Swindles, G.T., De Vleeschouwer, F., and Plunkett, G., 2010. Dating peat profiles using tephra: stratigraphy, geochemistry and chronology; Mires and Peat, v. 7, p. 1-9.

ter Braak, C.J.F., and Prentice, I.C., 1988. A theory of gradient analysis; Adv. Ecol. Res., v. 18, p. 271-317.

ter Braak, C.J.F., and Šmilauer. P., 1998. CANOCO for Windows (v. 4.0). Centre for Biometry, Wageningen, The Netherlands.

Turney, C.S.M., 1998. Extraction of rhyolitic component of Vedde microtephra from minerogenic lake sediments; Journal of Paleolimnology, v. 19, p. 199–206.

Watanabe, F.S. and Olsen, S.R, 1965. Test of an ascorbic acid method for determining phosphorus in water and $NaHCO_3$ extracts of soil. Soil Sci Soc Am Proc, v.29, p. 677–678.

Wolfe, A. and Härtling, J., 1996. The late quaternary development of three ancient tarns on southwestern Cumberland peninsula, Baffin Island, arctic Canada: Paleolimnological evidence from diatoms and sediment chemistry; Journal of Paleolimnology, v. 15(1), p. 1-18.

Zhou, Q., Gibson, C.E., and Zhu, Y., 2001. Evaluation of phosphorus bioavailability in sediments of three contrasting lakes in China and the UK. Chemosphere, v.42, p.221–225.

Appendix A: Maps

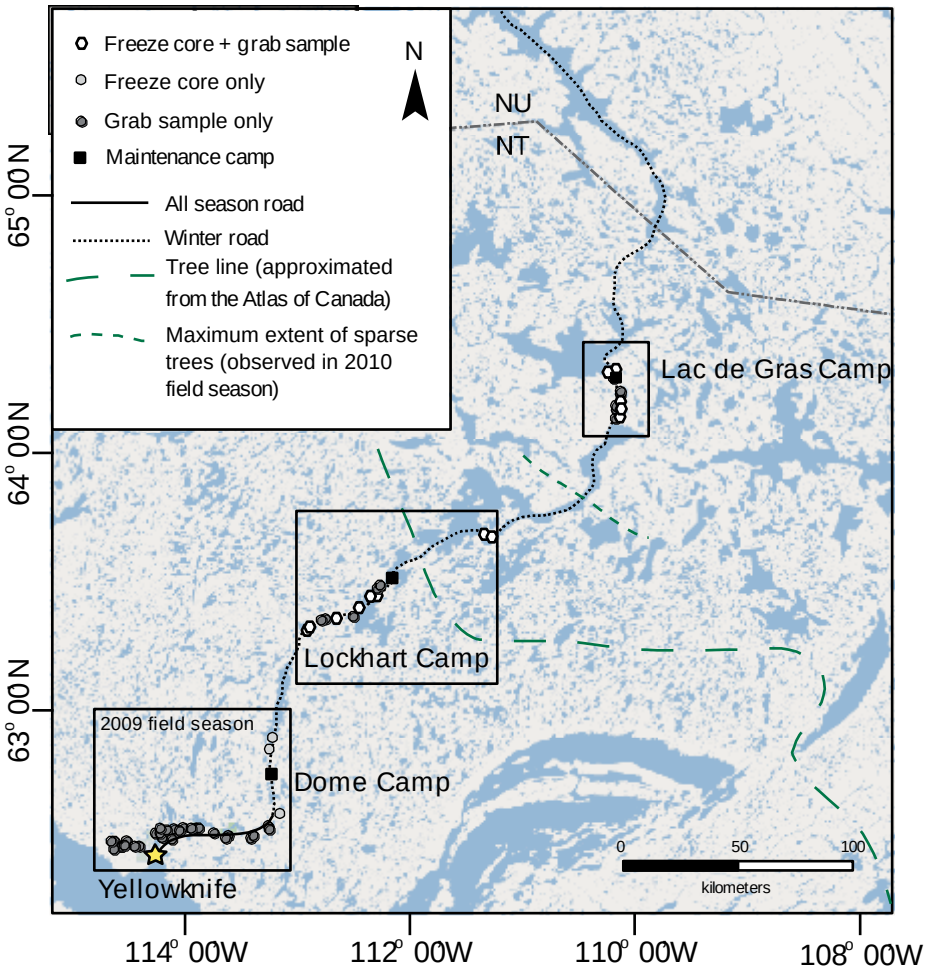

Figure A01 (shown again). Map showing sample locations and biogeographical regions: Boreal Forest (A), Sparse Trees (B), and Tundra (C) from the 2010 field season along the TCWR in the Northwest Territories as well as the 2009 field area near Yellowknife (map from Google Earth).

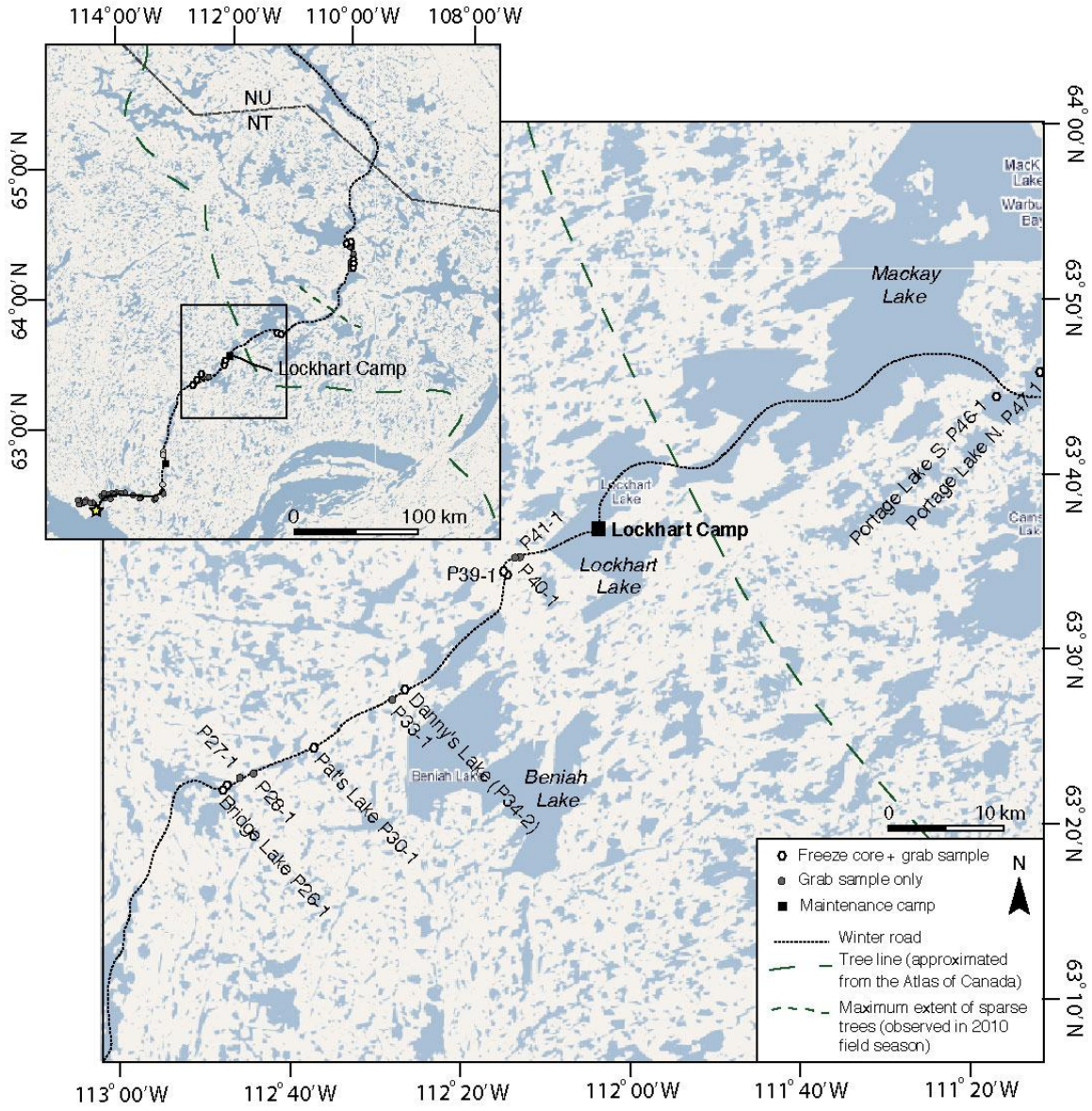

Figure A02. Map showing an enlargement of the area surrounding the Lockhart Camp. Coring sites from the 2010 field season are shown.

Figure A03. Map showing enlargement of the area surrounding Lac de Gras Camp. Coring sites from the 2010 field are shown.

Appendix B: Water Property Data

Figure B01. Temperature and dissolved oxygen depth profiles. Refer to Table B01 for data.

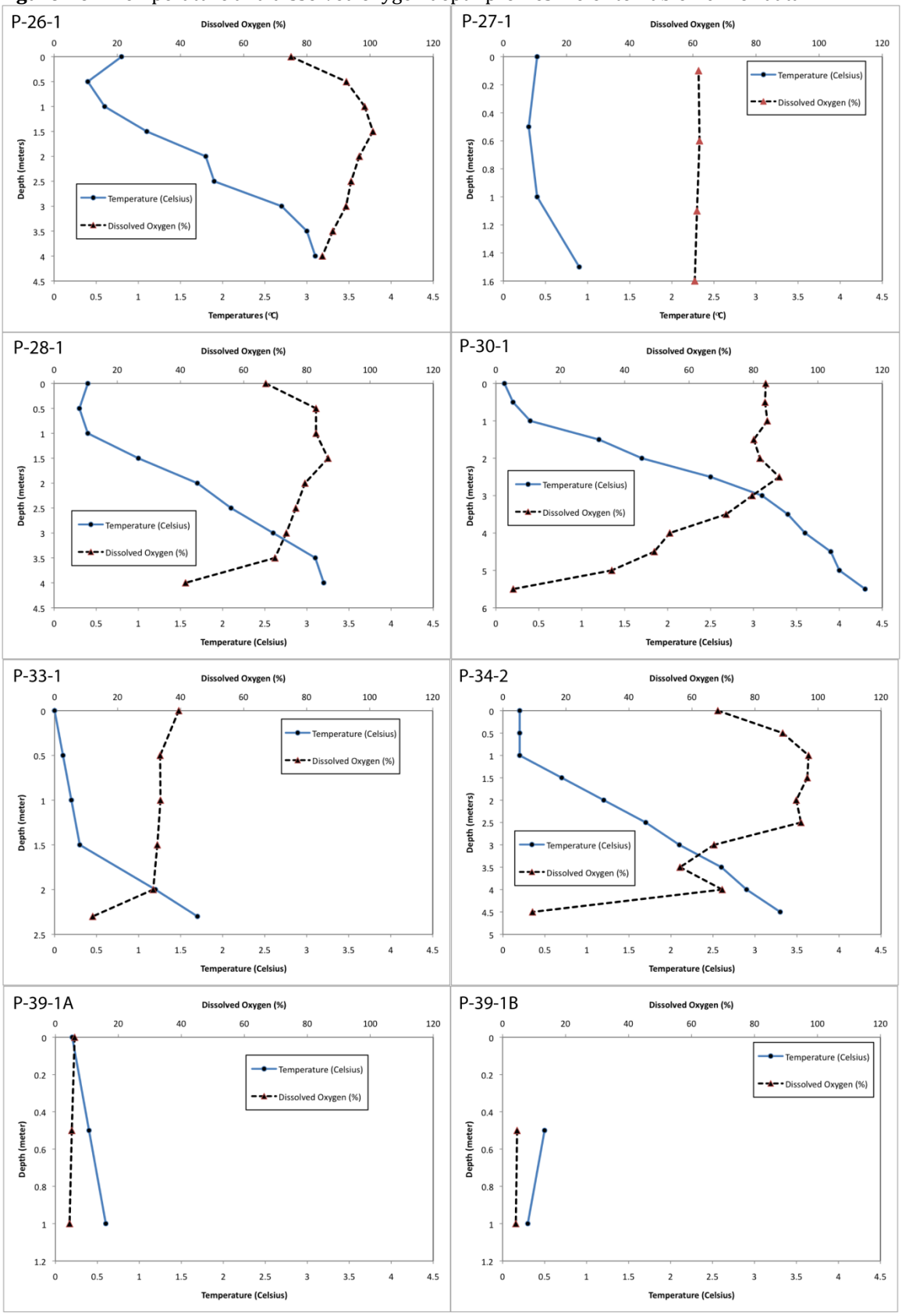

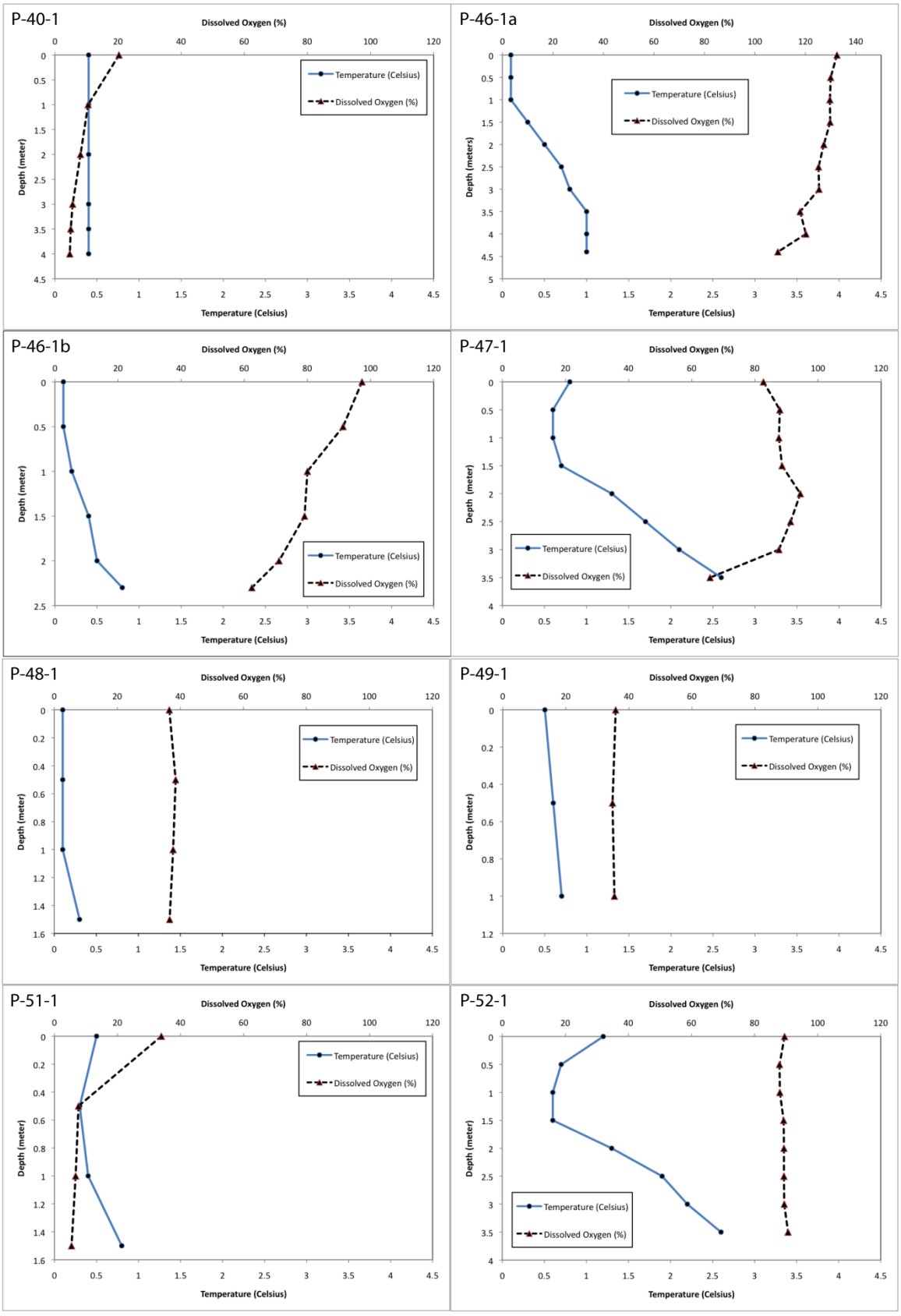
P-40-1
Dissolved Oxygen (%)
Depth (meter)
Temperature (Celsius)
Dissolved Oxygen (%)
Temperature (Celsius)
P-46-1a
Dissolved Oxygen (%)
Depth (meters)
Temperature (Celsius)
Dissolved Oxygen (%)
Temperature (Celsius)
P-46-1b
Dissolved Oxygen (%)
Depth (meter)
Temperature (Celsius)
Dissolved Oxygen (%)
Temperature (Celsius)
P-47-1
Dissolved Oxygen (%)
Depth (meter)
Temperature (Celsius)
Dissolved Oxygen (%)
Temperature (Celsius)
P-48-1
Dissolved Oxygen (%)
Depth (meter)
Temperature (Celsius)
Dissolved Oxygen (%)
Temperature (Celsius)
P-49-1
Dissolved Oxygen (%)
Depth (meter)
Temperature (Celsius)
Dissolved Oxygen (%)
Temperature (Celsius)
P-51-1
Dissolved Oxygen (%)
Depth (meter)
Temperature (Celsius)
Dissolved Oxygen (%)
Temperature (Celsius)
P-52-1
Dissolved Oxygen (%)
Depth (meter)
Temperature (Celsius)
Dissolved Oxygen (%)
Temperature (Celsius)

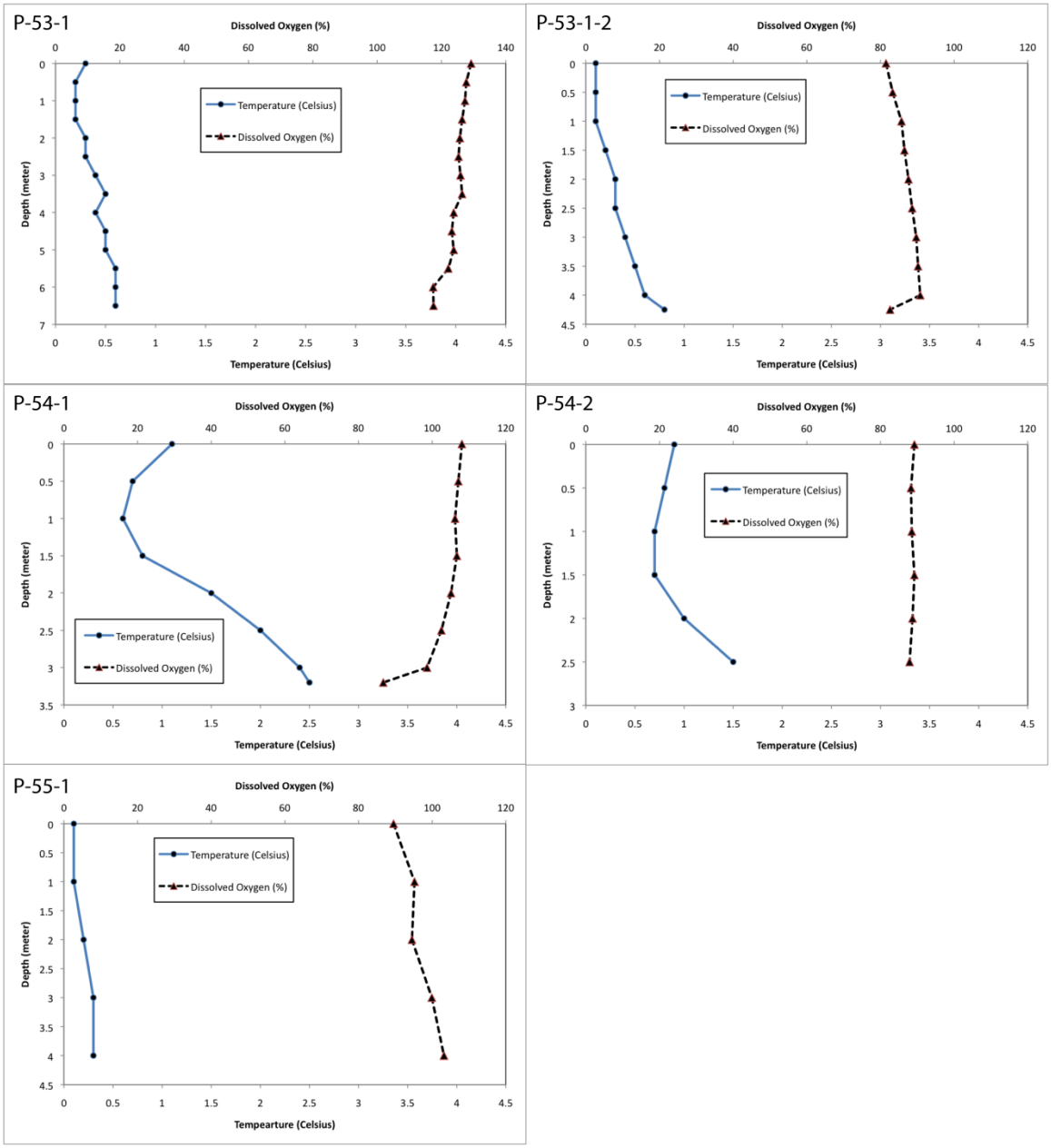
P-53-1
Dissolved Oxygen (%)
Temperature (Celsius)
Dissolved Oxygen (%)
Depth (meter)
Temperature (Celsius)
P-53-1-2
Dissolved Oxygen (%)
Temperature (Celsius)
Dissolved Oxygen (%)
Depth (meter)
Temperature (Celsius)
P-54-1
Dissolved Oxygen (%)
Temperature (Celsius)
Dissolved Oxygen (%)
Depth (meter)
Temperature (Celsius)
P-54-2
Dissolved Oxygen (%)
Temperature (Celsius)
Dissolved Oxygen (%)
Depth (meter)
Temperature (Celsius)
P-55-1
Dissolved Oxygen (%)
Temperature (Celsius)
Dissolved Oxygen (%)
Depth (meter)
Tempearture (Celsius)

Table B01. Water quality data. Units: meters (m), degrees Celsius (°C), percent (%), milligrams per liter (mg/L), microSiemens

Lake	Parameters		Depth (m) 0	0.5	1	1.5	2	2.5	3	3.5	4	4.5	5	5.5	6	6.5
Boreal Forest																
26.1	Temperature	(°C)	0.8	0.4	0.6	1.1	1.8	1.9	2.7	3	3.1					
	Dissolved Oxygen	(%)	75	92.5	98.3	100.9	96.6	94	92.4	88.2	84.9					
		(mg/L)	10.7	13.33	14.03	14.24	13.36	12.73	12.47	11.86	11.19					
	pH	(units)	7.68													
	Conductivity	(µS/cm)	18.7	18.7	18.9	18.7	18.5	18.5	18.5	18.5	18.7					
27.1	Temperature	(°C)	0.4	0.3	0.4	0.9										
	Dissolved Oxygen	(%)	60.6	61.3	62.1	61.8										
		(mg/L)	8.67	9.04	9.02	8.88										
	pH	(units)	7.29													
	Conductivity	(µS/cm)	26.8	25.2	24.9	25										
28.1	Temperature	(°C)	0.4	0.3	0.4	1	1.7	2.1	2.6	3.1	3.2					
	Dissolved Oxygen	(%)	67	82.9	82.9	86.7	79.4	76.5	73.5	69.9	41.6					
		(mg/L)	9.65	12.03	12.22	12.39	11	10.48	9.91	9.34	5.79					
	pH	(units)	7.28													
	Conductivity	(µS/cm)	18.6	19.1	19.5	19.8	19.8	20	20.1	20.3	20.9					
30.1	Temperature	(°C)	0.1	0.2	0.4	1.2	1.7	2.5	3.1	3.4	3.6	3.9	4	4.3		
	Dissolved Oxygen	(%)	83.8	83.6	84.3	80.1	82	88	79.6	71.5	54	49.2	36	5.4		
		(mg/L)	12.4	11.94	11.95	12.13	11.32	11.95	10.49	9.3	7.07	6.41	4.62	0.69		
	pH	(units)	7.14													
	Conductivity	(µS/cm)	14.9	14.8	14.8	14.8	14.7	14	14.8	15	15.5	16	16.5	19		
33.1	Temperature	(°C)	0	0.1	0.2	0.3	1.2	1.7								
	Dissolved Oxygen	(%)	39.4	33.5	33.6	32.6	31.3	12.1								
		(mg/L)	5.62	4.93	4.92	4.75	4.43	1.49								
	pH	(units)	6.75													
	Conductivity	(µS/cm)	33	33	32.8	33.2	35.2	45.8								
34.2	Temperature	(°C)	0.2	0.2	0.2	0.7	1.2	1.7	2.1	2.6	2.9	3.3				
	Dissolved Oxygen	(%)	68.2	88.8	97	96.6	93.1	94.6	67	56.2	69.6	9.4				
		(mg/L)	9.91	13.03	13.3	14.47	13.69	13.11	10.2	7.68	9.29	1.23				
	pH	(units)	6.61													
	Conductivity	(µS/cm)	12.8	22.7	27.4	27.4	27	27.1	27.3	27.4	28.2	32.8				
39.1	Temperature	(°C)	0.2	0.4	0.6											
	Dissolved Oxygen	(%)	6.1	5.2	4.5											
		(mg/L)	0.88	0.76	0.63											
	pH	(units)	6.31													
	Conductivity	(µS/cm)	43.9	43.7	44.2											
40.1	Temperature	(°C)	0.4	0.4	0.4	0.4	0.4	0.4								
	Dissolved Oxygen	(%)	20.3	10.5	8.1	5.6	5	4.7								
		(mg/L)	3.06	1.45	1.16	0.79	0.7	0.67								
	pH	(units)	6.41													
	Conductivity	(µS/cm)	93	95.3	95.1	95.7	95.9	95.9								
Sparse Trees																
46.1	Temperature	(°C)	0.1	0.1	0.1	0.3	0.5	0.7	0.8	1	1	1				
	Dissolved Oxygen	(%)	133	130	129.7	129.8	127.3	125.2	125.4	117.9	120.2	109				
		(mg/L)	19.3	19.04	19.03	18.94	18.43	17.99	18.01	16.76	17.14	16.2				
	pH		7.54													
	Conductivity	(µS/cm)	13.5	13.4	13.6	14.6	14.5	14.5	14.4	14.1	14.1	14.1				
47.1	Temperature	(°C)	0.8	0.6	0.6	0.7	1.3	1.7	2.1	2.6						
	Dissolved Oxygen	(%)	82.7	87.9	87.6	88.6	94.4	91.3	87.6	65.8						
		(mg/L)	12.1	12.74	12.77	12.74	13.24	12.64	12.08	9.07						
	pH		7.73													
	Conductivity	(µS/cm)	17.1	16.5	16.4	16.6	16.4	16.3	15.5	15.2						

Table B01 (cont.)

Lake	Parameters		Depth (m) 0	0.5	1	1.5	2	2.5	3	3.5	4	4.5	5	5.5	6	6.5
Tundra																
48.1	Temperature	(˚C)	0.1	0.1	0.1	0.3										
	Dissolved Oxygen	(%)	36.5	38.5	37.7	36.6										
		(mg/L)	5.29	5.61	5.45	5.34										
	pH		6.99													
	Conductivity	(µS/cm)	21.7	22.1	22	21.9										
49.1	Temperature	(˚C)	0.5	0.6	0.7											
	Dissolved Oxygen	(%)	35.8	34.8	35.4											
		(mg/L)	5.14	5.02	5.06											
	pH		7.7													
	Conductivity	(µS/cm)	21.9	21.9	22.4											
51.1	Temperature	(˚C)	0.5	0.3	0.4	0.8										
	Dissolved Oxygen	(%)	33.9	7.6	6.7	5.4										
		(mg/L)	4.41	1.08	0.93	0.75										
	pH		6.56													
	Conductivity	(µS/cm)	64.2	64.3	64.1	64.6										
52.1	Temperature	(˚C)	1.2	0.7	0.6	0.6	1.3	1.9	2.2	2.6						
	Dissolved Oxygen	(%)	89.5	87.9	88	89.2	89.3	89.3	89.4	90.6						
		(mg/L)	12.7	12.76	12.75	12.8	12.62	12.41	12.24	12.13						
	pH		7.7													
	Conductivity	(µS/cm)	12.1	12.6	12.6	12.6	12.4	12.1	12	11.8						
53.1A	Temperature	(˚C)	0.3	0.2	0.2	0.2	0.3	0.3	0.4	0.5	0.4	0.5	0.5	0.6	0.6	0.6
	Dissolved Oxygen	(%)	129	127.7	127.3	126.4	125.7	125.3	125.9	126.4	123.8	123	124	122	117	118
		(mg/L)	18.7	18.61	18.54	18.36	18.23	18.2	18.24	18.25	18.83	17.8	17.8	17.5	16.9	16.9
	pH		9.22													
	Conductivity	(µS/cm)	8.2	8	7.8	7.7	7.2	7.3	7.2	7	6.7	6.5	6.5	6.4	6.3	6.4
53.1B	Temperature	(˚C)	0.1	0.1	0.1	0.2	0.3	0.3	0.4	0.5	0.6	0.8				
	Dissolved Oxygen	(%)	81.5	83.3	85.7	86.5	87.6	88.6	89.7	90.2	90.8	82.6				
		(mg/L)	11.9	12.19	12.57	12.62	12.72	12.86	12.93	13	13.11	10.9				
	pH		7													
	Conductivity	(µS/cm)	8	8	7.9	7.7	7.6	7.5	7.2	7.1	7.3	9.7				
54.1	Temperature	(˚C)	1.1	0.7	0.6	0.8	1.5	2	2.4	2.5						
	Dissolved Oxygen	(%)	108	107.1	106.2	106.7	105.1	102.5	98.6	86.7						
		(mg/L)	15.3	15.4	15.34	15.17	14.65	14.07	13.32	11.11						
	pH		6.57													
	Conductivity	(µS/cm)	13.4	13.3	13.1	13.1	12.9	12.5	12.1	12						
54.2	Temperature	(˚C)	0.9	0.8	0.7	0.7	1	1.5								
	Dissolved Oxygen	(%)	89.2	88.3	88.5	89.2	88.7	87.9								
		(mg/L)	12.8	12.67	12.71	12.82	12.5	12.09								
	pH		7.11													
	Conductivity	(µS/cm)	11.8	11.7	11.6	11.6	11.9	11.8								
55.1	Temperature	(˚C)	0.1		0.1		0.2		0.3		0.3					
	Dissolved Oxygen	(%)	89.5		95.2		94.5		99.9		103.2					
		(mg/L)	13.3		13.97		13.29		14.51		14.98					
	pH		7.38													
	Conductivity	(µS/cm)	14		13.8		13.7		13.1		13.3					

Table BO2. ICP-MS and ICP-ES data from surface and bottom water samples.

LAKE	Al		As		B		Ba		Ce		Co		Cr	
	Top	Bottom	Top	Bottom	Top	Bottom	Top	Bottom	Top	Bottom	Top	Bottom	Top	Bottom
	(ppb)													
BOREAL FOREST														
26.1	11.300	10.000	0.240	0.190	2.350	1.915	3.370	4.440	0.052	0.046	0.025	0.025	0.140	0.145
27.1	18.500	17.900	0.265	0.260	3.050	2.970	6.290	5.890	0.145	0.140	0.025	0.025	0.185	0.180
28.1	18.850	16.100	0.260	0.300	2.140	2.070	5.810	5.600	0.133	0.129	0.052	0.053	0.220	0.200
30.1	61.800	50.000	0.220	0.180	2.290	2.280	4.030	5.150	0.376	0.303	0.025	0.172	0.230	0.220
33.1	35.500	38.800	0.200	0.240	4.405	5.080	5.785	6.970	0.464	0.520	0.057	0.071	0.245	0.280
34.2	55.700	51.950	0.240	0.215	5.030	4.165	3.820	3.815	0.444	0.439	0.025	0.025	0.300	0.240
39.1	231.400	227.900	0.550	0.580	3.120	3.780	17.220	17.710	2.212	2.265	0.936	0.796	0.790	0.800
40.1	732.800	727.350	1.560	1.510	3.910	3.835	32.010	31.580	6.141	6.051	4.384	4.409	1.800	1.775
MIN	11.300	10.000	0.200	0.180	2.140	1.915	3.370	3.815	0.052	0.046	0.025	0.025	0.140	0.145
MAX	732.800	727.350	1.560	1.510	5.030	5.080	32.010	31.580	6.141	6.051	4.384	4.409	1.800	1.775
MEDIAN	45.600	44.400	0.250	0.250	3.085	3.375	5.798	5.745	0.410	0.371	0.039	0.062	0.238	0.230
MEAN	145.731	142.500	0.442	0.434	3.287	3.262	9.792	10.144	1.246	1.236	0.691	0.697	0.489	0.480
SPARSE TREES														
46.1	7.200	2.500	0.250	0.180	2.275	1.490	3.880	3.190	0.126	0.029	0.025	0.025	0.050	0.050
47.1	11.650	6.300	0.240	0.190	1.925	1.370	4.510	3.760	0.178	0.072	0.068	0.059	0.100	0.100
MIN	7.200	2.500	0.240	0.180	1.925	1.370	3.880	3.190	0.126	0.029	0.025	0.025	0.050	0.050
MAX	11.650	6.300	0.250	0.190	2.275	1.490	4.510	3.760	0.178	0.072	0.068	0.059	0.100	0.100
MEDIAN	9.425	4.400	0.245	0.185	2.100	1.430	4.195	3.475	0.152	0.051	0.047	0.042	0.075	0.075
MEAN	9.425	4.400	0.245	0.185	2.100	1.430	4.195	3.475	0.152	0.051	0.047	0.042	0.075	0.075
ARCTIC TUNDRA														
48.1	17.400	14.100	0.380	0.310	2.790	2.690	8.220	7.720	0.255	0.174	0.420	0.231	0.130	0.140
49.1	47.550	46.000	0.850	0.800	3.165	3.280	5.900	5.620	0.178	0.122	0.358	0.362	0.330	0.310
51.1	89.700	79.800	1.220	1.170	4.780	4.350	19.850	19.440	0.508	0.466	2.627	2.499	0.670	0.630
52.1A	15.600	6.100	0.450	0.160	1.940	1.000	4.180	1.750	0.114	0.016	0.086	0.025	0.050	0.050
52.1B	13.600	6.800	0.320	0.170	1.660	1.200	2.590	1.800	0.082	0.018	0.025	0.025	0.050	0.050
53.1A	16.500	35.950	0.200	0.265	1.650	0.900	2.780	2.230	0.101	0.115	0.025	0.117	0.120	0.210
53.1B	8.300	6.250	0.210	0.140	1.390	1.225	2.960	2.265	0.051	0.020	0.025	0.025	0.050	0.050
54.1	11.050	7.700	0.290	0.230	2.420	2.010	4.495	3.930	0.042	0.023	0.025	0.025	0.115	0.100
54.2	17.400	7.650	0.530	0.240	2.430	2.075	3.920	3.960	0.085	0.029	0.087	0.127	0.050	0.050
55.1	4.400	2.400	0.550	0.250	1.460	1.370	3.170	2.800	0.036	0.015	0.025	0.025	0.050	0.050
MIN	4.400	2.400	0.200	0.140	1.390	0.900	2.590	1.750	0.036	0.015	0.025	0.025	0.050	0.050
MAX	89.700	79.800	1.220	1.170	4.780	4.350	19.850	19.440	0.508	0.466	2.627	2.499	0.670	0.630
MEDIAN	16.050	7.675	0.415	0.245	2.180	1.690	4.050	3.365	0.093	0.026	0.056	0.071	0.083	0.075
MEAN	24.150	21.275	0.500	0.374	2.369	2.010	5.807	5.152	0.145	0.100	0.370	0.346	0.162	0.164
FULL LAKESET														
MIN	4.400	2.400	0.200	0.140	1.390	0.900	2.590	1.750	0.036	0.015	0.025	0.025	0.050	0.050
MAX	732.800	727.350	1.560	1.510	5.030	5.080	32.010	31.580	6.141	6.051	4.384	4.409	1.800	1.775
MEDIAN	17.400	15.100	0.278	0.240	2.385	2.073	4.338	4.200	0.139	0.118	0.039	0.056	0.135	0.163
MEAN	71.310	68.078	0.451	0.379	2.709	2.453	7.240	6.981	0.586	0.550	0.466	0.456	0.284	0.282

Table BO2 (cont.)

LAKE	Cs		Cu		Gd		La		Li		Mn		Nd	
	Top	Bottom	Top	Bottom	Top	Bottom	Top	Bottom	Top	Bottom	Top	Bottom	Top	Bottom
								(ppb)						
BOREAL FOREST														
26.1	0.013	0.012	0.520	0.320	0.008	0.007	0.038	0.037	2.308	2.071	1.220	11.940	0.037	0.036
27.1	0.018	0.017	0.555	0.530	0.017	0.016	0.097	0.087	2.875	2.722	4.880	5.180	0.096	0.092
28.1	0.018	0.016	1.020	7.780	0.010	0.011	0.080	0.078	2.788	2.763	17.470	18.980	0.067	0.065
30.1	0.020	0.020	1.370	0.970	0.037	0.030	0.223	0.177	1.574	1.427	3.620	47.470	0.224	0.177
33.1	0.013	0.013	1.015	0.920	0.043	0.048	0.328	0.346	2.886	2.969	12.050	17.800	0.276	0.302
34.2	0.016	0.013	1.450	1.325	0.041	0.040	0.322	0.313	3.791	3.360	1.740	4.690	0.268	0.268
39.1	0.033	0.032	2.490	2.990	0.128	0.130	1.126	1.147	4.959	4.999	89.830	89.710	1.007	1.012
40.1	0.067	0.066	3.780	3.485	0.332	0.322	3.092	3.050	13.471	13.146	284.320	283.375	2.684	2.695
MIN	0.013	0.012	0.520	0.320	0.008	0.007	0.038	0.037	1.574	1.427	1.220	4.690	0.037	0.036
MAX	0.067	0.066	3.780	7.780	0.332	0.322	3.092	3.050	13.471	13.146	284.320	283.375	2.684	2.695
MEDIAN	0.018	0.017	1.195	1.148	0.039	0.035	0.273	0.245	2.880	2.866	8.465	18.390	0.246	0.222
MEAN	0.025	0.024	1.525	2.290	0.077	0.075	0.663	0.654	4.331	4.182	51.891	59.893	0.582	0.581
SPARSE TREES														
46.1	0.013	0.011	0.780	0.500	0.006	0.003	0.069	0.024	2.349	2.192	4.965	1.730	0.055	0.022
47.1	0.012	0.011	0.745	0.490	0.011	0.003	0.109	0.051	2.491	2.204	10.435	17.540	0.099	0.051
MIN	0.012	0.011	0.745	0.490	0.006	0.003	0.069	0.024	2.349	2.192	4.965	1.730	0.055	0.022
MAX	0.013	0.011	0.780	0.500	0.011	0.003	0.109	0.051	2.491	2.204	10.435	17.540	0.099	0.051
MEDIAN	0.012	0.011	0.763	0.495	0.009	0.003	0.089	0.038	2.420	2.198	7.700	9.635	0.077	0.036
MEAN	0.012	0.011	0.763	0.495	0.009	0.003	0.089	0.038	2.420	2.198	7.700	9.635	0.077	0.036
ARCTIC TUNDRA														
48.1	0.021	0.022	1.870	1.400	0.020	0.014	0.128	0.092	2.588	2.574	9.510	6.120	0.145	0.104
49.1	0.020	0.030	2.640	2.340	0.014	0.012	0.097	0.068	6.858	6.896	36.550	37.210	0.099	0.077
51.1	0.132	0.082	2.050	1.670	0.035	0.034	0.239	0.217	10.696	10.246	212.300	206.880	0.255	0.239
52.1A	0.017	0.019	1.240	0.780	0.009	0.003	0.061	0.005	2.689	1.523	5.100	0.930	0.058	0.010
52.1B	0.031	0.018	1.770	0.520	0.005	0.003	0.040	0.010	2.077	1.710	1.680	0.580	0.037	0.011
53.1A	0.015	0.018	1.210	0.825	0.007	0.016	0.056	0.055	1.922	1.470	1.530	4.670	0.052	0.064
53.1B	0.011	0.029	0.800	0.830	0.003	0.003	0.031	0.012	1.754	1.587	0.650	0.355	0.028	0.014
54.1	0.019	0.030	1.150	0.800	0.003	0.003	0.024	0.013	3.316	2.926	1.470	2.590	0.027	0.016
54.2	0.019	0.023	1.380	0.990	0.007	0.003	0.045	0.017	3.065	2.987	5.850	19.275	0.042	0.018
55.1	0.014	0.005	1.350	0.850	0.003	0.003	0.018	0.005	1.577	1.732	9.160	1.280	0.021	0.011
MIN	0.011	0.005	0.800	0.520	0.003	0.003	0.018	0.005	1.577	1.470	0.650	0.355	0.021	0.010
MAX	0.132	0.082	2.640	2.340	0.035	0.034	0.239	0.217	10.696	10.246	212.300	206.880	0.255	0.239
MEDIAN	0.019	0.022	1.365	0.840	0.007	0.003	0.051	0.015	2.639	2.153	5.475	3.630	0.047	0.017
MEAN	0.030	0.028	1.546	1.101	0.010	0.009	0.074	0.049	3.654	3.365	28.380	27.989	0.076	0.056
FULL LAKESET														
MIN	0.011	0.005	0.520	0.320	0.003	0.003	0.018	0.005	1.574	1.427	0.650	0.355	0.021	0.010
MAX	0.132	0.082	3.780	7.780	0.332	0.322	3.092	3.050	13.471	13.146	284.320	283.375	2.684	2.695
MEDIAN	0.018	0.019	1.295	0.885	0.010	0.011	0.088	0.062	2.739	2.648	5.475	9.030	0.082	0.064
MEAN	0.026	0.024	1.459	1.516	0.037	0.035	0.311	0.290	3.802	3.575	35.717	38.915	0.279	0.264

Table BO2 (cont.)

LAKE	Ni		Pb		Pr		Rb		Sm		Sr		U	
	Top	Bottom	Top	Bottom	Top	Bottom	Top	Bottom	Top	Bottom	Top	Bottom	Top	Bottom
								(ppb)						
BOREAL FOREST														
26.1	0.190	0.190	0.047	0.022	0.009	0.009	1.821	1.597	0.008	0.008	15.040	13.755	0.800	0.742
27.1	0.190	0.190	0.029	0.017	0.023	0.022	2.259	2.142	0.019	0.018	20.305	19.390	1.045	1.023
28.1	0.190	0.190	0.109	0.225	0.017	0.017	2.763	2.789	0.012	0.014	15.345	15.290	1.063	1.040
30.1	0.800	0.830	0.067	0.017	0.055	0.045	2.274	2.121	0.041	0.034	9.870	10.590	0.904	0.685
33.1	0.295	0.290	0.145	0.087	0.072	0.078	2.460	2.591	0.052	0.056	23.255	24.720	1.356	1.461
34.2	0.600	0.480	0.115	0.050	0.070	0.069	2.658	2.295	0.047	0.047	16.610	15.950	0.863	0.690
39.1	1.390	1.350	0.848	0.342	0.266	0.266	3.956	3.934	0.163	0.165	45.600	42.360	0.454	0.458
40.1	3.200	3.050	0.240	0.190	0.702	0.689	7.936	7.760	0.434	0.429	88.190	87.405	1.501	1.474
MIN	0.190	0.190	0.029	0.017	0.009	0.009	1.821	1.597	0.008	0.008	9.870	10.590	0.454	0.458
MAX	3.200	3.050	0.848	0.342	0.702	0.689	7.936	7.760	0.434	0.429	88.190	87.405	1.501	1.474
MEDIAN	0.448	0.385	0.112	0.068	0.063	0.057	2.559	2.443	0.044	0.040	18.458	17.670	0.974	0.883
MEAN	0.857	0.821	0.200	0.119	0.152	0.149	3.266	3.153	0.097	0.096	29.277	28.683	0.998	0.946
SPARSE TREES														
46.1	0.305	0.290	0.075	0.005	0.015	0.006	1.997	1.846	0.009	0.003	13.850	13.100	0.120	0.055
47.1	0.315	0.310	0.089	0.016	0.025	0.013	1.989	1.785	0.015	0.007	15.790	15.030	0.105	0.076
MIN	0.305	0.290	0.075	0.005	0.015	0.006	1.989	1.785	0.009	0.003	13.850	13.100	0.105	0.055
MAX	0.315	0.310	0.089	0.016	0.025	0.013	1.997	1.846	0.015	0.007	15.790	15.030	0.120	0.076
MEDIAN	0.310	0.300	0.082	0.011	0.020	0.009	1.993	1.816	0.012	0.005	14.820	14.065	0.113	0.065
MEAN	0.310	0.300	0.082	0.011	0.020	0.009	1.993	1.816	0.012	0.005	14.820	14.065	0.113	0.065
ARCTIC TUNDRA														
48.1	3.670	3.780	0.108	0.046	0.036	0.026	2.670	2.673	0.025	0.019	17.810	18.010	0.037	0.021
49.1	2.485	2.540	0.135	0.030	0.024	0.017	3.313	3.332	0.017	0.013	15.730	15.830	0.066	0.036
51.1	5.640	5.020	0.157	0.102	0.063	0.059	5.684	5.570	0.045	0.042	47.770	44.510	0.069	0.059
52.1A	0.550	0.250	0.107	0.018	0.014	0.003	1.775	1.072	0.010	0.003	9.310	4.640	0.047	0.060
52.1B	0.410	0.290	0.404	0.016	0.010	0.003	1.483	1.179	0.005	0.003	5.920	4.930	0.064	0.028
53.1A	0.540	0.430	0.077	0.051	0.013	0.027	1.545	1.134	0.009	0.023	6.280	4.755	0.059	0.057
53.1B	0.470	0.395	0.055	0.017	0.007	0.003	1.366	1.238	0.005	0.003	5.910	5.115	0.069	0.063
54.1	0.880	0.760	0.090	0.013	0.006	0.003	2.203	1.868	0.005	0.003	10.280	9.050	0.033	0.024
54.2	0.840	0.915	0.090	0.012	0.012	0.003	2.102	2.013	0.009	0.003	8.210	8.320	0.048	0.026
55.1	0.770	0.980	0.120	0.005	0.006	0.003	1.823	1.867	0.003	0.003	10.190	11.120	0.056	0.061
MIN	0.410	0.250	0.055	0.005	0.006	0.003	1.366	1.072	0.003	0.003	5.910	4.640	0.033	0.021
MAX	5.640	5.020	0.404	0.102	0.063	0.059	5.684	5.570	0.045	0.042	47.770	44.510	0.069	0.063
MEDIAN	0.805	0.838	0.108	0.018	0.012	0.003	1.963	1.868	0.009	0.003	9.750	8.685	0.057	0.047
MEAN	1.626	1.536	0.134	0.031	0.019	0.014	2.396	2.194	0.013	0.011	13.741	12.628	0.055	0.044
FULL LAKESET														
MIN	0.190	0.190	0.029	0.005	0.006	0.003	1.366	1.072	0.003	0.003	5.910	4.640	0.033	0.021
MAX	5.640	5.020	0.848	0.342	0.702	0.689	7.936	7.760	0.434	0.429	88.190	87.405	1.501	1.474
MEDIAN	0.575	0.455	0.108	0.020	0.020	0.017	2.231	2.067	0.014	0.013	15.193	14.393	0.087	0.062
MEAN	1.187	1.127	0.155	0.064	0.072	0.068	2.704	2.540	0.047	0.044	20.063	19.194	0.438	0.407

Table BO2 (cont.)

LAKE	V		Y		Yb		Zn		Ca		Cl	
	Top	Bottom	Top	Bottom	Top	Bottom	Top	Bottom	Top	Bottom	Top	Bottom
	(ppb)								(ppm)			
BOREAL FOREST												
26.1	0.050	0.120	0.034	0.032	0.003	0.003	1.570	0.995	3.101	2.911	1.320	1.145
27.1	0.100	0.050	0.070	0.068	0.006	0.006	2.385	1.860	4.252	4.132	1.585	1.480
28.1	0.185	0.220	0.046	0.044	0.003	0.003	8.695	3.300	3.082	3.064	1.485	1.340
30.1	0.130	0.150	0.162	0.149	0.014	0.014	6.560	3.010	2.384	2.513	0.350	0.330
33.1	0.155	0.330	0.220	0.229	0.018	0.018	3.830	4.630	5.346	5.641	1.230	1.320
34.2	0.170	0.160	0.193	0.177	0.017	0.017	6.850	2.415	3.901	3.840	0.690	0.620
39.1	0.830	0.930	0.483	0.475	0.044	0.042	6.520	9.800	8.939	8.838	1.020	1.040
40.1	2.530	2.440	1.231	1.217	0.099	0.099	5.220	3.380	18.358	18.077	1.760	1.680
MIN	0.050	0.050	0.034	0.032	0.003	0.003	1.570	0.995	2.384	2.513	0.350	0.330
MAX	2.530	2.440	1.231	1.217	0.099	0.099	8.695	9.800	18.358	18.077	1.760	1.680
MEDIAN	0.163	0.190	0.178	0.163	0.016	0.016	5.870	3.155	4.076	3.986	1.275	1.233
MEAN	0.519	0.550	0.305	0.299	0.025	0.025	5.204	3.674	6.170	6.127	1.180	1.119
SPARSE TREES												
46.1	0.155	0.050	0.022	0.005	0.003	0.003	7.390	0.920	2.370	2.238	0.785	0.600
47.1	0.155	0.050	0.030	0.016	0.003	0.003	3.355	0.770	2.725	2.518	0.820	0.700
MIN	0.155	0.050	0.022	0.005	0.003	0.003	3.355	0.770	2.370	2.238	0.785	0.600
MAX	0.155	0.050	0.030	0.016	0.003	0.003	7.390	0.920	2.725	2.518	0.820	0.700
MEDIAN	0.155	0.050	0.026	0.011	0.003	0.003	5.373	0.845	2.547	2.378	0.803	0.650
MEAN	0.155	0.050	0.026	0.011	0.003	0.003	5.373	0.845	2.547	2.378	0.803	0.650
ARCTIC TUNDRA												
48.1	0.170	0.120	0.064	0.047	0.003	0.003	7.360	3.560	3.476	3.571	1.100	1.110
49.1	0.260	0.190	0.078	0.067	0.008	0.008	6.495	2.790	3.226	3.139	0.475	0.520
51.1	0.570	0.520	0.171	0.158	0.018	0.017	21.960	2.450	8.546	8.587	2.310	2.250
52.1A	0.350	0.050	0.040	0.005	0.003	0.003	3.040	1.000	1.731	0.818	0.830	0.450
52.1B	0.200	0.050	0.026	0.005	0.003	0.003	6.110	0.620	1.025	0.851	0.610	0.450
53.1A	0.050	0.180	0.032	0.069	0.003	0.006	4.890	1.330	1.054	0.798	0.420	0.280
53.1B	0.050	0.050	0.018	0.005	0.003	0.003	2.430	0.930	0.978	0.858	0.340	0.340
54.1	0.050	0.050	0.017	0.011	0.003	0.003	2.605	2.510	1.732	1.534	0.755	0.630
54.2	0.190	0.050	0.033	0.015	0.003	0.003	2.750	0.845	1.385	1.415	0.660	0.625
55.1	0.310	0.050	0.012	0.005	0.003	0.003	1.790	0.680	1.352	1.472	1.460	1.370
MIN	0.050	0.050	0.012	0.005	0.003	0.003	1.790	0.620	0.978	0.798	0.340	0.280
MAX	0.570	0.520	0.171	0.158	0.018	0.017	21.960	3.560	8.546	8.587	2.310	2.250
MEDIAN	0.195	0.050	0.033	0.013	0.003	0.003	3.965	1.165	1.558	1.443	0.708	0.573
MEAN	0.220	0.131	0.049	0.039	0.005	0.005	5.943	1.672	2.450	2.304	0.896	0.803
Full Lakeset												
MIN	0.050	0.050	0.012	0.005	0.003	0.003	1.570	0.620	0.978	0.798	0.340	0.280
MAX	2.530	2.440	1.231	1.217	0.099	0.099	21.960	9.800	18.358	18.077	2.310	2.250
MEDIAN	0.170	0.120	0.043	0.046	0.003	0.003	5.055	2.138	2.903	2.714	0.825	0.665
MEAN	0.333	0.291	0.149	0.140	0.013	0.013	5.590	2.390	3.948	3.841	1.000	0.914

Table B02 (cont.)

LAKE	Fe		K		Mg		Na		S		Si	
	Top	Bottom	Top	Bottom	Top	Bottom	Top	Bottom	Top	Bottom	Top	Bottom
	(ppm)											
BOREAL FOREST												
26.1	0.015	0.041	0.987	0.840	1.086	0.979	2.098	1.869	0.329	0.295	0.459	0.496
27.1	0.170	0.180	1.223	1.189	1.419	1.395	2.667	2.604	0.415	0.402	0.887	0.894
28.1	0.064	0.065	1.220	1.327	1.176	1.172	2.314	2.272	0.353	0.374	0.572	0.592
30.1	0.024	0.064	0.713	0.637	1.133	1.066	1.576	1.374	0.604	0.490	0.785	0.895
33.1	0.402	0.445	1.480	1.534	2.310	2.371	3.563	3.733	1.306	1.358	1.069	1.149
34.2	0.097	0.163	1.775	1.601	2.100	2.058	3.429	3.114	1.713	1.577	0.767	1.041
39.1	2.542	2.608	2.030	2.047	3.081	3.062	4.569	4.563	0.995	0.986	3.065	3.023
40.1	9.259	9.476	3.674	3.522	6.275	6.199	8.903	8.643	1.077	1.060	5.448	5.287
MIN	0.015	0.041	0.713	0.637	1.086	0.979	1.576	1.374	0.329	0.295	0.459	0.496
MAX	9.259	9.476	3.674	3.522	6.275	6.199	8.903	8.643	1.713	1.577	5.448	5.287
MEDIAN	0.133	0.172	1.351	1.431	1.759	1.726	3.048	2.859	0.800	0.738	0.836	0.968
MEAN	1.572	1.630	1.638	1.587	2.322	2.288	3.640	3.522	0.849	0.818	1.631	1.672
SPARSE TREES												
46.1	0.010	0.005	0.887	0.799	0.976	0.943	1.081	0.958	0.779	0.727	0.115	0.089
47.1	0.069	0.039	0.903	0.761	1.093	0.982	1.139	0.929	0.798	0.632	0.190	0.216
MIN	0.010	0.005	0.887	0.761	0.976	0.943	1.081	0.929	0.779	0.632	0.115	0.089
MAX	0.069	0.039	0.903	0.799	1.093	0.982	1.139	0.958	0.798	0.727	0.190	0.216
MEDIAN	0.039	0.022	0.895	0.780	1.035	0.962	1.110	0.944	0.788	0.680	0.153	0.153
MEAN	0.039	0.022	0.895	0.780	1.035	0.962	1.110	0.944	0.788	0.680	0.153	0.153
ARCTIC TUNDRA												
48.1	0.073	0.072	1.235	1.246	1.459	1.506	1.310	1.336	1.449	1.495	0.174	0.169
49.1	0.579	0.621	1.448	1.427	1.971	1.929	1.472	1.441	0.959	0.933	0.255	0.251
51.1	4.110	3.995	2.406	2.348	4.939	4.967	2.783	2.699	3.201	3.281	1.850	1.840
52.1A	0.023	0.005	0.745	0.418	0.994	0.494	0.846	0.462	0.859	0.432	0.207	0.106
52.1B	0.010	0.005	0.589	0.452	0.622	0.518	0.669	0.515	0.575	0.481	0.123	0.096
53.1A	0.017	0.260	0.610	0.440	0.604	0.467	0.626	0.447	0.639	0.500	0.136	0.127
53.1B	0.005	0.005	0.541	0.500	0.560	0.497	0.551	0.539	0.612	0.560	0.118	0.112
54.1	0.023	0.018	0.822	0.732	1.037	0.926	0.914	0.813	0.826	0.715	0.173	0.171
54.2	0.031	0.019	0.811	0.767	0.871	0.875	0.854	0.815	0.913	0.856	0.204	0.207
55.1	0.019	0.005	0.877	0.843	0.883	0.925	1.174	1.119	1.021	1.012	0.042	0.031
MIN	0.005	0.005	0.541	0.418	0.560	0.467	0.551	0.447	0.575	0.432	0.042	0.031
MAX	4.110	3.995	2.406	2.348	4.939	4.967	2.783	2.699	3.201	3.281	1.850	1.840
MEDIAN	0.023	0.018	0.817	0.749	0.939	0.900	0.884	0.814	0.886	0.785	0.173	0.148
MEAN	0.489	0.500	1.008	0.917	1.394	1.310	1.120	1.019	1.105	1.026	0.328	0.311
Full Lakeset												
MIN	0.005	0.005	0.541	0.418	0.560	0.467	0.551	0.447	0.329	0.295	0.042	0.031
MAX	9.259	9.476	3.674	3.522	6.275	6.199	8.903	8.643	3.201	3.281	5.448	5.287
MEDIAN	0.047	0.065	0.945	0.841	1.113	1.024	1.391	1.355	0.843	0.721	0.231	0.234
MEAN	0.877	0.905	1.249	1.171	1.730	1.666	2.127	2.012	0.971	0.908	0.832	0.840

Table BO3. Dissolved organic and inorganic carbon, nutrients (bottom samples only), and geochemistry of surface and bottom water samples.

LAKE	C DOC		C DIC		δ^{13}C DOC	δ^{13}C DOC	δ^{13}C DIC	δ^{13}C DIC	Ammonia	Kjeldahl	Phosphorus	Phosphorus
	Top	Bottom	Top	Bottom	Top	Bottom	Top	Bottom	(N) Total	Nitrogen	(NaHCO3	Total
	ppm				vpdb						(µg/g)	
BOREAL FOREST												
26.1	9.05	7.73	5.83	7.46	-25.94	-26.46	-10.6	-13.51	12.5	17700	35	1720
27.1	10.83	9.94	10.15	9.2	-26.06	-25.18	-12.46	-12.25	38.9	18400	49	973
28.1	9.89	11	4.52	9.95	-26.57	-25.88	-9.25	-14.22	59.5	15400	11	1420
30.1	9.96	8.75	5.9	8.09	-26.56	-25.19	-12.43	-15.47	13.2	13400	22	1090
33.1	9.35	9.89	13.93	10.2	-25.26	-25.98	-13.66	-12.72	44.4	15000	25	889
34.2	14.26	11.54	8.39	9.11	-26.22	-26.52	-11.64	-15.08	6.46	10500	25	1890
39.1	27.13	32.53	19.79	21.54	-26.43	-26.61	-16.12	-15.97	3.39	5740	7.9	523
40.1	92.94	94.73	45.35	49.05	-27.08	-26.98	-18.16	-16.87	42.6	18800	25	809
MIN	9.050	7.730	4.520	7.460	-27.080	-26.980	-18.160	-16.870	3.390	5740.000	7.900	523.000
MAX	92.940	94.730	45.350	49.050	-25.260	-25.180	-9.250	-12.250	59.500	18800.000	49.000	1890.000
MEDIAN	10.395	10.470	9.270	9.575	-26.325	-26.220	-12.445	-14.650	26.050	15200.000	25.000	1031.500
MEAN	22.926	23.264	14.233	15.575	-26.265	-26.100	-13.040	-14.511	27.619	14367.500	24.988	1164.250
SPARSE TREES												
46.1	4.07	3.43	5.1	4.6	-25.21	-24.36	-9.62	-8.68	22.7	5450	7.9	650
47.1	5.67	4.2	7.82	6.41	-23.73	-24.93	-10.01	-11.75	68.2	13500	15	1260
MIN	4.070	3.430	5.100	4.600	-25.210	-24.930	-10.010	-11.750	22.700	5450.000	7.900	650.000
MAX	5.670	4.200	7.820	6.410	-23.730	-24.360	-9.620	-8.680	68.200	13500.000	15.000	1260.000
MEDIAN	4.870	3.815	6.460	5.505	-24.470	-24.645	-9.815	-10.215	45.450	9475.000	11.450	955.000
MEAN	4.870	3.815	6.460	5.505	-24.470	-24.645	-9.815	-10.215	45.450	9475.000	11.450	955.000
ARCTIC TUNDRA												
48.1	6.21	7.06	11.66	12.5	-24.83	-25.09	-13.85	-13.62	0.44	2560	28	732
49.1	15.41	14.28	13.91	13.3	-25.9	-26.44	-15.87	-15.91	0.81	5370	56	792
51.1	21.41	17.47	25.85	23.16	-26.01	-26.16	-15.17	-15.42	7.82	3490	27	535
52.1A	5.19	4.09	5.26	6.2	-24.73	-25.86	-13.44	-13.35	4.38	2260	13	480
52.1B	4.42	3.64	3.87	2.1	-26.19	-26.2	-11.64	-11.32	0.91	438	7.9	85.9
53.1A	3.32	2.82	2.37	1.26	-26.49	-26.32	-12.84	-11	1.5	1800	11	493
53.1B	3.5	3.38	2.54	1.9	-26.51	-26.57	-12.2	-10.66	4.05	4800	8	763
54.1	6.72	5.49	6.24	5.18	-26.09	-25.35	-13.09	-14.77	3.14	9120	12	1270
54.2	6.31	7.04	4.68	7.05	-24.24	-23.38	-12.93	-13.36	4.26	3760	25	411
55.1	3.73	3.75	3.73	1.95	-25.17	-26.2	-11.87	-10.06	5.01	1240	22	740
MIN	3.320	2.820	2.370	1.260	-26.510	-26.570	-15.870	-15.910	0.440	438.000	7.900	85.900
MAX	21.410	17.470	25.850	23.160	-24.240	-23.380	-11.640	-10.060	7.820	9120.000	56.000	1270.000
MEDIAN	5.700	4.790	4.970	5.690	-25.955	-26.180	-13.010	-13.355	3.595	3025.000	17.500	633.500
MEAN	7.622	6.902	8.011	7.460	-25.616	-25.757	-13.290	-12.947	3.232	3483.800	20.990	630.190
FULL LAKESET												
MIN	3.320	2.820	2.370	1.260	-27.080	-26.980	-18.160	-16.870	0.440	438.000	7.900	85.900
MAX	92.940	94.730	45.350	49.050	-23.730	-23.380	-9.250	-8.680	68.200	18800.000	56.000	1890.000
MEDIAN	7.885	7.395	6.070	7.775	-26.035	-26.070	-12.650	-13.435	5.735	5595.000	22.000	777.500
MEAN	13.469	13.138	10.345	10.511	-25.761	-25.783	-12.843	-13.300	17.209	8436.400	21.635	876.295

Table BO3 (cont.)

LAKE	Alkalinity		Br		Cl		Cond		F		NO3		pH		SO4	
	Top	Bottom	Top	Bottom	Top	Bottom	Top	Bottom	Top	Bottom	Top	Bottom	Top	Bottom	Top	Bottom
	(ppm)						(µS/cm)		(ppm)				(units)		(ppm)	
BOREAL FOREST																
26.1	11	11	0.021	0.026	1.128	1.025	33.64	33.6	0.1	0.091	0.019	0.145	6.41	6.61	0.776	0.71
27.1	17	16	0.022	0.019	1.41	1.342	44.64	42.3	0.121	0.119	0.05	0.044	7.04	7.03	1.038	1.002
28.1	14	13	0.029	0.071	1.309	1.221	36.53	36.24	0.082	0.092	0.061	0.019	6.64	6.68	0.784	0.817
30.1	8	9	0.03	0.02	0.2915	0.254	30.145	28.98	0.0665	0.059	0.1615	0.452	6.875	6.79	1.588	1.312
33.1	24	26	0.02	0.019	1.118	1.158	61.34	63.34	0.123	0.129	0.216	0.2	6.77	6.86	3.904	4.128
34.2	16	16	0.019	0.029	0.583	0.421	51.68	50.69	0.128	0.11	0.053	0.191	6.94	7.03	5.068	4.745
39.1	34	34	0.019	0.019	0.875	0.907	76.06	75.63	0.092	0.09	0.054	0.043	7.02	6.92	2.192	2.244
40.1	72	68	0.088	0.082	1.873	1.573	147.2	148.5	0.078	0.086	0.032	0.02	7.33	7.31	0.5	0.43
MIN	8.000	9.000	0.019	0.019	0.292	0.254	30.145	28.980	0.067	0.059	0.019	0.019	6.410	6.610	0.500	0.430
MAX	72.000	68.000	0.088	0.082	1.873	1.573	147.200	148.500	0.128	0.129	0.216	0.452	7.330	7.310	5.068	4.745
MEDIAN	16.500	16.000	0.022	0.023	1.123	1.092	48.160	46.495	0.096	0.092	0.054	0.095	6.908	6.890	1.313	1.157
MEAN	24.500	24.125	0.031	0.036	1.073	0.988	60.154	59.910	0.099	0.097	0.081	0.139	6.878	6.904	1.981	1.924
SPARSE TREES																
46.1	8	7	0.019	0.019	0.706	0.602	28.32	25.74	0.085	0.079	0.022	0.019	7.21	7.15	2.35	2.233
47.1	8	8	0.019	0.019	0.702	0.615	30.27	28.1	0.077	0.07	0.061	0.074	7.24	7.24	2.328	1.893
MIN	8.000	7.000	0.019	0.019	0.702	0.602	28.320	25.740	0.077	0.070	0.022	0.019	7.210	7.150	2.328	1.893
MAX	8.000	8.000	0.019	0.019	0.706	0.615	30.270	28.100	0.085	0.079	0.061	0.074	7.240	7.240	2.350	2.233
MEDIAN	8.000	7.500	0.019	0.019	0.704	0.609	29.295	26.920	0.081	0.075	0.042	0.047	7.225	7.195	2.339	2.063
MEAN	8.000	7.500	0.019	0.019	0.704	0.609	29.295	26.920	0.081	0.075	0.042	0.047	7.225	7.195	2.339	2.063
ARCTIC TUNDRA																
48.1	10	11	0.031	0.029	0.953	0.96	44.31	45.64	0.039	0.039	0.233	0.229	6.8	6.81	4.174	4.257
49.1	12.5	1	0.039	0.034	0.455	0.447	44.97	44.05	0.0355	0.041	0.028	0.019	6.785	6.8	2.4385	2.45
51.1	35	34	0.044	0.048	2.33	2.178	105.8	104.5	0.041	0.045	0.019	0.019	6.83	6.79	9.694	9.754
52.1A	4	2	0.031	0.038	0.571	0.499	26.76	14.3	0.028	0.017	0.182	0.035	7.08	7.11	2.457	1.21
52.1B	3	2	0.038	0.04	0.562	0.439	18.63	15.27	0.024	0.02	0.02	0.019	6.99	7	1.645	1.293
53.1A	2	2	0.027	0.021	0.372	0.249	16.94	14.12	0.032	0.019	0.019	0.019	7.24	7.27	1.763	1.345
53.1B	2	1	0.04	0.037	0.32	0.285	16.64	15.215	0.034	0.0195	0.019	0.019	7.03	6.995	1.651	1.468
54.1	5	7	0.04	0.034	0.653	0.529	27.63	25.3	0.024	0.024	0.106	0.067	7.02	6.98	2.236	1.965
54.2	3	4	0.025	0.025	0.575	0.774	25.06	25.93	0.03	0.026	0.087	0.052	7.14	7.11	2.514	2.557
55.1	4	3	0.042	0.046	1.284	1.219	27.1	27.69	0.022	0.022	0.054	0.034	7.05	6.96	2.87	2.789
MIN	2.000	1.000	0.025	0.021	0.320	0.249	16.640	14.120	0.022	0.017	0.019	0.019	6.785	6.790	1.645	1.210
MAX	35.000	34.000	0.044	0.048	2.330	2.178	105.800	104.500	0.041	0.045	0.233	0.229	7.240	7.270	9.694	9.754
MEDIAN	4.000	2.500	0.039	0.036	0.573	0.514	26.930	25.615	0.031	0.023	0.041	0.027	7.025	6.988	2.448	2.208
MEAN	8.050	6.700	0.036	0.035	0.808	0.758	35.384	33.202	0.031	0.027	0.077	0.051	6.997	6.983	3.144	2.909
FULL LAKESET																
MIN	2.000	1.000	0.019	0.019	0.292	0.249	16.640	14.120	0.022	0.017	0.019	0.019	6.410	6.610	0.500	0.430
MAX	72.000	68.000	0.088	0.082	2.330	2.178	147.200	148.500	0.128	0.129	0.233	0.452	7.330	7.310	9.694	9.754
MEDIAN	9.000	8.500	0.030	0.029	0.704	0.695	31.955	31.290	0.054	0.052	0.054	0.039	7.020	6.988	2.282	1.929
MEAN	14.625	13.750	0.032	0.034	0.904	0.835	44.683	43.257	0.063	0.060	0.075	0.086	6.972	6.972	2.599	2.430

Appendix C: Freeze Core Catalogue

Table C01. Sediment cores collected during the 2010 field season and lake metadata. Cores are ordered from south to north and are broken into three groups. Group A (Boreal Forest) lies below the southern limit of the treeline, Group B (Sparse Trees) lies between the southern and northern limits of the treeline, and Group C (Tundra) lies above the northern limit of the treeline.

Lake (#)	Surface Area (hectares)	Depth (m)	Core name	Coordinates (decimal minutes)	Corer Type	Face #	Sect #	Length (cm)	Figure #
BOREAL FOREST									
P-26-1 (Bridge S)	119.5	4.5	ROAD10-BRIDGE1	N63°23.297 W112°51.768	2F	1	1	60.9	CO1
						2	1	64.8	CO2
			ROAD10-BRIDGE2		1F	1	1	45.1	CO3
							2	53.5	CO4
			26-1-(2-4)		Glew		Top - Middle - Bottom		
P-27-1 (Bridge N)	11.9	2	27-1-(1-3)	N63°28.616 W112°50.972	Glew		Top - Middle - Bottom		
P-28-1	21.3	4.5	28-1-(2-4)	N63°23 974 W112°50.514	Glew		Top - Middle - Bottom		
P-30-1 (Pat's)	45	5.5	ROAD10-PAT'S LAKE	N63°25.195 W112°41.314	1F	1	1	36.9	CO5
							2	34.6	CO6
							3	80.8	CO7
			30-1-(2-4)		Glew		Top - Middle - Bottom		
P-33-1 (Problem)	54	2.3	33-1-(2-4)	N63°27.551 W112°32.785	Glew		Top - Middle - Bottom		
P-34-2 (Danny's)	19.2	4.4	ROAD10-DANNY'S LAKE	N63°28.547 W112°32.25	2F	1	1	69.4	CO8
							2	48.6	CO9
						2	1	33.4	C10
							2	37.8	C11
							3	45	C12
			34-2-(2-4)		Glew		Top - Middle - Bottom		
P-39-1	37.3	1	ROAD10-39-1B	N63°35 103 W112°18.427	1F	1	1	29.3	C15
		1.1	ROAD10-39-1A	N63°35 105 W112°18.436	2F	1	1	27.3	C13
						2	1	27.9	C14
		1.25	39-1-(2-4)	N63°35 141 W112°18.393	Glew		Top - Middle - Bottom		
P-40-1	11.1	1.5	40-1-(2-4)	N63°35 141 W112°17.649	Glew		Top - Middle - Bottom		
SPARSE TREES									
P-46-1 (Portage S)	1108.8	3.6	ROAD10-46-1	N63°44.963 W111°18.560	2F	1	1	33.3	C16
						2	1	36.9	C17
			46-1-(2-5)		Glew		Top - Middle - Bottom		
		2.5	46-1-(6-8)	N63°44.599 W111°14.486	Glew		Top - Middle - Bottom		
P-47-1 (Portage N)	194.9	4.85	ROAD10-47-1	N63°44.538 W111°12.957	1F	1	1	40.4	C18
							2	45.3	
			47-1-(2-4)		Glew		Top - Middle - Bottom		

Notes: Two face freeze corer (2F), one face freeze corer (1F), and the Glew corer (Glew). The number of sections that make up the freeze core were included (Sect #). For Glew cores, subsamples were taken from the surface (Top), the middle of the core (Middle), and the base of the core (Bottom). Units: meters (m), centimeters (cm).

Lake (#)	Surface Area (hectares)	Depth (m)	Core name	Coordinates (decimal minutes)	Corer 1F/2F	Face #	Sect #	Length (cm)	Figure #
ARCTIC TUNDRA									
Mackay	97600	1.5	MK-(2*,3*,4,5)	N64˚14.592 W110˚06.995	Glew	T - M - B (* no middle collected)			
P-49-1	29.8	3.5	ROAD10-49-1A	N64˚15.571 W110˚05.878	2F	1	1	38	C19
							2	32.8	
						2	1	54.1	
							2	34.2	
			49-1-(2-4)		Glew	Top - Middle - Bottom			
		1.5	ROAD10-49-1B	N64˚17.76 W110˚03.288	1F	1	1	60	C20
							2	51.2	C21
P-51-1	2.3	1.5	51-1-(2*,3,4)	N64˚16.605 W110˚05.015	Glew	T - M - B (* no middle collected)			
P-52-1 (Horseshoe)	505.1	4	ROAD10-52-1	N64˚17.381 W110˚03.701	2F	1	1	52.6	C22
							2	49	
						2	1	55	C23
							2	49.7	C24
			52-1-(2 & 4-5)		Glew	Top - Middle - Bottom			
			52-1-1-(2-3)		Glew	Top - Middle - Bottom			
P-53-1 (Gravel Pit N)	531	6.5	53-1-(2-4)	N64˚19.921 W109˚59.921	Glew	Top - Middle - Bottom			
		4.25	53-1-2-(2-4)	N64º22 554, W110º00.944	Glew	Top - Middle - Bottom			
P-54-1 (Abe)	210.7	3.5	54-1-(2-4)	N64˚24 717 W110˚06.199	Glew	Top - Middle - Bottom			
P-54-2 (Echo)	45.7	3	ROAD10-ECHO	N64˚25.114 W110˚06.449	2F	1	1	44.5	C25
							2	43.2	
						2	1	52	
							2	34.5	
P-55-1 (Lac de Gras)	57800	4	ROAD10-Lacdegras	N64˚25 794 W110˚08.168	2F	1	1	44.7	C26
						2	1	49.2	C27
			LG-(2*,3-5)		Glew	T - M - B (* no middle collected)			

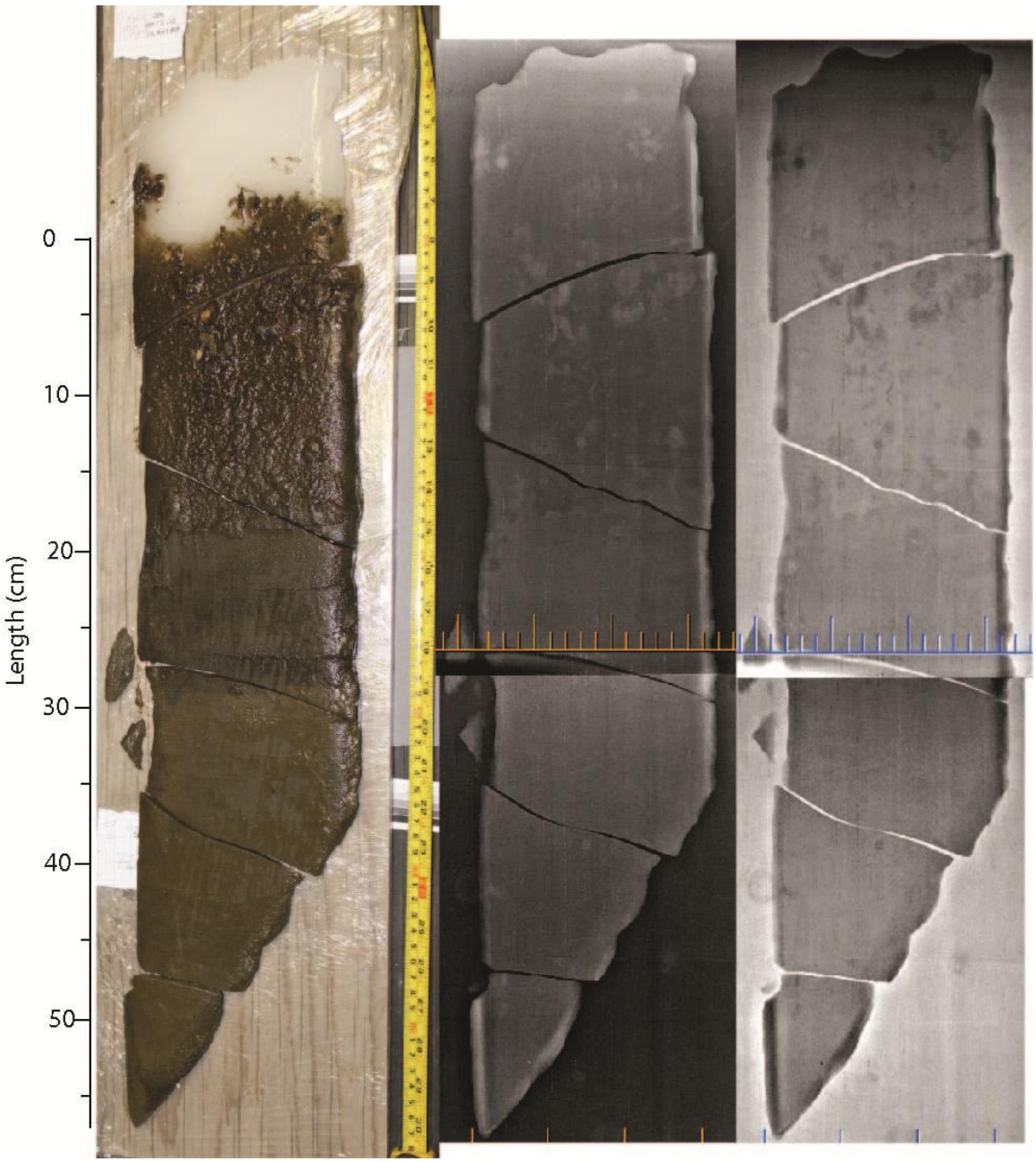

Figure C01. Freeze core ROAD10-BRIDGE1, Face 1 of 2: (left) light photograph; (middle) positive X-Ray; (right) negative X-Ray. Note: The big bars on the X-Ray scale are separated by 5 cm and the small bars are separated by 1 cm.

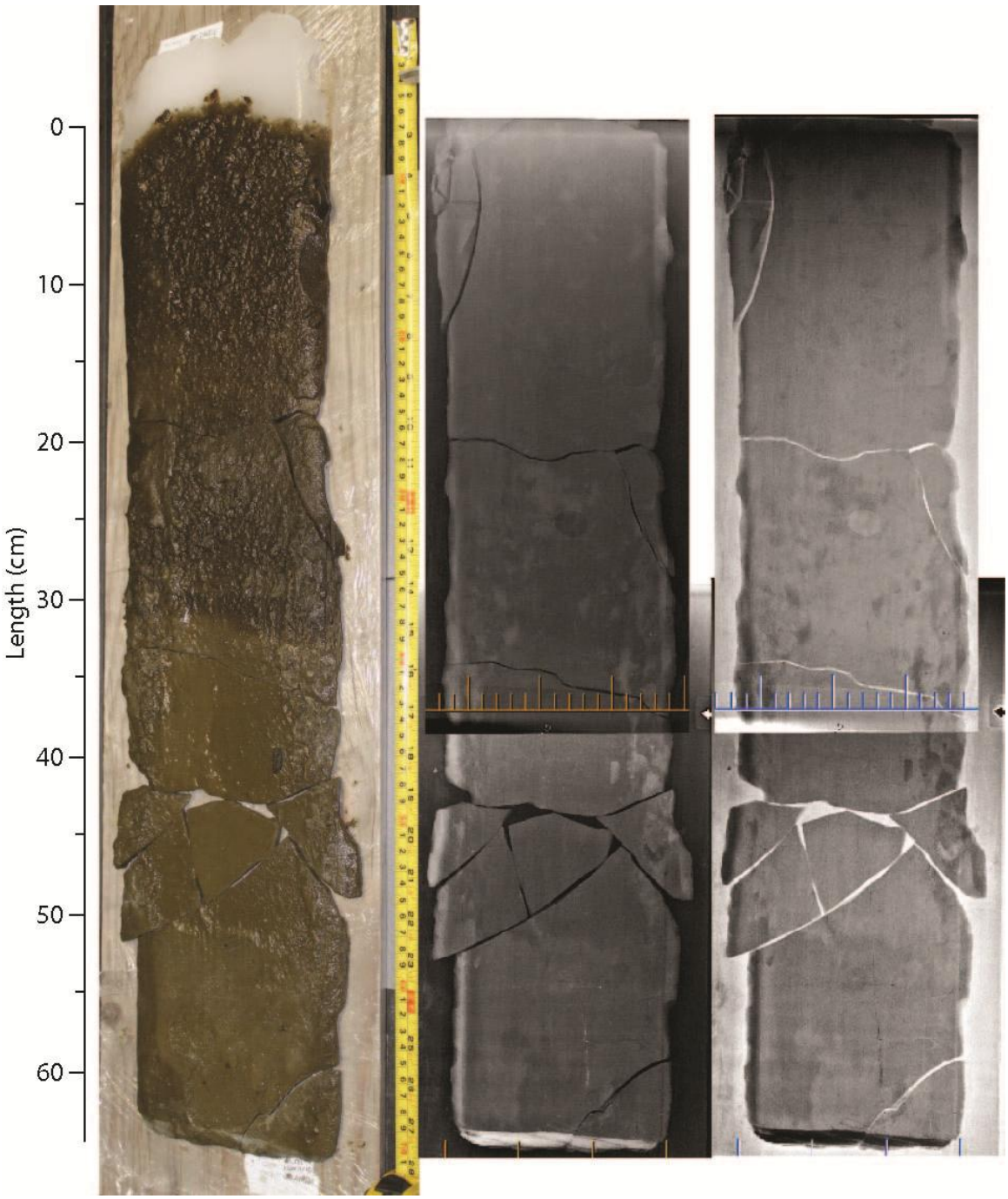

Figure C02. Freeze core ROAD10-BRIDGE1, Face 2 of 2: (left) light photograph; (middle) positive X-Ray; (right) negative X-Ray. Note: The big bars on the X-Ray scale are separated by 5 cm and the small bars are separated by 1 cm.

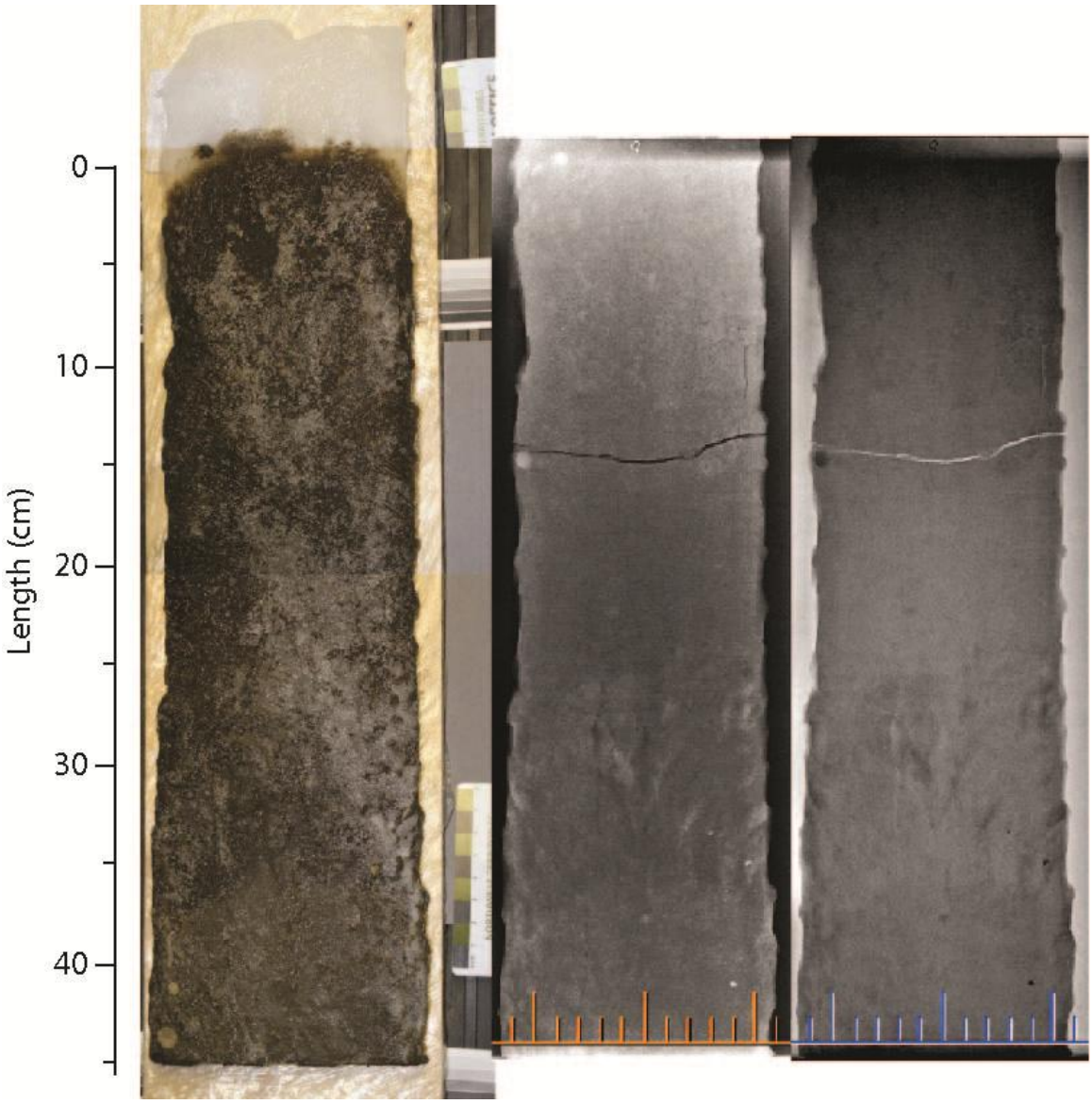

Figure C03. Freeze core ROAD10-BRIDGE2, Face 1 of 1, Section 1 of 2: (left) light photograph; (middle) positive X-Ray; (right) negative X-Ray. Note: The big bars on the X-Ray scale are separated by 5 cm and the small bars are separated by 1 cm.

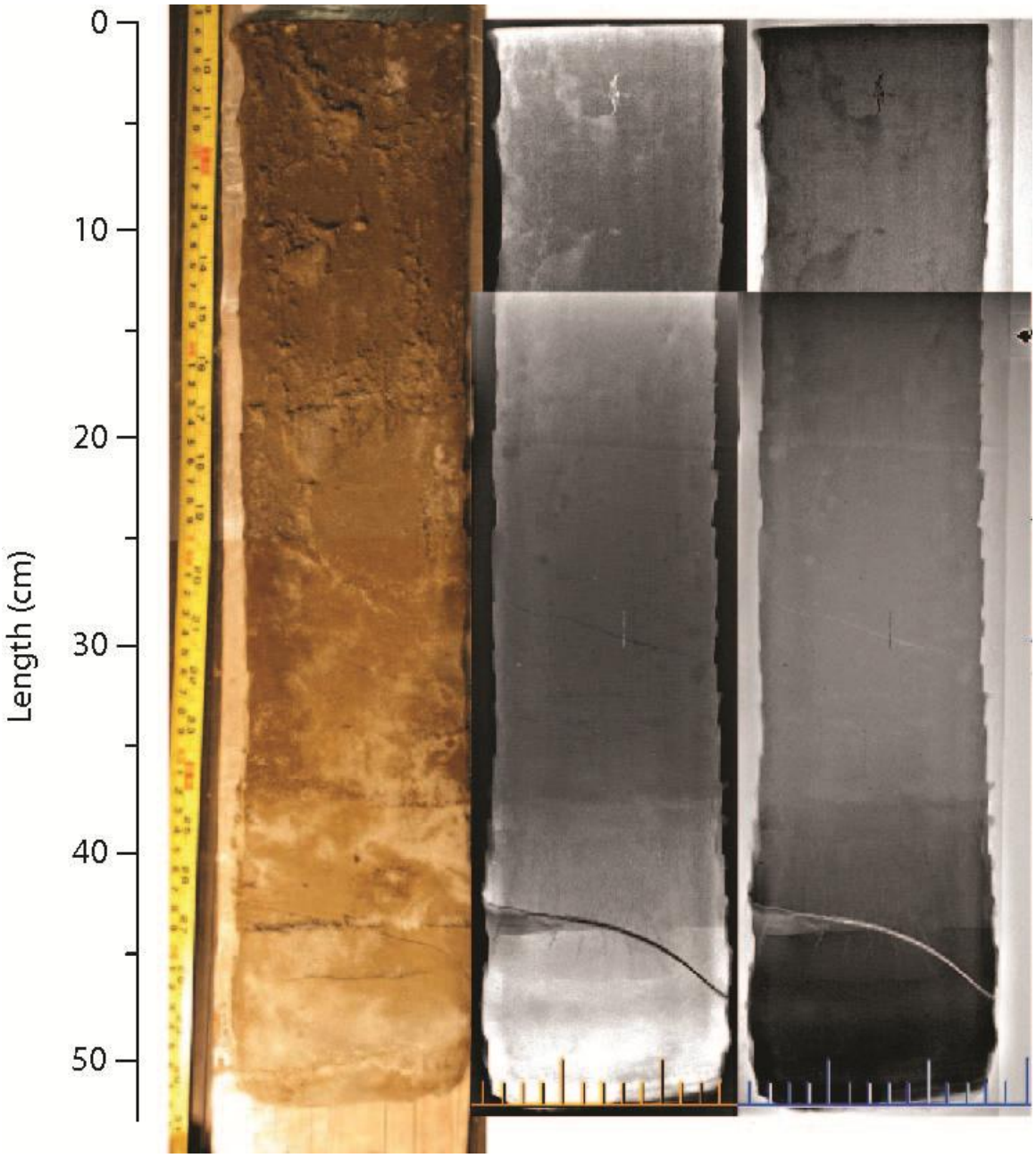

Figure C04. Freeze core ROAD10-BRIDGE2, Face 1 of 1, Section 2 of 2: (left) light photograph; (middle) positive X-Ray; (right) negative X-Ray. Note: The big bars on the X-Ray scale are separated by 5 cm and the small bars are separated by 1 cm.

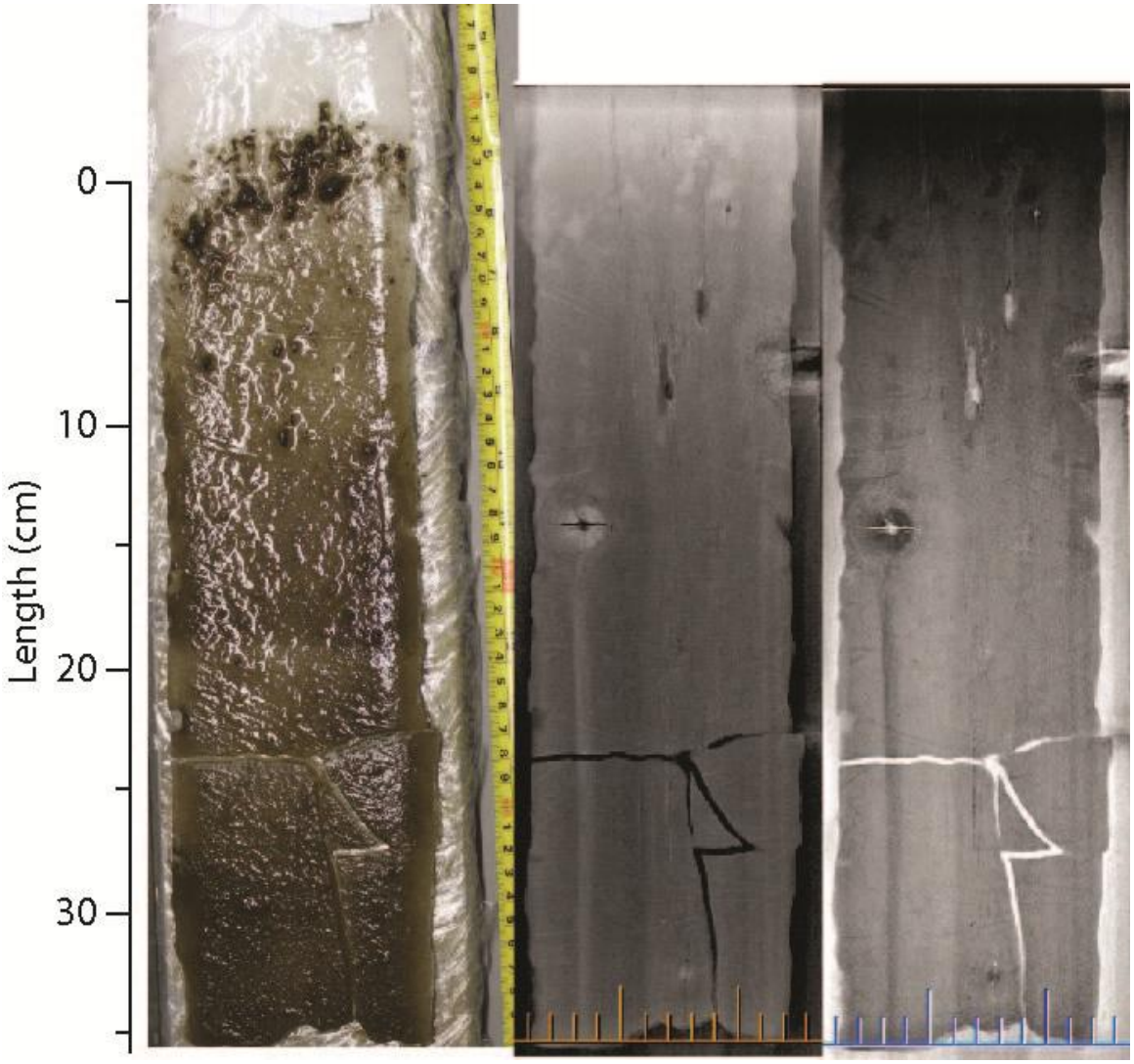

Figure C05. Freeze core ROAD10-PAT'S LAKE, Face 1 of 1, Section 1 of 3: (left) light photograph; (middle) positive X-Ray; (right) negative X-Ray. Note: The big bars on the X-Ray scale are separated by 5 cm and the small bars are separated by 1 cm. Also note: knots from the wooden board below show up in the X-Ray images.

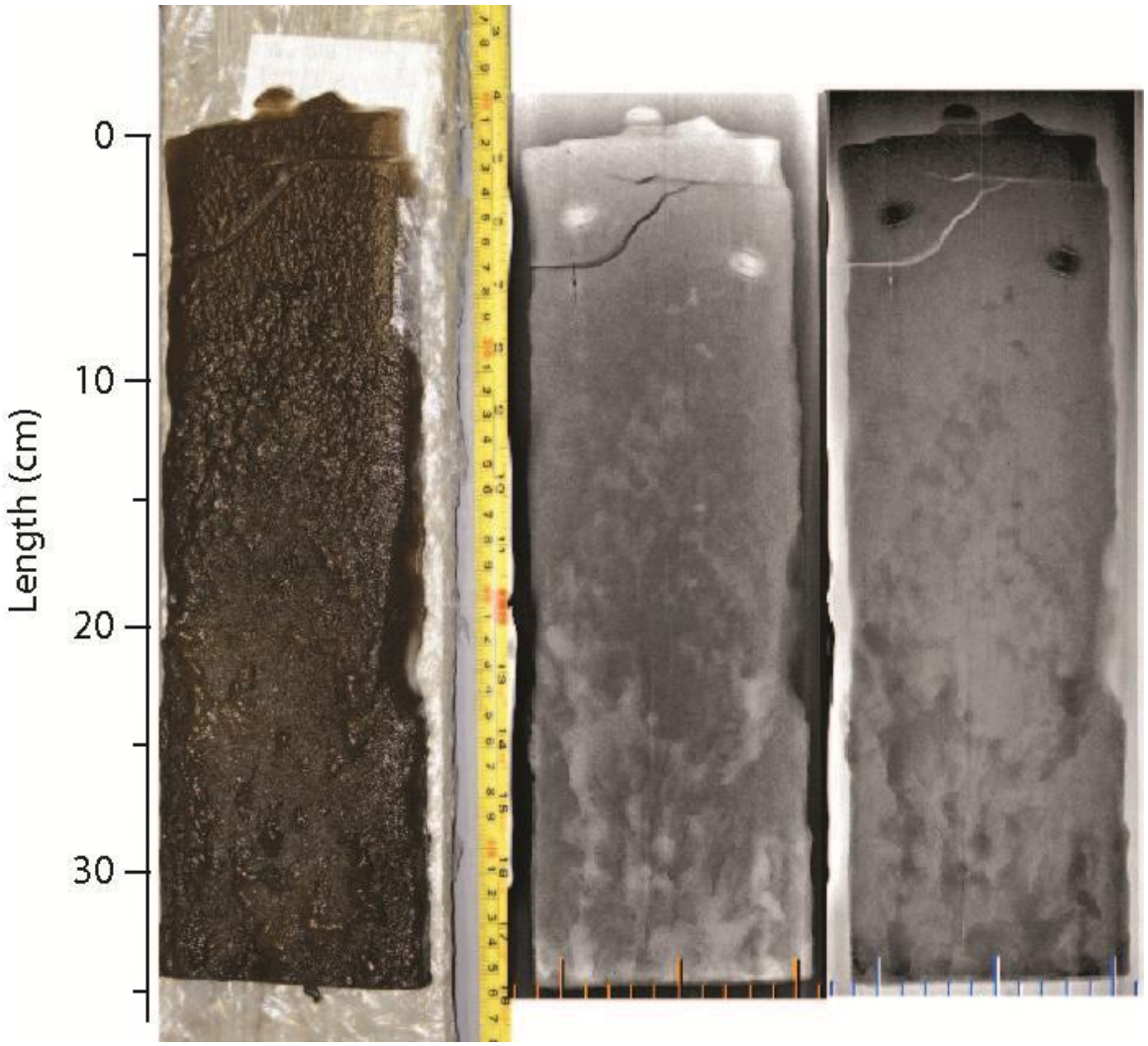

Figure C06. Freeze core ROAD10-PAT'S LAKE, Face 1 of 1, Section 2 of 3: (left) light photograph; (middle) positive X-Ray; (right) negative X-Ray. The big bars on the X-Ray scale are separated by 5 cm and the small bars are separated by 1 cm. Also note: knots from the wooden board below show up in the X-Ray images.

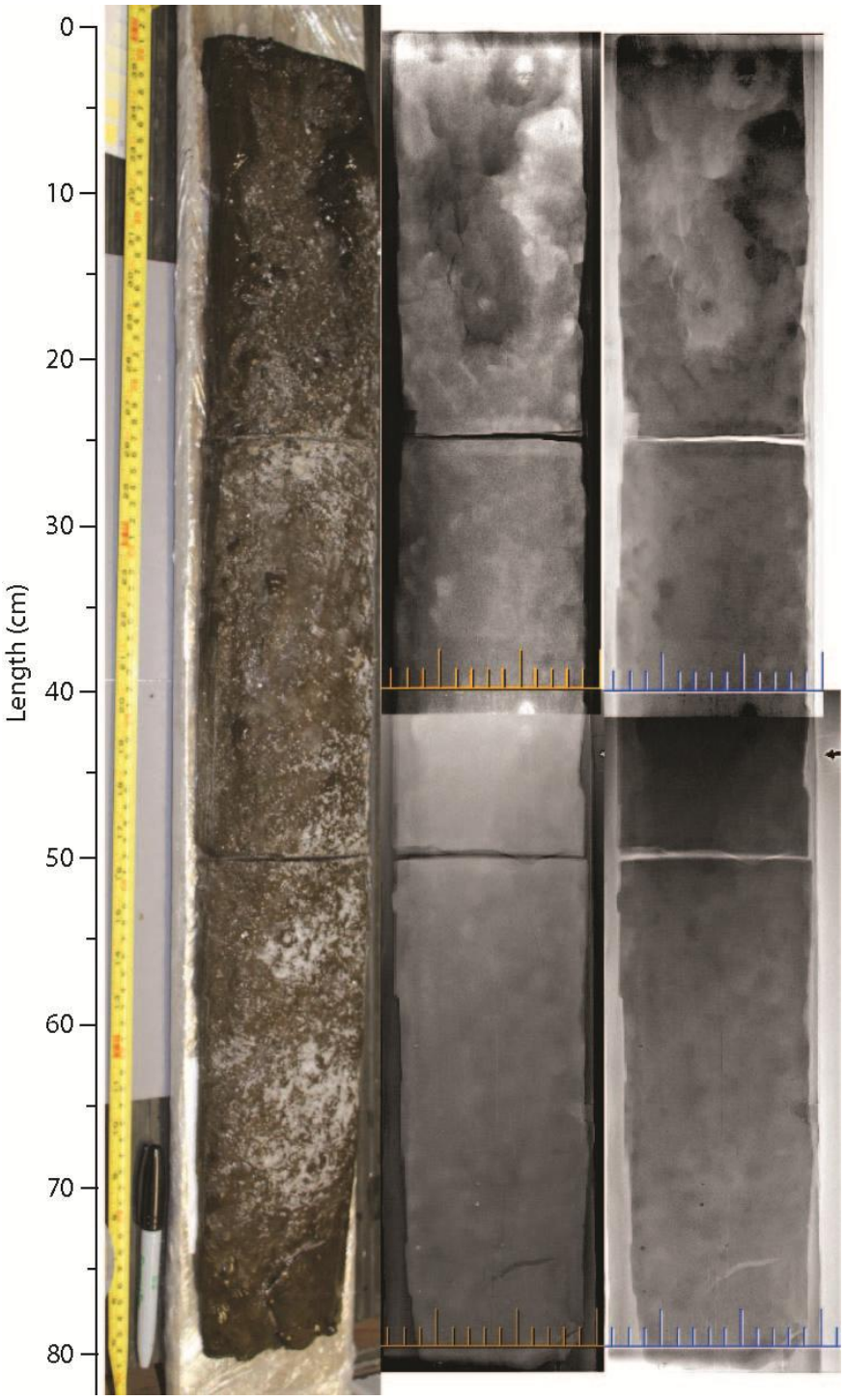

Figure C07. Freeze core ROAD10-PAT'S LAKE, Face 1 of 1, Section 3 of 3: (left) light photograph; (middle) positive X-Ray; (right) negative X-Ray. The big bars on the X-Ray scale are separated by 5 cm and the small bars are separated by 1 cm.

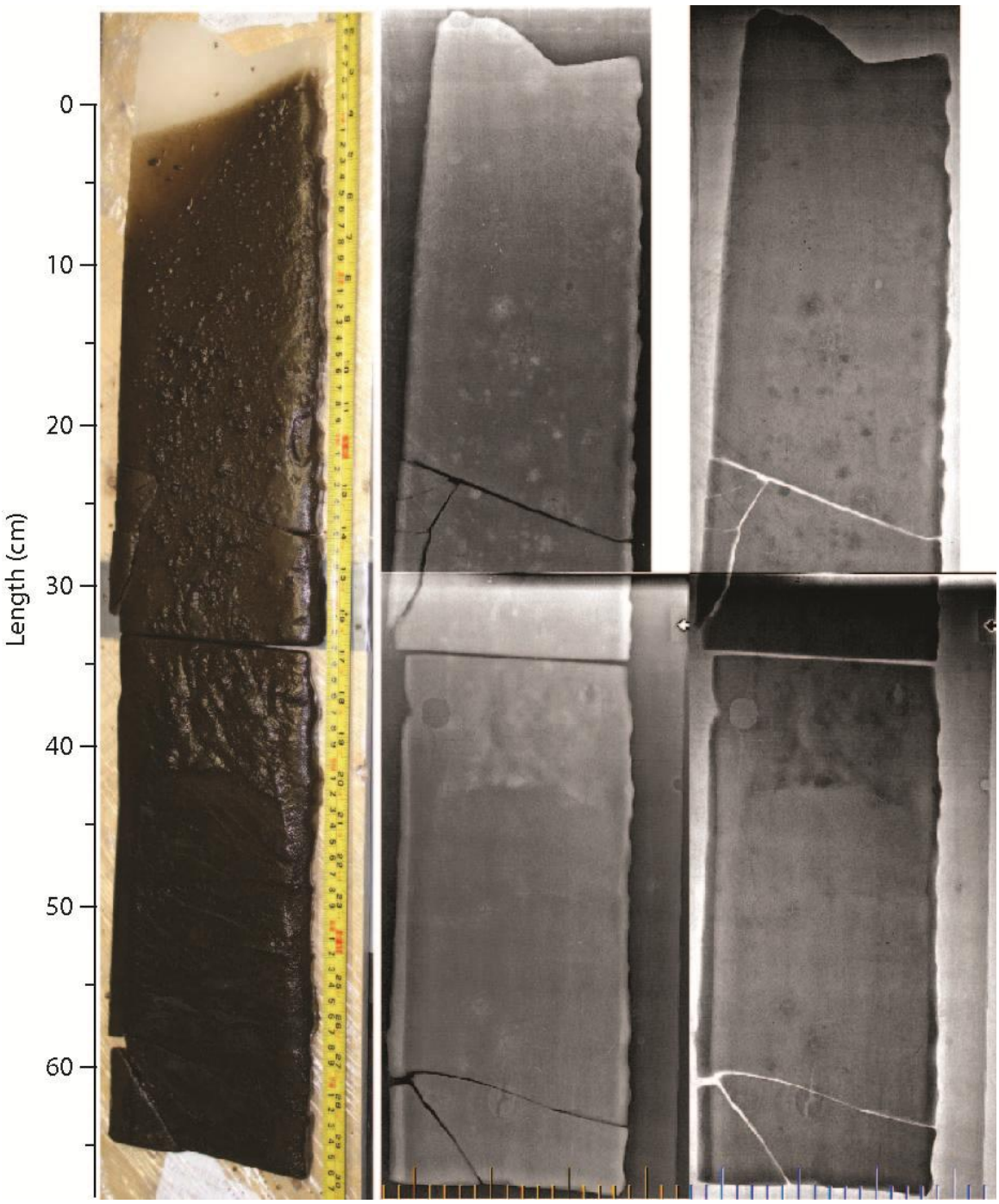

Figure C08. Freeze core ROAD10-DANNY'S LAKE, Face 1 of 2, Section 1 of 2: (left) light photograph; (middle) positive X-Ray; (right) negative X-Ray. The big bars on the X-Ray scale are separated by 5 cm and the small bars are separated by 1 cm.

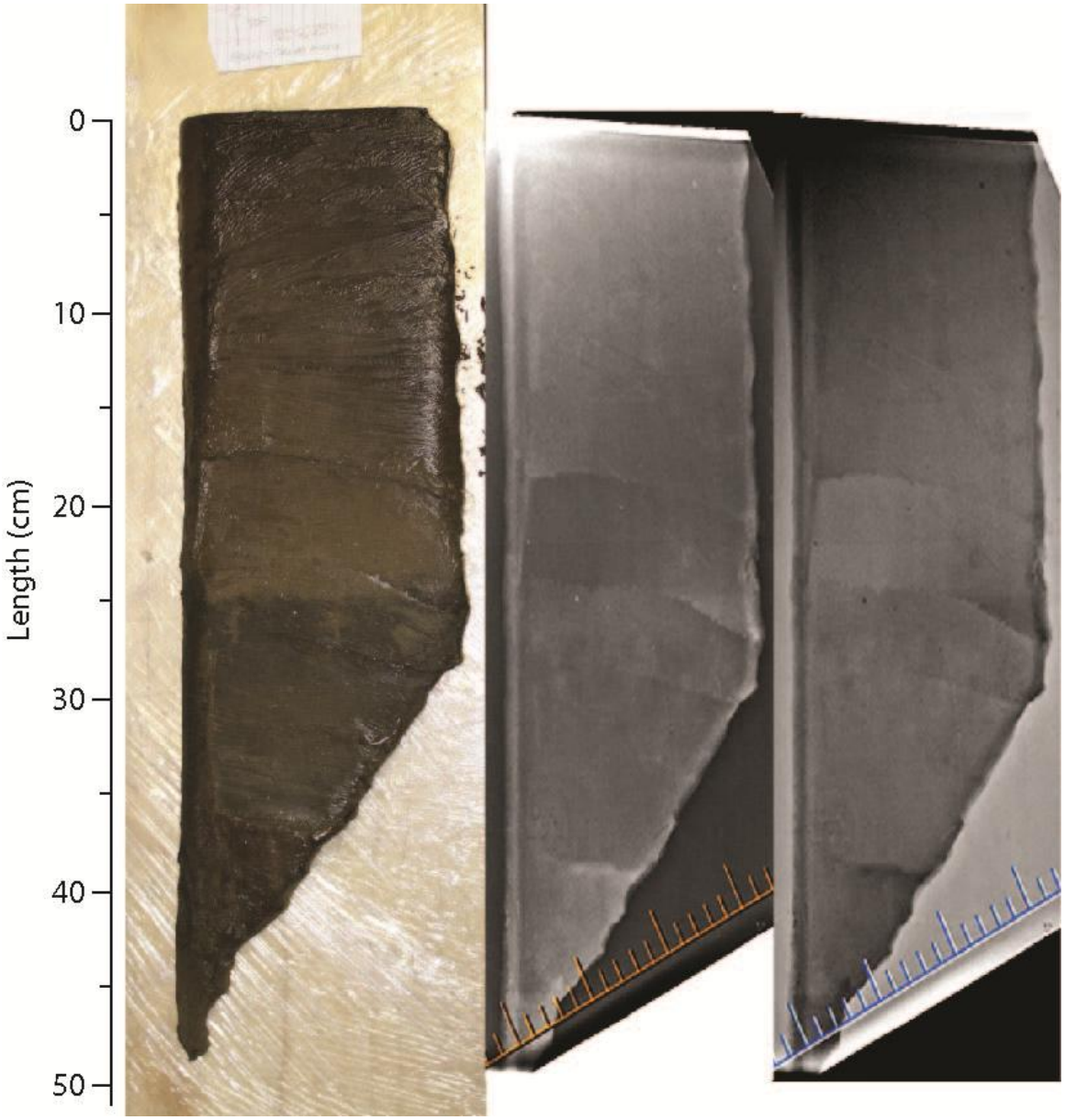

Figure C09. Freeze core ROAD10-DANNY'S LAKE, Face 1 of 2, Section 2 of 2: (left) light photograph; (middle) positive X-Ray; (right) negative X-Ray. The big bars on the X-Ray scale are separated by 5 cm and the small bars are separated by 1 cm.

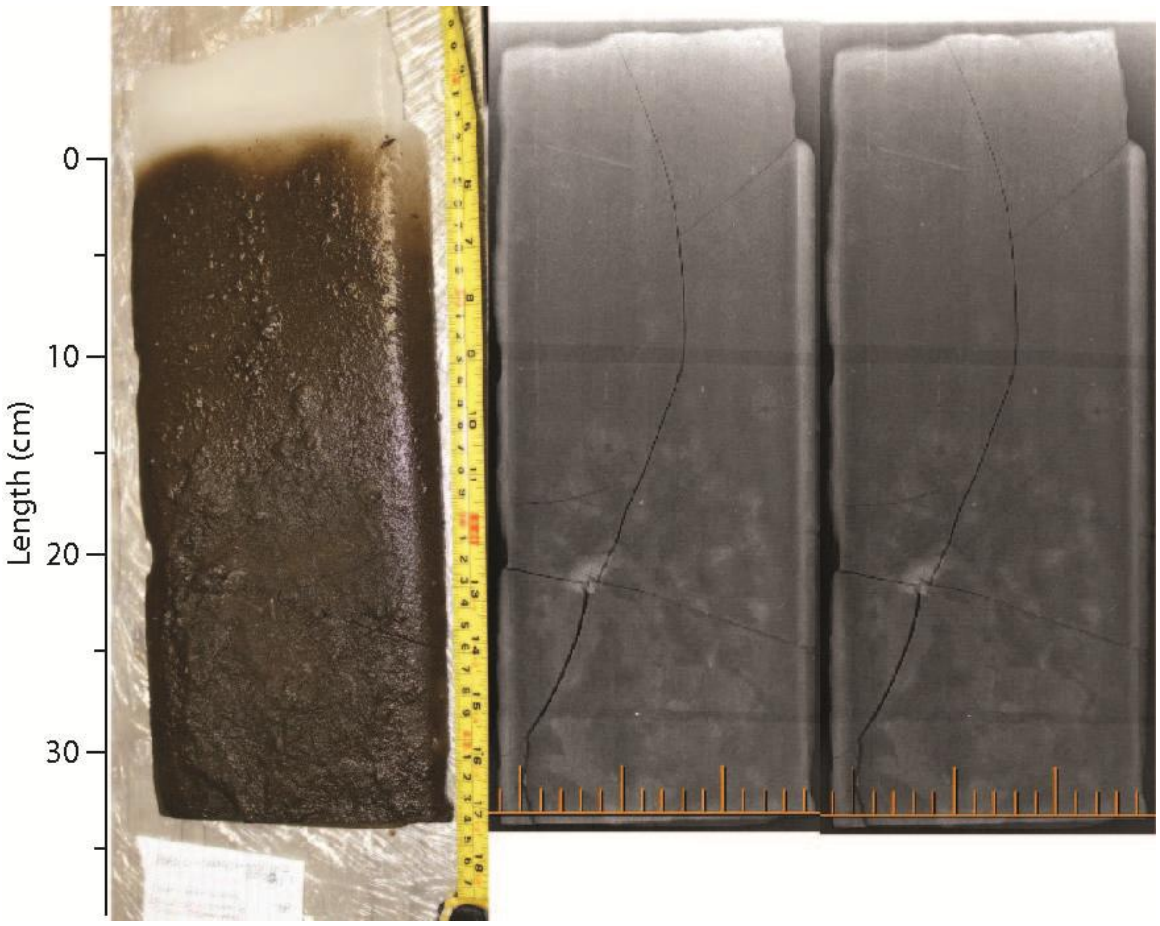

Figure C10. Freeze core ROAD10-DANNY'S LAKE, Face 2 of 2, Section 1 of 3: (left) light photograph; (middle) positive X-Ray; (right) negative X-Ray. The big bars on the X-Ray scale are separated by 5 cm and the small bars are separated by 1 cm.

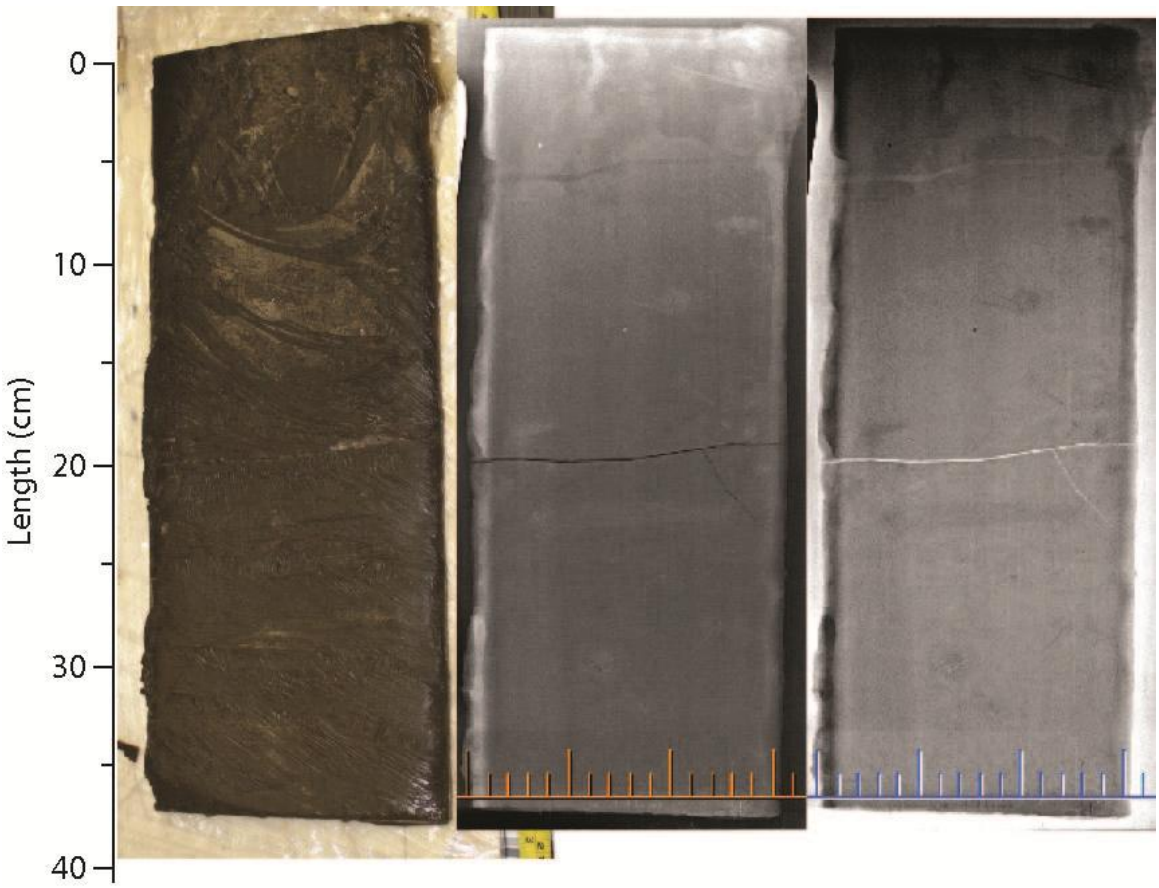

Figure C11. Freeze core ROAD10-DANNY'S LAKE, Face 2 of 2, Section 2 of 3: (left) light photograph; (middle) positive X-Ray; (right) negative X-Ray. The big bars on the X-Ray scale are separated by 5 cm and the small bars are separated by 1 cm.

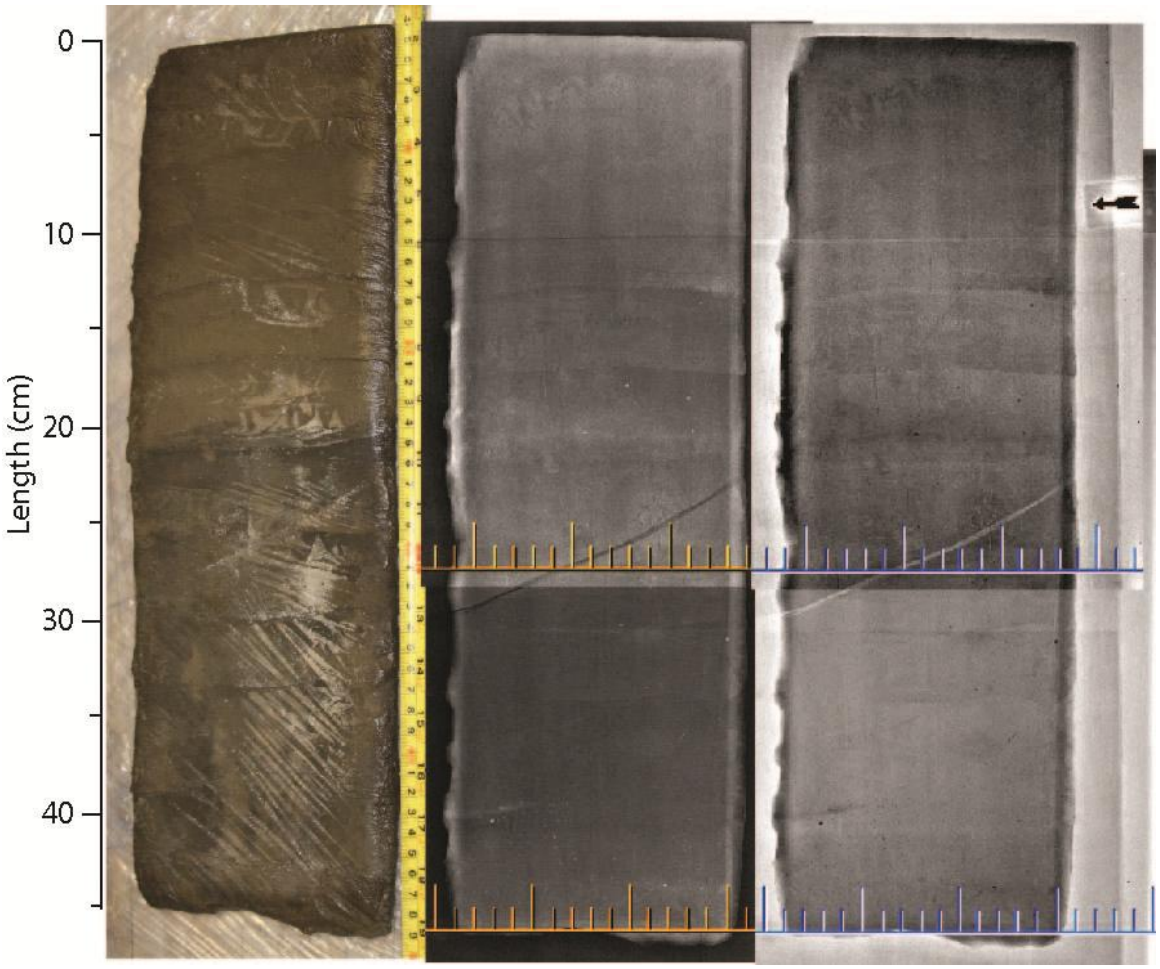

Figure C12. Freeze core ROAD10-DANNY'S LAKE, Face 2 of 2, Section 3 of 3: (left) light photograph; (middle) positive X-Ray; (right) negative X-Ray. The big bars on the X-Ray scale are separated by 5 cm and the small bars are separated by 1 cm.

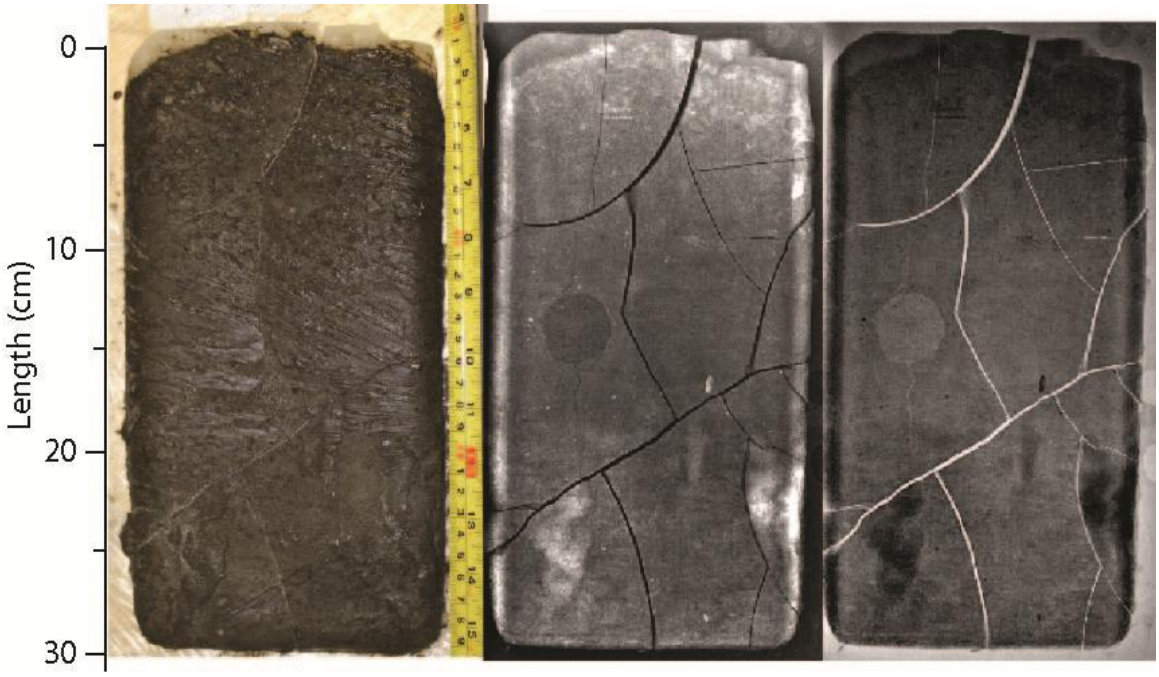

Figure C13. Freeze core ROAD10-39-1A, Face 1 of 2, Section 1 of 1: (left) light photograph; (middle) positive X-Ray; (right) negative X-Ray. The big bars on the X-Ray scale are separated by 5 cm and the small bars are separated by 1 cm.

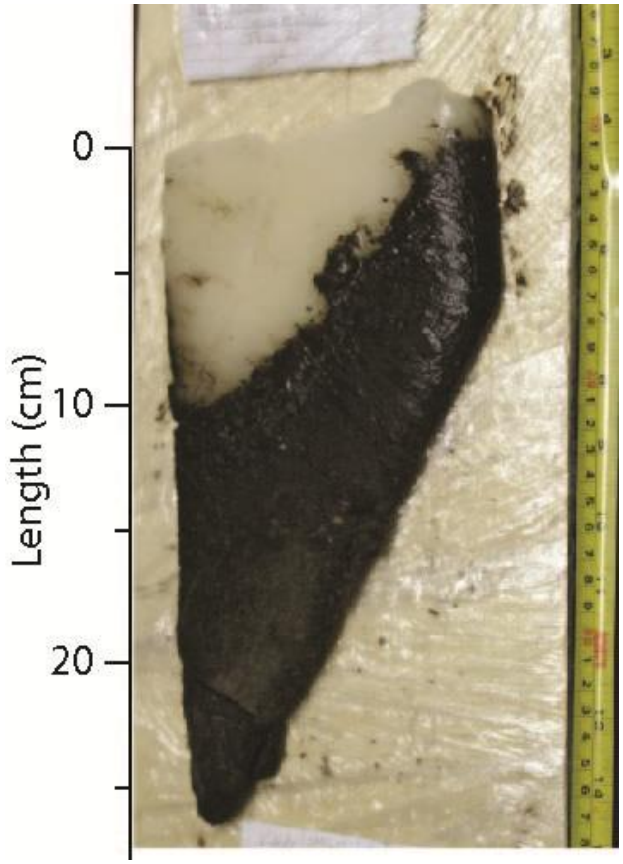

Figure C14. Freeze core ROAD10-39-1A, Face 2 of 2, Section 1 of 1: light photograph only.

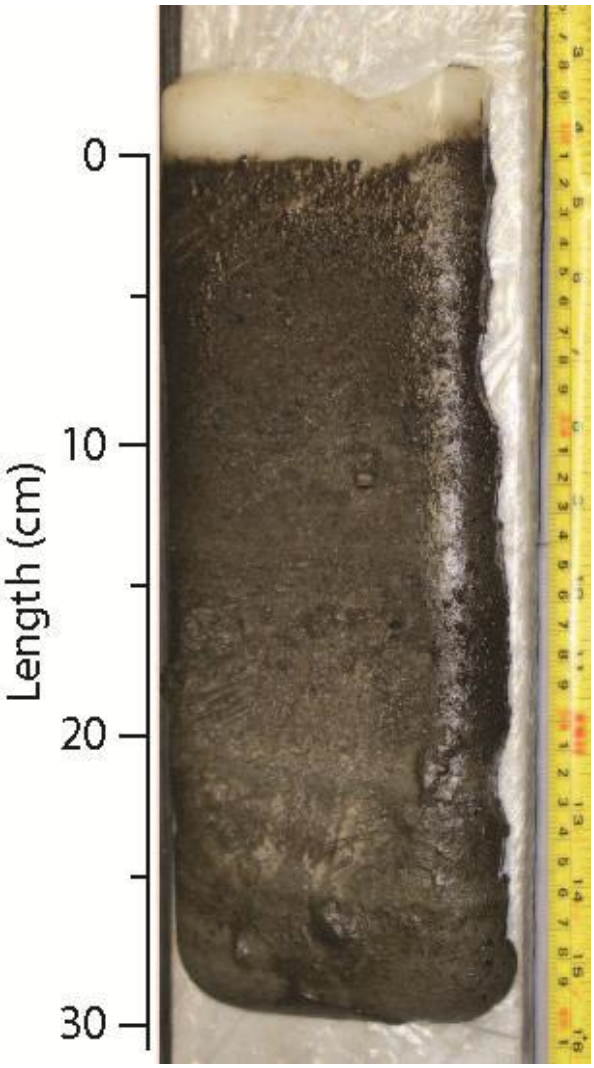

Figure C15. Freeze core ROAD10-39-1B, Face 1 of 1, Section 1 of 1: light photograph only.

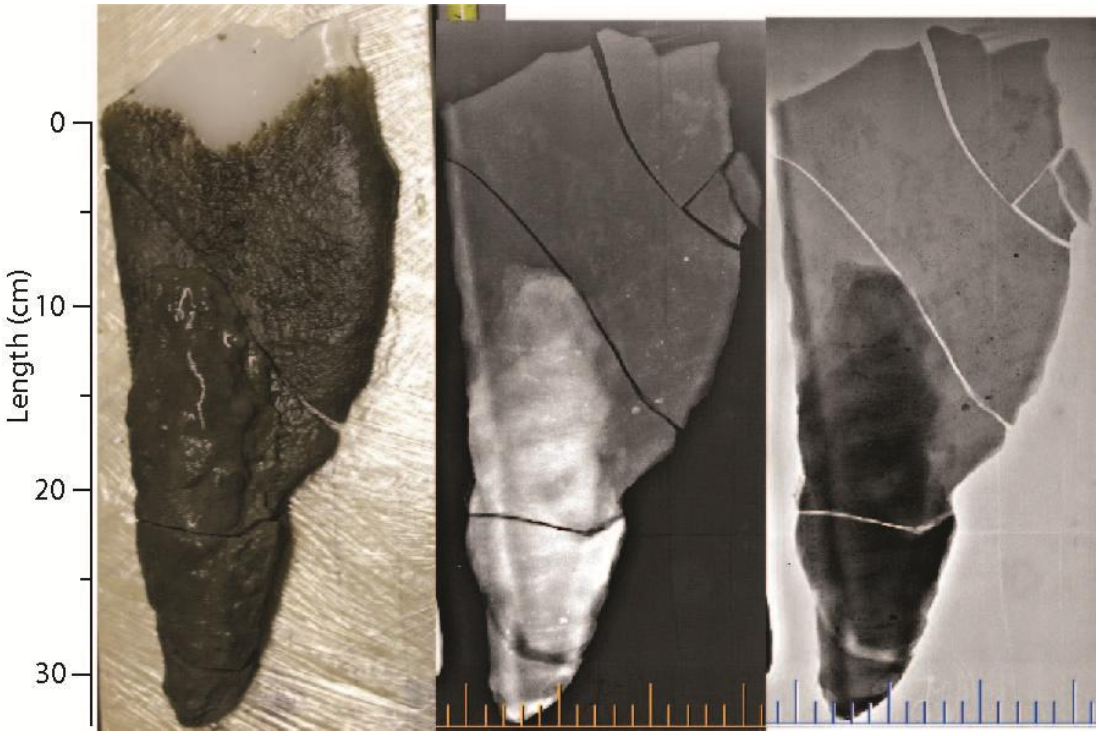

Figure C16. Freeze core ROAD10-46-1, Face 1 of 2, Section 1 of 1: (left) light photograph; (middle) positive X-Ray; (right) negative X-Ray. The big bars on the X-Ray scale are separated by 5 cm and the small bars are separated by 1 cm.

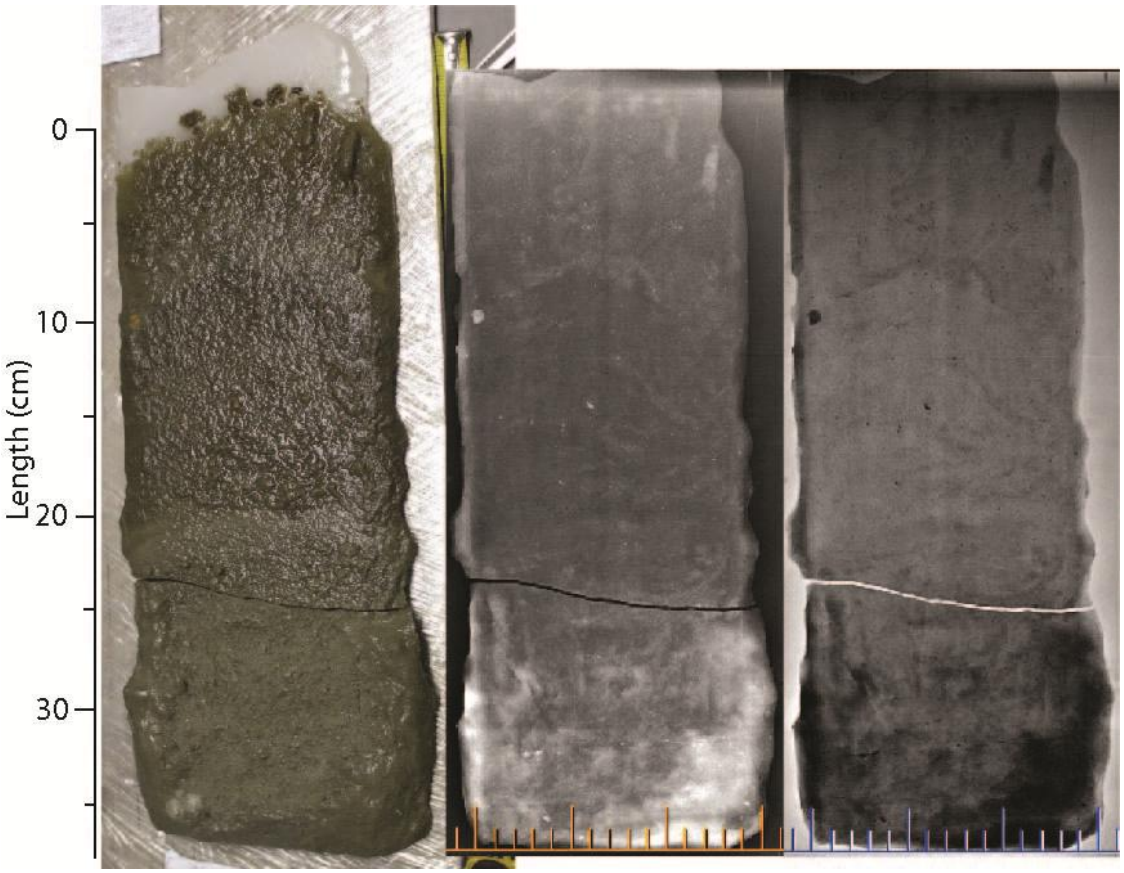

Figure C17. Freeze core ROAD10-46-1, Face 2 of 2, Section 1 of 1: (left) light photograph; (middle) positive X-Ray; (right) negative X-Ray. The big bars on the X-Ray scale are separated by 5 cm and the small bars are separated by 1 cm.

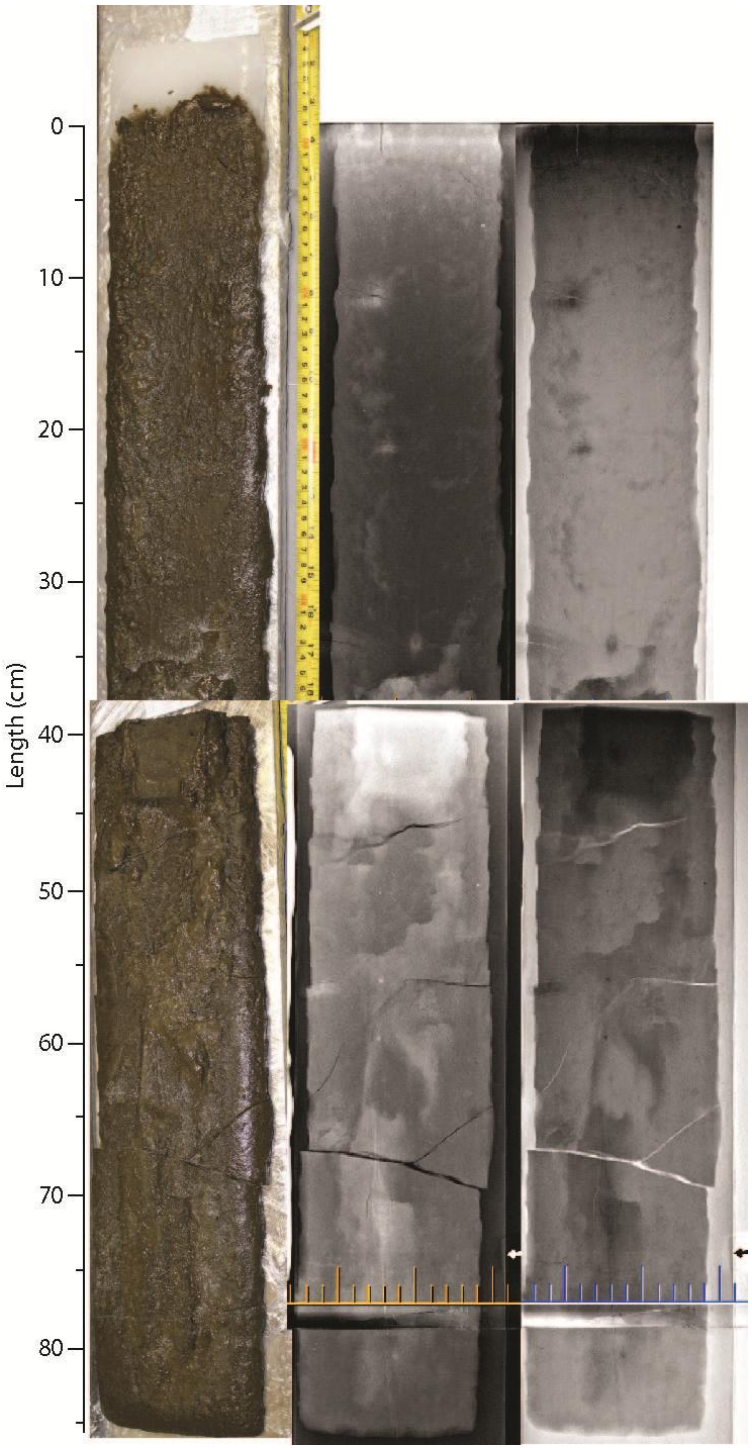

Figure C18. Freeze core ROAD10-47-1, Face 1 of 1, Section 1 of 2: (left) light photograph; (middle) positive X-Ray; (right) negative X-Ray. The big bars on the X-Ray scale are separated by 5 cm and the small bars are separated by 1 cm.

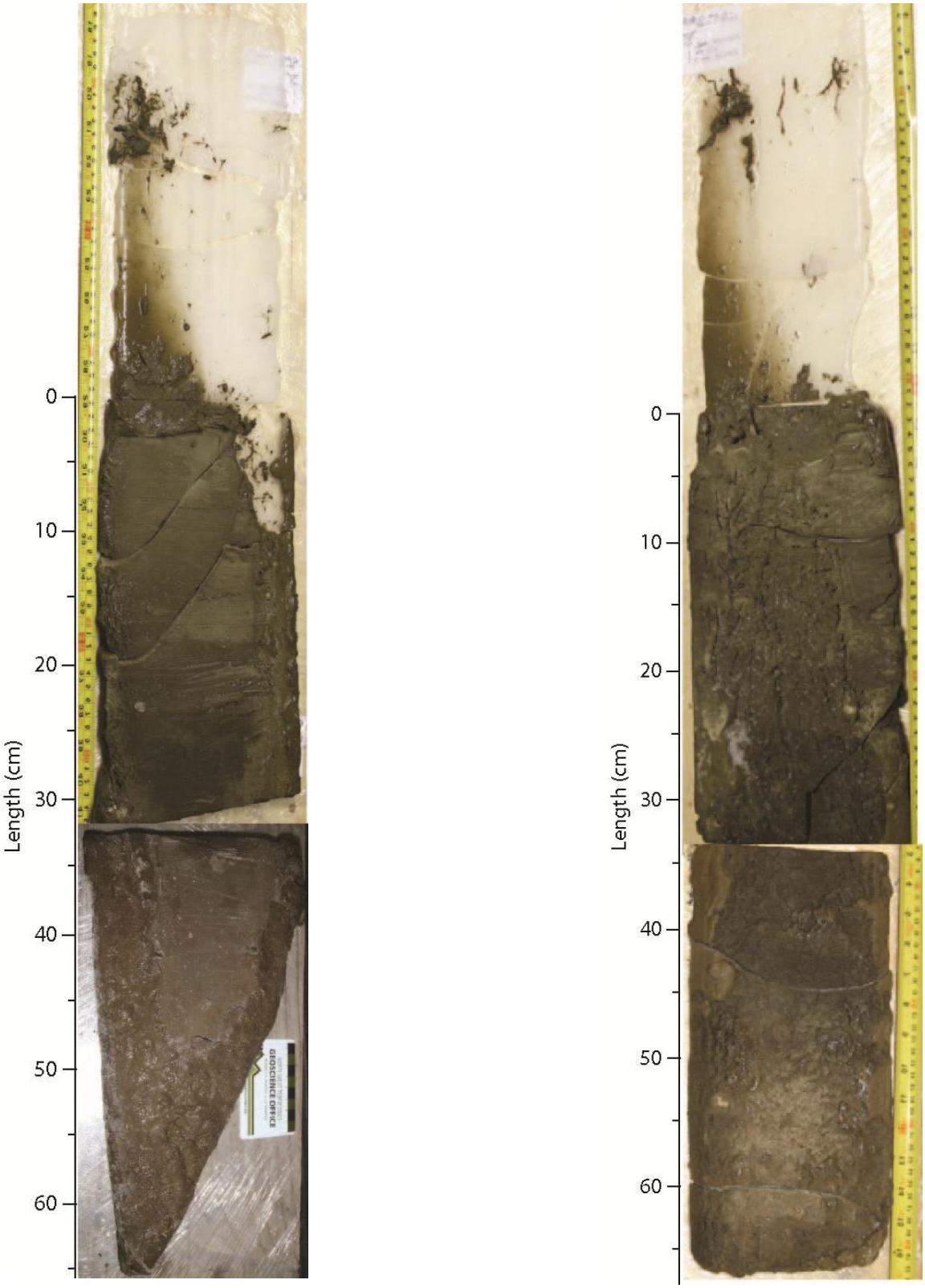

Figure C19. Light photographs of freeze core ROAD10-49-1A. Face 1 of 2 (left), Sections 1 and 2 of 2. Face 2 of 2 (right), Sections 1 and 2 of 2.

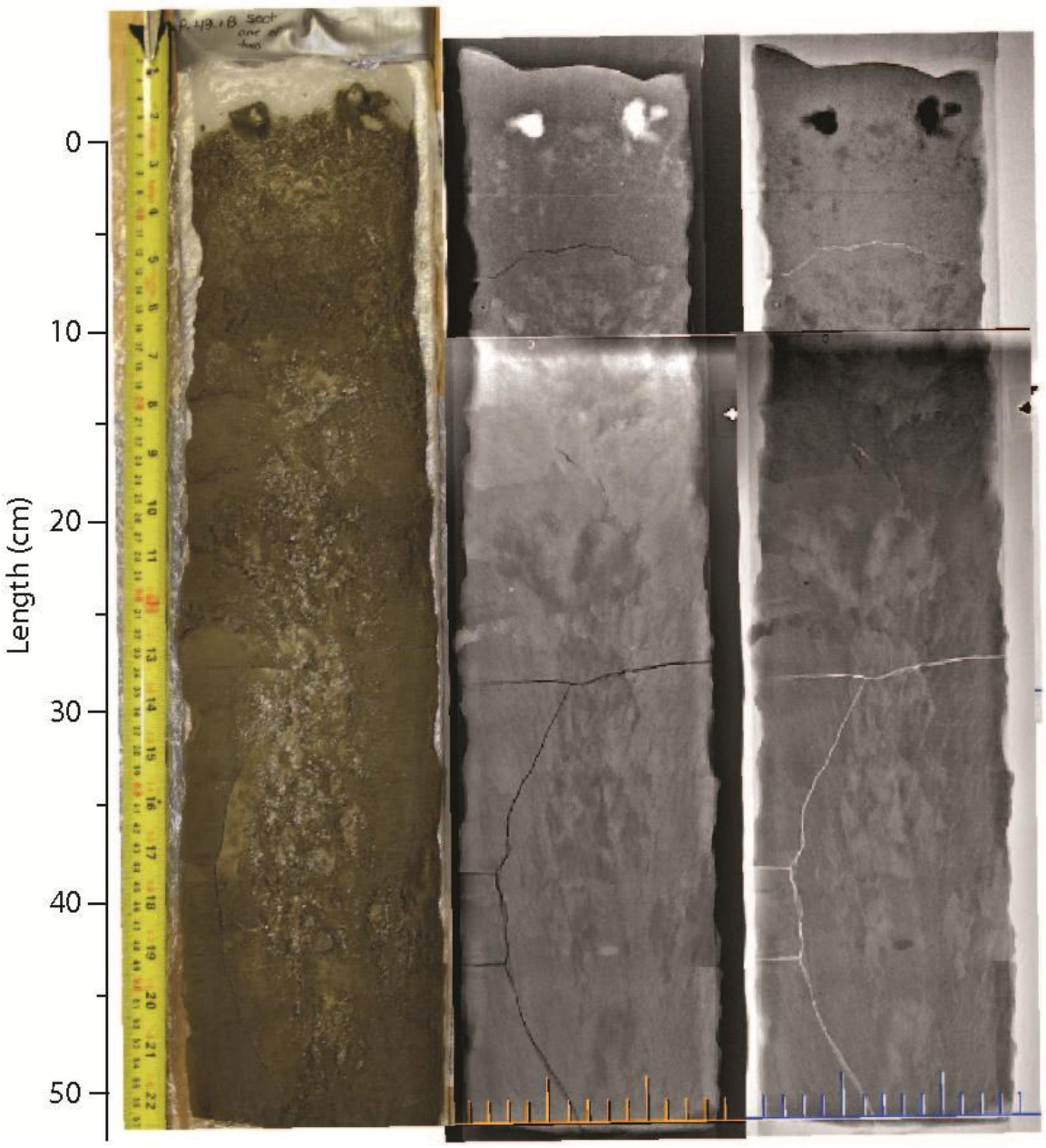

Figure C20. Freeze core ROAD10-49-1B, Face 1 of 1, Section 1 of 2: (left) light photograph; (middle) positive X-Ray; (right) negative X-Ray. The big bars on the X-Ray scale are separated by 5 cm and the small bars are separated by 1 cm.

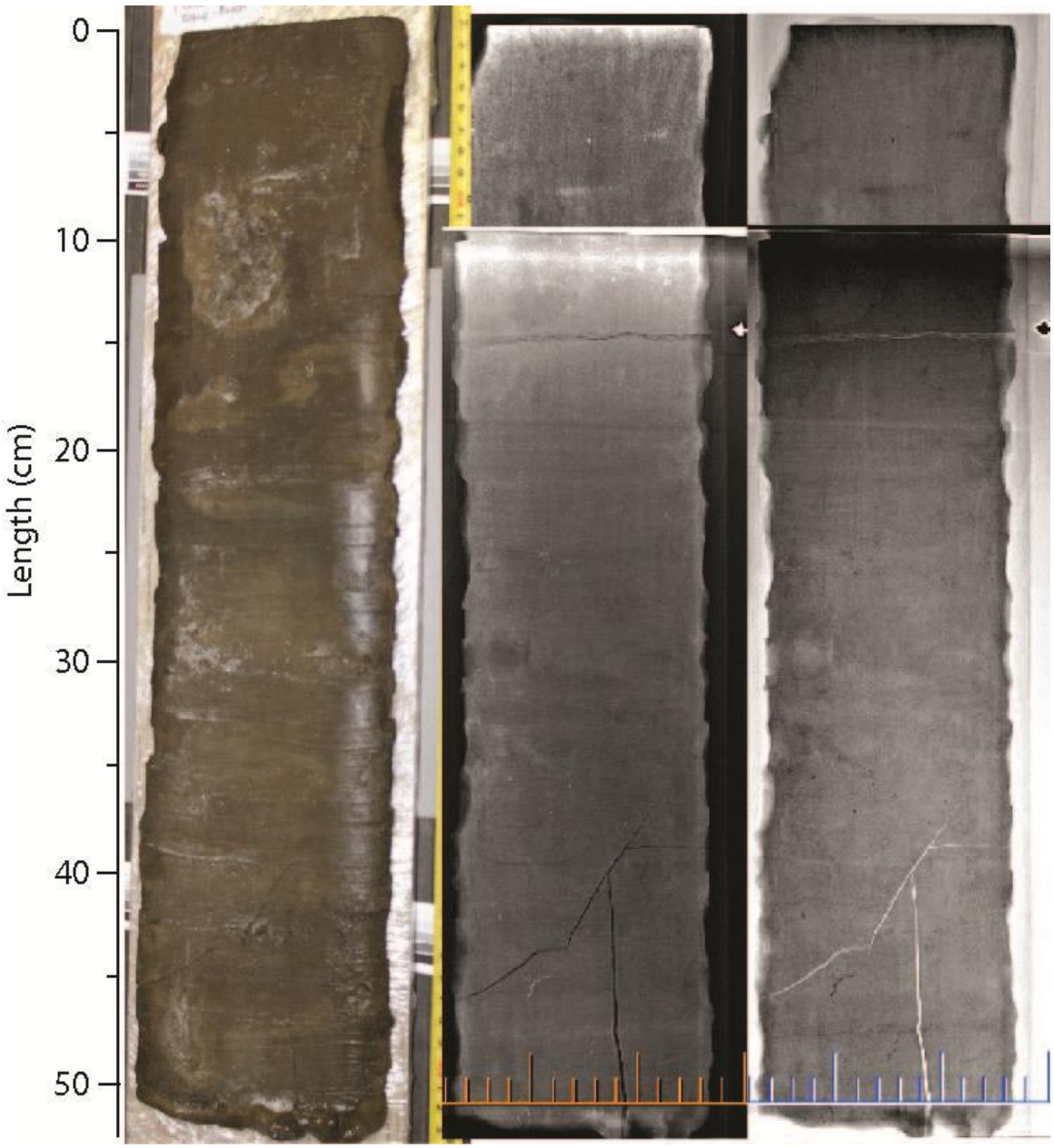

Figure C21. Freeze core ROAD10-49-1B, Face 1 of 1, Section 2 of 2: (left) light photograph; (middle) positive X-Ray; (right) negative X-Ray. The big bars on the X-Ray scale are separated by 5 cm and the small bars are separated by 1 cm.

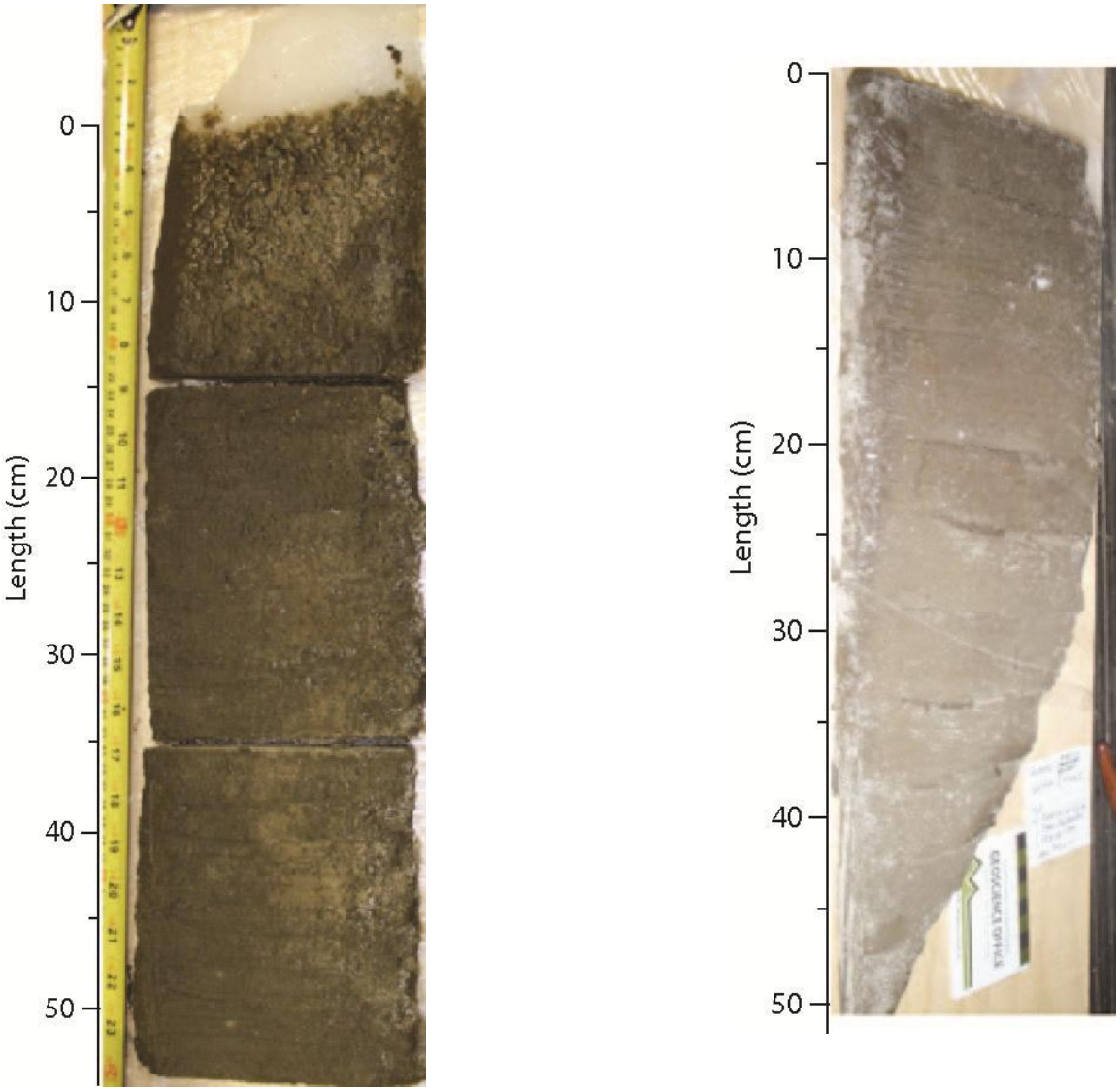

Figure C22. Freeze core ROAD10-52-1, Face 1 of 2, Sections 1 & 2: (left) light photograph of Section 1; (right) light photograph of Section 2.

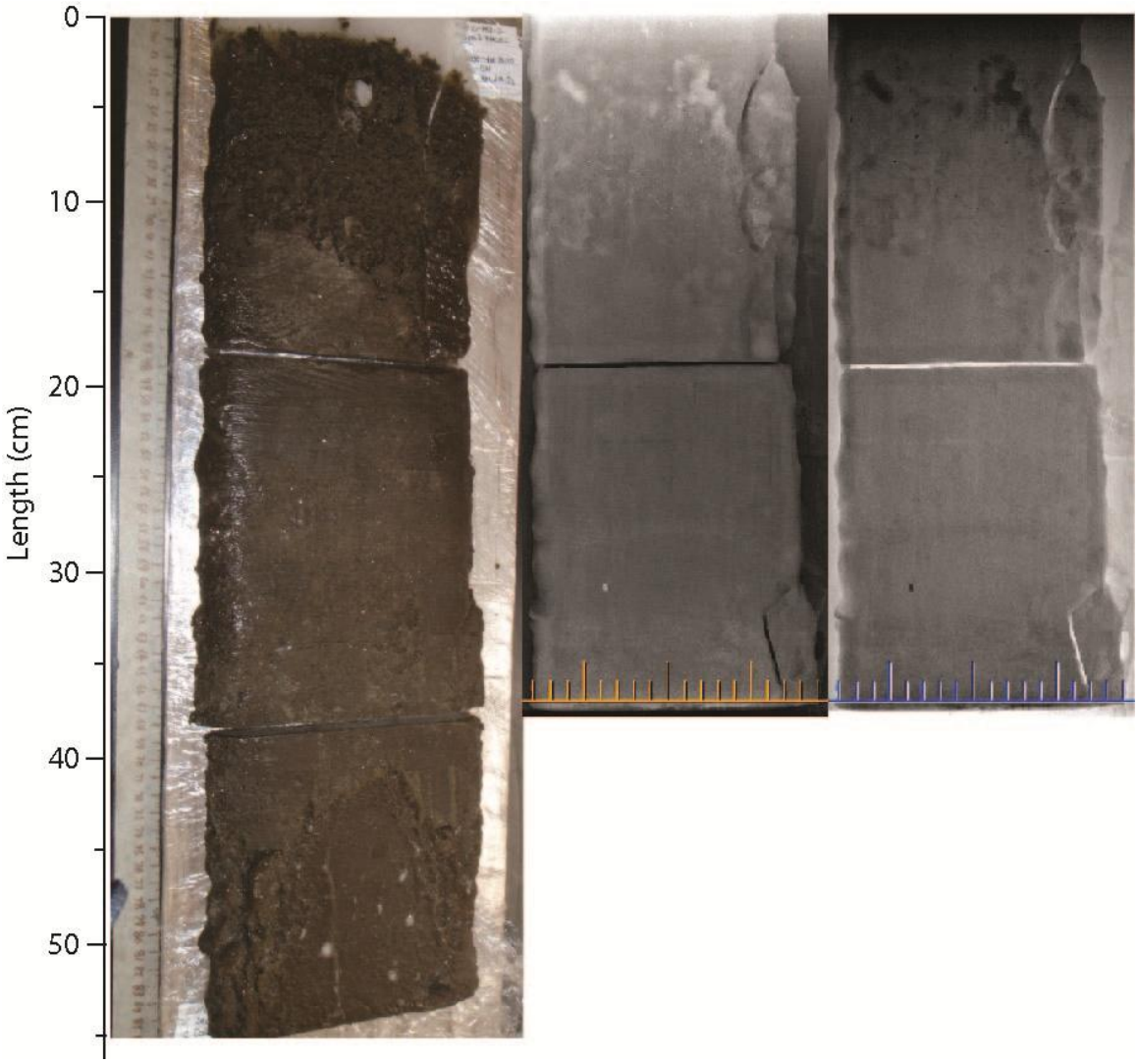

Figure C23. Freeze core ROAD10-52-1, Face 2 of 2, Section 1 of 2: (left) light photograph; (middle) positive X-Ray; (right) negative X-Ray. The big bars on the X-Ray scale are separated by 5 cm and the small bars are separated by 1 cm.

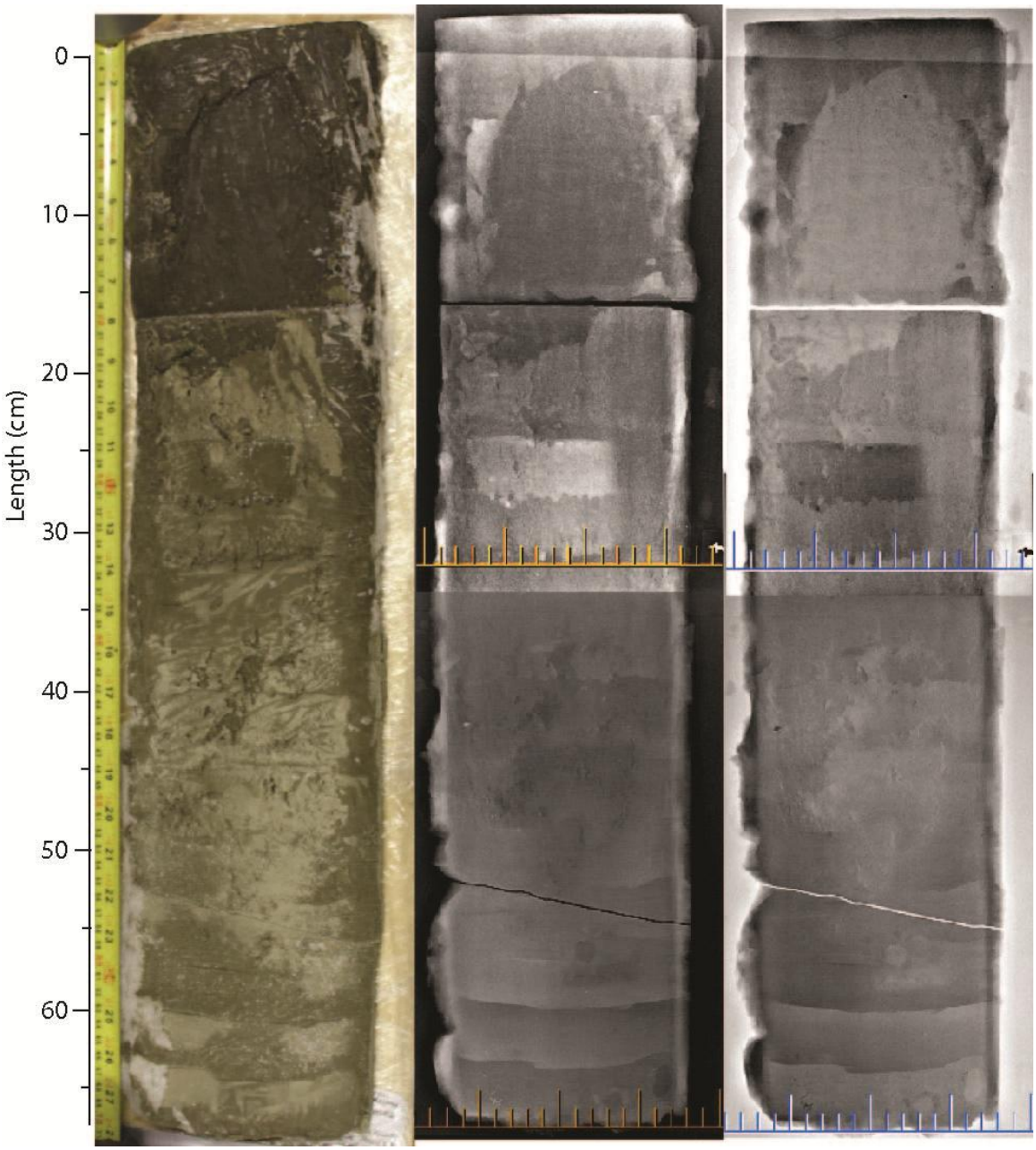

Figure C24. Freeze core ROAD10-52-1, Face 2 of 2, Section 2 of 2: (left) light photograph; (middle) positive X-Ray; (right) negative X-Ray. The big bars on the X-Ray scale are separated by 5 cm and the small bars are separated by 1 cm.

Figure C25. Freeze core ROAD10-ECHO, Face 1 of 2, Sections 1 & 2: (left) light photograph of Section 1; (right) light photograph of Section 2.

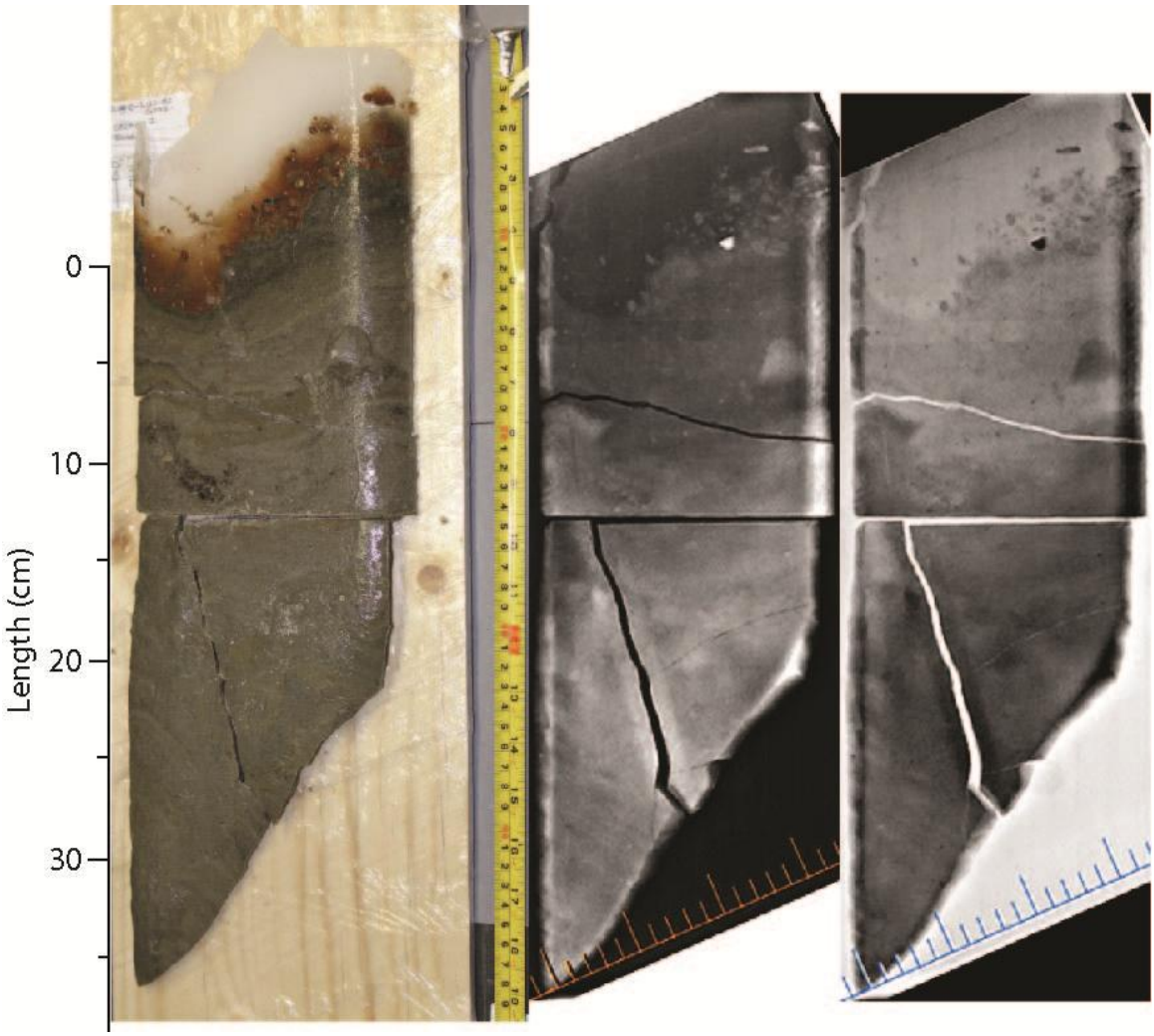

Figure C26. Freeze core ROAD10-Lacdegras, Face 1 of 2, Section 1 of 1: (left) light photograph; (middle) positive X-Ray; (right) negative X-Ray. The big bars on the X-Ray scale are separated by 5 cm and the small bars are separated by 1 cm.

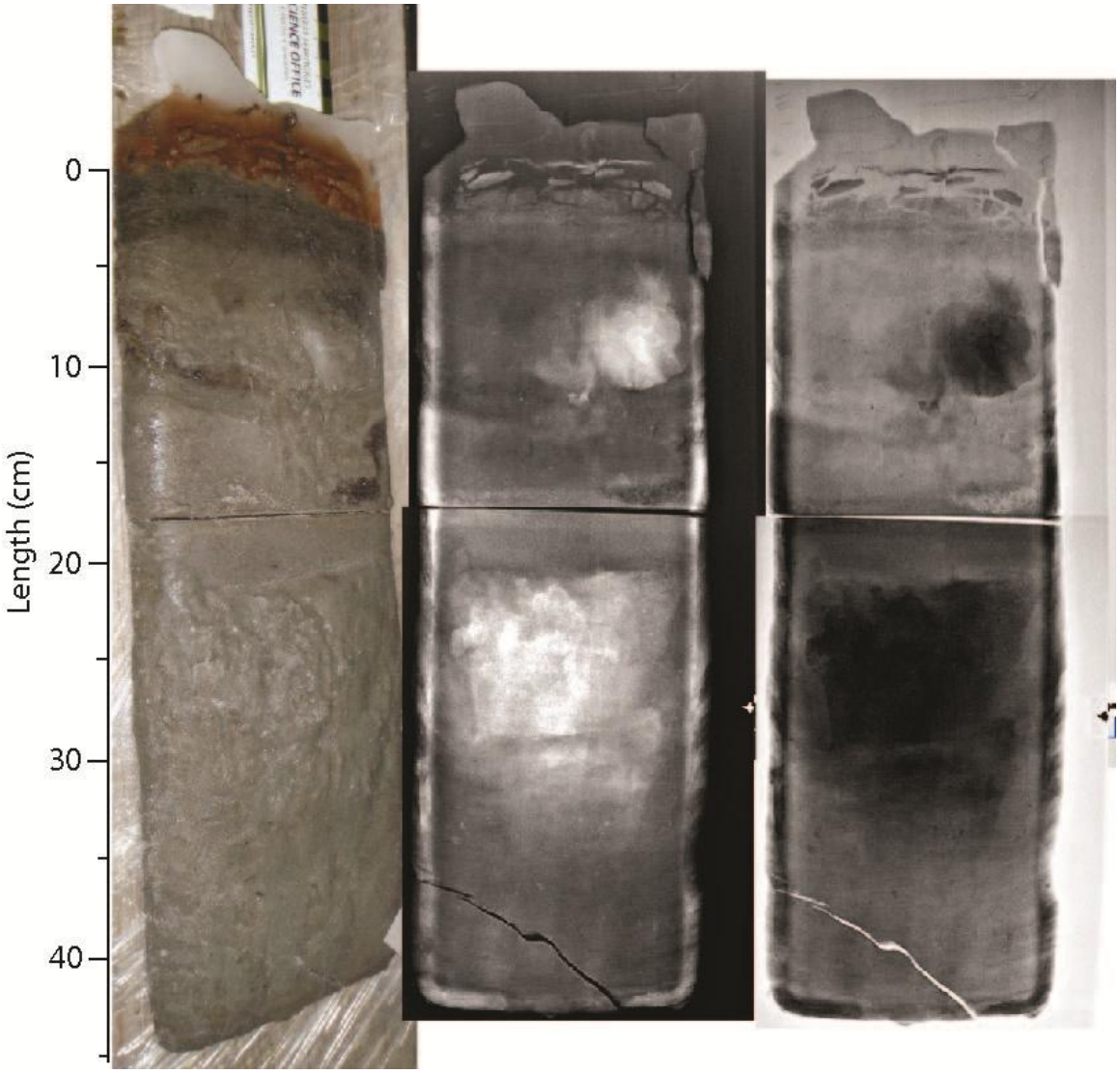

Figure C27. Freeze core ROAD10-Lacdegras, Face 2 of 2, Section 1 of 1: (left) light photograph; (middle) positive X-Ray; (right) negative X-Ray. The big bars on the X-Ray scale are separated by 5 cm and the small bars are separated by 1 cm.

Appendix D: Chronology

Table D01. AMS radiocarbon dates from TCWR freeze cores.

Lake	Corer	Face	Sect	Sample ID	14 C Age (uncalibrated)	+/-	Depth (cm)	UBA (#)	Material Dated
Tibbitt	1F		1	TibA_20cm	67	22	20	UBA-17353	Bulk
			1	TibA_40cm	1409	20	40	UBA-17354	Bulk
			1	TibA_80cm	2046	26	80	UBA-17355	Bulk
			2	ROAD09-TIBBITT01-A55-55.5cm	2390	40	138.25		Bulk
Waite	1F		1	WAITE15	995	24	16.9	UBA-16433	Bulk
			1	WAITE25	1129	22	29.1	UBA-16434	Bulk
			1	WAITE39	1455	23	43.2	UBA-16435	Bulk
			1	WAITE53	1519	22	57.8	UBA-16436	Bulk
			1	ROAD09-WAITE01-A65-67.5cm	1520	40	66.3		Bulk
			2	WaiteB_110	2107	29	109.7	UBA-15638	Twig
			2	ROAD09-WAITE01-B79-81cm	2580	40	154		Bulk
			3	ROAD09-WAITE01-C22-23cm	2920	40	185		Bulk
			3	ROAD09-WAITE01-C-43-43.75cm	3460	40	205.1		Bulk
P34-2 (Danny's)	2F	2	1	P34-F2_5.7cm	693	21	5.7	UBA-17359	Bulk
			1	P34-F2_10.2cm	855	23	10.2	UBA-17360	Bulk
			1	Danny_2_1_ChipA	1329	23	15	UBA-16543	Bulk
			1	P34-F2_21.9cm	1617	25	21.9	UBA-17361	Bulk
			1	P34-F2_27.8	1659	21	27.8	UBA-17431	Bulk
			1	Danny_2_1_6/9	1916	25	32.6	UBA-16544	Bulk
			1	P34-F2_37.6cm	2659	32	37.6	UBA-17432	Bulk
			2	Danny_2_2_ChipB	2912	24	45	UBA-16545	Bulk
			2	Danny_2_2_132/135	3604	25	56.9	UBA-16546	Bulk
			2	Danny_2_2_5	5039	51	70.1	UBA-16547	Bulk
			3	Danny_2_3_ChipC	5834	29	85.1	UBA-16548	Bulk
			3	Danny_2_3_200	8112	32	95.5	UBA-16439	Bulk
			3	Danny_2_3_20	7450	30	113.6	UBA-16440	Bulk
P39-1A	2F	1	1	P39-1A-F1_10cm	3597	26	10	UBA-17344	Bulk
			1	P39-1A-F1_19cm	3701	24	19	UBA-17345	Bulk
			1	P39-1A-F1_29cm	5385	35	29	UBA-17346	Bulk
P47-1	2F	2	1	P47_13.5	4218	38	13.5	UBA-17159	Bulk
			1	P47_41	4885	37	41	UBA-17160	Bulk
			1	P47_63	5333	35	63	UBA-17161	Bulk
			1	P47_86.5	5878	34	86.5	UBA-17162	Bulk
P49-1B	1F		1	P49-1B-F1_19.5cm	1925	25	19.5	UBA-17347	Bulk
			2	P49-1B-F1_64.5cm	3675	24	64.5	UBA-17348	Bulk
			2	P49-1B-F1_100cm	5663	26	100	UBA-17349	Bulk
P52-1	2F	2	1	P52-F2_9cm	178	25	9	UBA-17350	Bulk
			1	P52_18	1148	42	18	UBA-17163	Bulk
			1	P52-F2_28cm	2763	22	28	UBA-17351	Bulk
			1	P52-F2_38cm	3343	23	38	UBA-17352	Bulk
			1	P52_45	5916	58	55	UBA-17165	Bulk
			2	P52_80	7488	40	80	UBA-17166	Bulk
			2	P52_106	8011	43	106	UBA-17167	Bulk
Lac de Gras	2F	2	1	LG-F2_19cm	3299	38	19	UBA-17356	Bulk
				LG-F2_32cm	1607	29	32	UBA-17357	Bulk
				LG-F2_46cm	2144	35	46	UBA-17358	Bulk

Note: UBA (#) is code that Chronos Lab (Queens University Belfast) gives to radiocarbon samples. Samples without a UBA code were submitted to Beta Analytic Inc. All dates are uncalibrated.

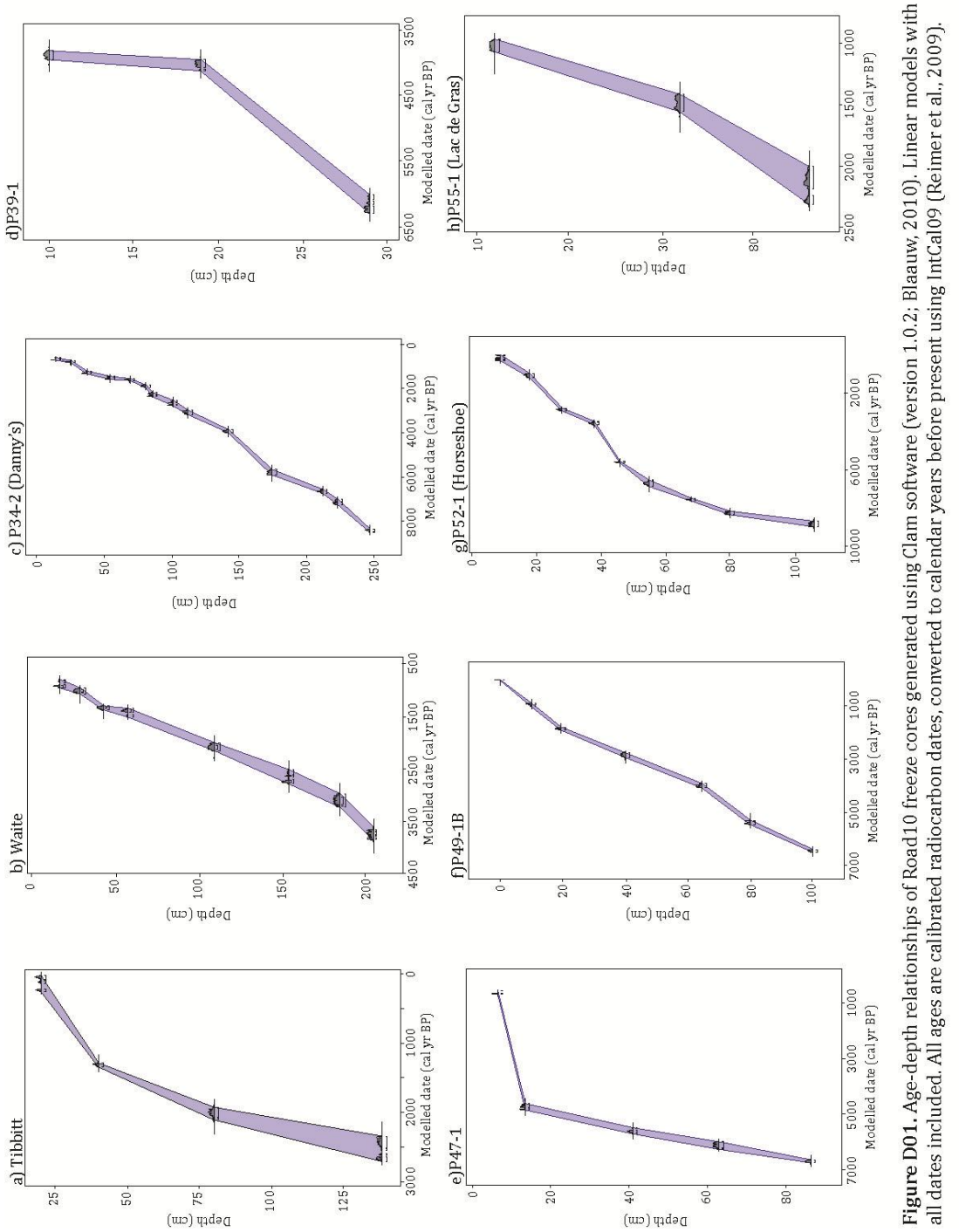

Figure D01. Age-depth relationships of Road10 freeze cores generated using Clam software (version 1.0.2; Blaauw, 2010). Linear models with all dates included. All ages are calibrated radiocarbon dates, converted to calendar years before present using IntCal09 (Reimer et al., 2009).